nature COMMUNICATIONS

ARTICLE

https://doi.org/10.1038/s41467-020-15479-3 OPEN

Check for updates

An intracellular membrane protein GEP1 regulates xanthurenic acid induced gametogenesis of malaria parasites

Yuanyuan Jiang[1,4], Jun Wei[1,4], Huiting Cui[1,4], Chuanyuan Liu[1], Yuan Zhi[1], ZhengZheng Jiang[1], Zhenkui Li[1], Shaoneng Li[1], Zhenke Yang[1], Xu Wang[1], Pengge Qian[1], Cui Zhang[1], Chuanqi Zhong[1], Xin-zhuan Su[3] & Jing Yuan [1,2✉]

Gametocytes differentiation to gametes (gametogenesis) within mosquitos is essential for malaria parasite transmission. Both reduction in temperature and mosquito-derived XA or elevated pH are required for triggering cGMP/PKG dependent gametogenesis. However, the parasite molecule for sensing or transducing these environmental signals to initiate gametogenesis remains unknown. Here we perform a CRISPR/Cas9-based functional screening of 59 membrane proteins expressed in the gametocytes of *Plasmodium yoelii* and identify that GEP1 is required for XA-stimulated gametogenesis. GEP1 disruption abolishes XA-stimulated cGMP synthesis and the subsequent signaling and cellular events, such as Ca^{2+} mobilization, gamete formation, and gametes egress out of erythrocytes. GEP1 interacts with GCα, a cGMP synthesizing enzyme in gametocytes. Both GEP1 and GCα are expressed in cytoplasmic puncta of both male and female gametocytes. Depletion of GCα impairs XA-stimulated gametogenesis, mimicking the defect of GEP1 disruption. The identification of GEP1 being essential for gametogenesis provides a potential new target for intervention of parasite transmission.

[1] State Key Laboratory of Cellular Stress Biology, Innovation Center for Cell Signaling Network, School of Life Sciences, Xiamen University, 361102 Xiamen, Fujian, China. [2] Lingnan Guangdong Laboratory of Modern Agriculture, 510642 Guangzhou, China. [3] Laboratory of Malaria and Vector Research, National Institute of Allergy and Infectious Diseases, National Institutes of Health, Bethesda, MD 20892, USA. [4] These authors contributed equally: Yuanyuan Jiang, Jun Wei, Huiting Cui. ✉email: yuanjing@xmu.edu.cn

Male and female gametocytes are sexual precursor cells essential for malaria parasite transmission. Within 10–15 min after being taken up by a mosquito, gametocytes differentiate into gametes in mosquito midgut, a process known as gametogenesis. A female gametocyte forms a rounded female gamete, whereas a male gametocyte undergoes three mitotic divisions, assembles eight intracytoplasmic axonemes, and produces eight flagellated male gametes[1]. Both male and female gametes egress from their residing erythrocytes via an inside-out mechanism, during which the parasitophorus vacuole membrane (PVM) ruptures prior to the opening of the erythrocyte membrane (EM)[2]. After the release from erythrocytes, the male and female gametes fertilize to produce zygotes and then the motile ookinetes that penetrate mosquito midgut wall to develop into oocysts each containing thousands of sporozoites. The sporozoites then migrate to mosquito salivary glands and are injected into a new host when the mosquito bites again.

Gametogenesis is triggered by two stimuli, a drop in temperature of approximately 5 °C[3,4] and the presence of xanthurenic acid (XA) that is a metabolite of tryptophan from mosquito[5,6]. An additional signal reported to induce gametogenesis is an increase in pH from 7.4 to 8[4]. Since the groundbreaking discovery of XA as a trigger for *Plasmodium* gametogenesis in mosquitoes, studies have shown that XA can enhance parasite guanylyl cyclase (GC) activity on gametocyte membrane fraction, leading to increased level of second messenger 3'−5'-cyclic guanosine monophosphate (cGMP)[7]. Two integral membrane GC proteins (GCα and GCβ) are found in *Plasmodium* parasites. GCα has been implicated to be responsible for cGMP synthesis during gametogenesis because disruption of GCβ has no effect on XA-induced gametogenesis[8–10]. The increased level of cGMP activates cGMP-dependent protein kinase G (PKG) that functions as a master regulator of the downstream signaling events during gametogenesis[11]. Inhibition of PKG using Compound 2 (C2) prevented gametocytes rounding up, gamete formation of both sexes, and gametes egress from erythrocytes in *P. falciparum* and *P. berghei*[11,12]. PKG-dependent Ca^{2+} mobilization was also observed in the cytosol of *P. falciparum* and *P. berghei* gametocytes 10–15 s after addition of XA[13,14]. PKG activates the synthesis of inositol (1,4,5)-trisphosphate (IP3) via phosphoinositide metabolism and triggers cytosolic mobilization of Ca^{2+} that likely originates from the endoplasmic reticulum[15]. Unfortunately, the molecule(s) responsible for sensing XA or transducing the XA-stimulated signal to activate the cGMP-PKG signaling remain unknown.

Membrane proteins are known to play critical roles in sensing, transporting, and/or transducing environmental signals to initiate cellular responses. To identify potential molecules involved in sensing or transducing XA signal during gametogenesis, we perform CRISPR/Cas9-mediated genetic deletion screens of 59 candidate genes encoding integral membrane proteins expressed in gametocytes of the rodent malaria parasite *P. yoelii*. We identify a multiple-spanning membrane protein GEP1 (gametogenesis essential protein 1) that was essential for XA-stimulated gametogenesis. Disruption of GEP1 completely abolishes XA-stimulated gametogenesis of both sexes. Parasites deficient of GEP1 show no synthesis of XA-stimulated cGMP and no downstream cellular and signaling events such as Ca^{2+} mobilization, parasite egress out of PVM and EM, genome replication and axoneme assembly in male gametocytes, and release of translational repression in female gametocytes. GEP1 interacts with GCα in gametocytes, and GCα depletion also impairs XA-stimulated gametogenesis, mimicking the effects of GEP1 disruption. This study identifies a molecule essential for the initiation of gametogenesis and a potential target for blocking parasite transmission.

Results

GEP1 is essential for XA-stimulated gametogenesis. To identify membrane proteins critical in sensing XA or transducing XA-induced signal during gametogenesis, we identified 59 *P. yoelii* genes that are expressed in gametocytes and encode proteins with 1 to 22 predicted transmembrane domains (TMs) from the PlasmoDB database (Supplementary Table 1). We designed single guide RNA (sgRNA) to disrupt each of these genes using CRISPR/Cas9 methods[16,17] and were able to successfully knockout (KO) 45 (76%) of the genes in the *P. yoelii* 17XNL strain, obtaining at least two cloned lines for each mutant (Supplementary Fig. 1a, c, d, i). The remaining 14 genes (24%) were refractory to repeated deletion attempts using three independent sgRNA sequences, suggesting their essential roles for asexual blood-stage growth.

The 45 gene deletion mutants proliferated asexually in mouse blood normally and were able to produce both male and female gametocytes although the gametocytemia level varied among these mutants (Supplementary Fig. 2, Supplementary Fig. 3a). Next we measured the gametogenesis of male gametocyte by counting exflagellation centers (ECs) formed in vitro after stimulation with 50 μM XA at 22 °C. Only one mutant (PY17X_1116300 disruption) showed complete deficiency in EC formation and male gamete release (Fig. 1a–c). The PY17X_1116300 gene contains four exons (Fig. 1d) encoding a putative amino acid transporter protein that is essential for gametogenesis; we therefore name the gene *gep1* for gametogenesis essential protein 1. As controls, disruption of *P. yoelii cdpk4* or *map2* also caused defect in EC formation (Fig. 1a), confirming the phenotypes observed in *P. berghei*[13,18]. Consequently, the Δ*gep1* mutant parasite produced no ookinete in in vitro culture (Supplementary Fig. 3b), oocyst in *Anopheles stephensi* midgut (Fig. 1f), or sporozoite in mosquito salivary gland (Supplementary Fig. 3c).

To further confirm the phenotype of Δ*gep1*, we generated three additional *gep1* mutant parasites (Δ*gep1n*, Δ*gep1fl*, and Δ*gep1mScarlet*) (Fig. 1d, Supplementary Fig. 1c–e). The Δ*gep1n* parasite had a 464 bp deletion at the 5' coding region, causing a frameshift for the remaining coding region. The Δ*gep1fl* parasite had the whole *gep1* coding region deleted, and the Δ*gep1mScarlet* parasite had its *gep1* coding regions replaced with a gene encoding red florescent protein mScarlet. These mutations were confirmed by PCR and DNA sequencing (Supplementary Fig. 1j, k), and the mutant parasites displayed developmental phenotypes similar to those of Δ*gep1* in both mouse and mosquito stages (Fig. 1e, f, Supplementary Fig. 3a–c). We also reintroduced the 558 bp deleted segment plus a sextuple HA epitope (6HA) into the Δ*gep1* parasite to rescue the gene function using Cas9-mediated homologous replacement (Fig. 1d, Supplementary Fig. 1b, j). Two clones of the rescued parasite (Δ*gep1/gep1::6HA*c1 and Δ*gep1/gep1::6HA*c2) showed expression of the GEP1::6HA protein in both Western blotting and immunofluorescence analysis (IFA) (Supplementary Fig. 3d, e). Importantly, both clones produced wild type (WT) levels of EC in vitro (Fig. 1e) and midgut oocyst in mosquitoes (Fig. 1f). The GEP1 protein is well-conserved among *P. yoelii, P. berghei*, and the human *P. falciparum* parasites (Supplementary Fig. 4), suggesting conserved function. Deletion of *P. berghei gep1* gene (PBANKA_1115100) resulted in parasite clones that failed to form XA-stimulated ECs in vitro and midgut oocyst in mosquitoes (Supplementary Fig. 1l, m, Supplementary Fig. 3f–h). Together, these results demonstrate that GEP1 depletion completely block male gametogenesis and mosquito transmission of malaria parasites.

GEP1 is expressed in cytosol puncta of gametocytes. GEP1 is a *Plasmodium*-specific protein with 905 residues and 14 predicted

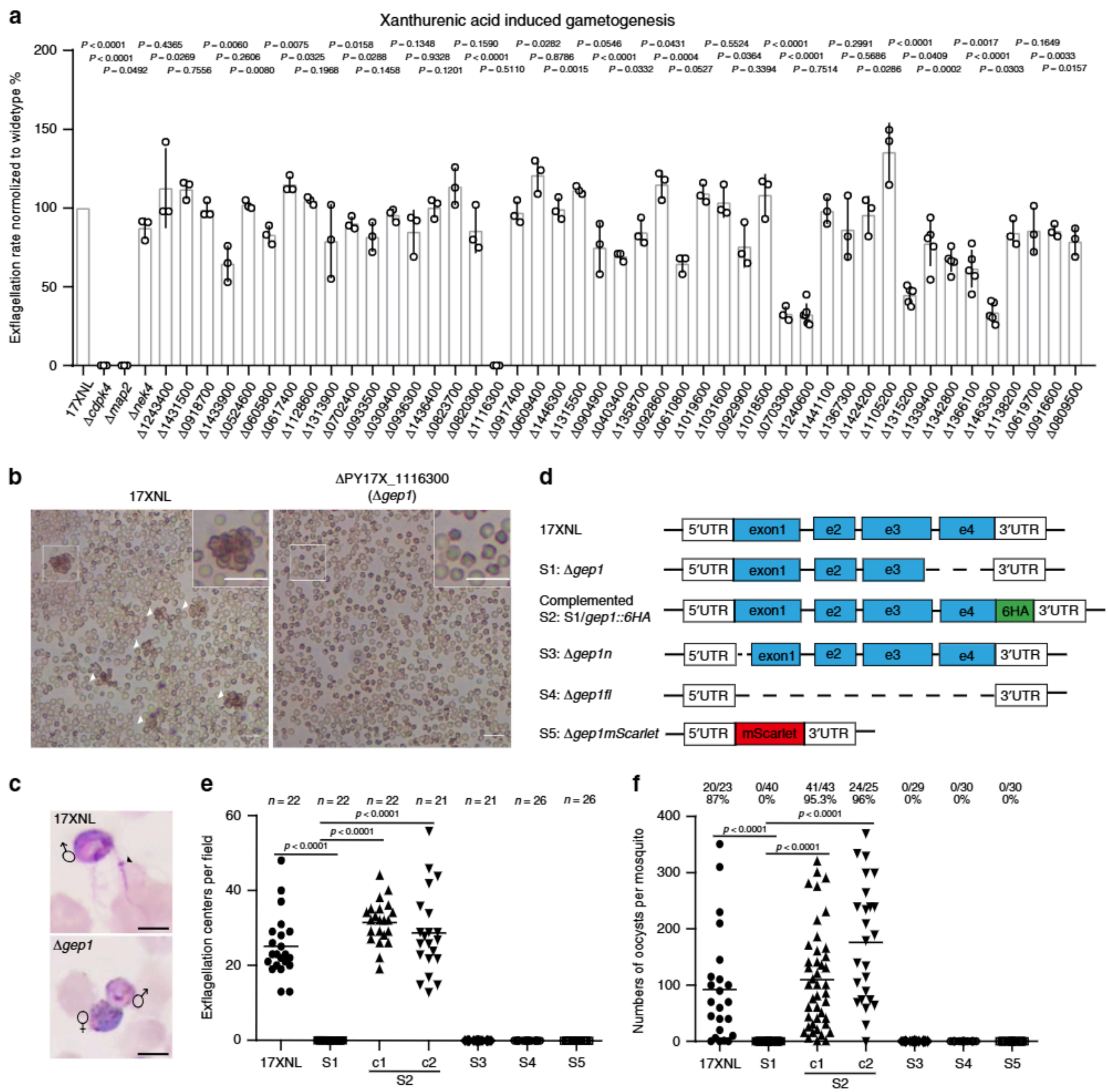

Fig. 1 Membrane proteins screening identified *gep1* essential for gametogenesis. **a** In vitro XA stimulated exflagellation rates for *P. yoelii* 17XNL wild type (WT) and 45 mutant strains each with a specific gene disruption. The exflagellation rate of each mutant was normalized with that of WT parallelly tested each time. The numbers for the gene name are the gene IDs derived in PlasmoDB. Data are shown as mean ± SD from $n = 3$ independent experiments for strains except $n = 5$ for *Δ1315200*, *Δ1339400*, *Δ1342800*, *Δ1366100* and *Δ1463300*, and $n = 6$ for *Δ1240600*. **b** Representative images of XA stimulated exflagellation centers (ECs, white arrows) under light microscope (10×). Scale bar = 20 µm. **c** Images of the exflagellated male gametes (Black arrow) after Giemsa staining under light microscope (100×). Scale bar = 5 µm. **d** Diagrams of WT *gep1* gene structure and various mutants: S1 (*Δgep1*), deletion in C-terminus; S2 (*Δgep1/gep1::6HA*), reconstructed *gep1* with a 6HA tag; S3 (*Δgep1n*), deletion in N-terminus; S4 (*Δgep1fl*), deletion of the full coding region; S5 (*Δgep1mScarlet*), coding region replaced with *mScarlet* gene. **e** XA-stimulated EC counts from WT and the *gep1* mutants. c1 and c2 are two clones of S2 parasite. *n* is the numbers of microscopic fields counted (40×). **f** Oocyst counts from WT and the *gep1* mutants. Oocysts are counted from the mosquito midguts 7 days post blood feeding. *x*/*y* on the top is the number of mosquito containing oocyst/the number of mosquito dissected; the percentage number is the mosquito infection prevalence. Experiments were independently repeated six times in **b**, and three times in **c**, **e**, and **f**. Two-tailed unpaired Student's *t* test was applied in **a**, **e**, and **f**. Source data of **a**, **e**, and **f** are provided as a Source Data file.

TMs (Fig. 2a). Previous transcriptomic study indicated the *gep1* gene is transcribed in gametocytes and ookinetes, but not asexual blood stages of *P. falciparum* and *P. berghei*[19,20]. To investigate protein expression and localization, we tagged the endogenous GEP1 with 6HA at N-terminus (Supplementary Fig. 1g, j), generating *6HA::gep1* parasite that had normal development throughout the life cycle (Supplementary Fig. 5a). The GEP1 protein is expressed in gametocytes and ookinetes, but not in asexual blood stages and other mosquito stages of the *6HA::gep1* parasite (Fig. 2b, c). We also tagged the GEP1 protein with quadruple Myc (4Myc) (Supplementary Fig. 1j, Supplementary Fig. 5b) and observed similar expression pattern in the *4Myc::gep1* parasite (Fig. 2d). In addition, mScarlet fluorescent signals driven by the endogenous *gep1* promoter were detected only in

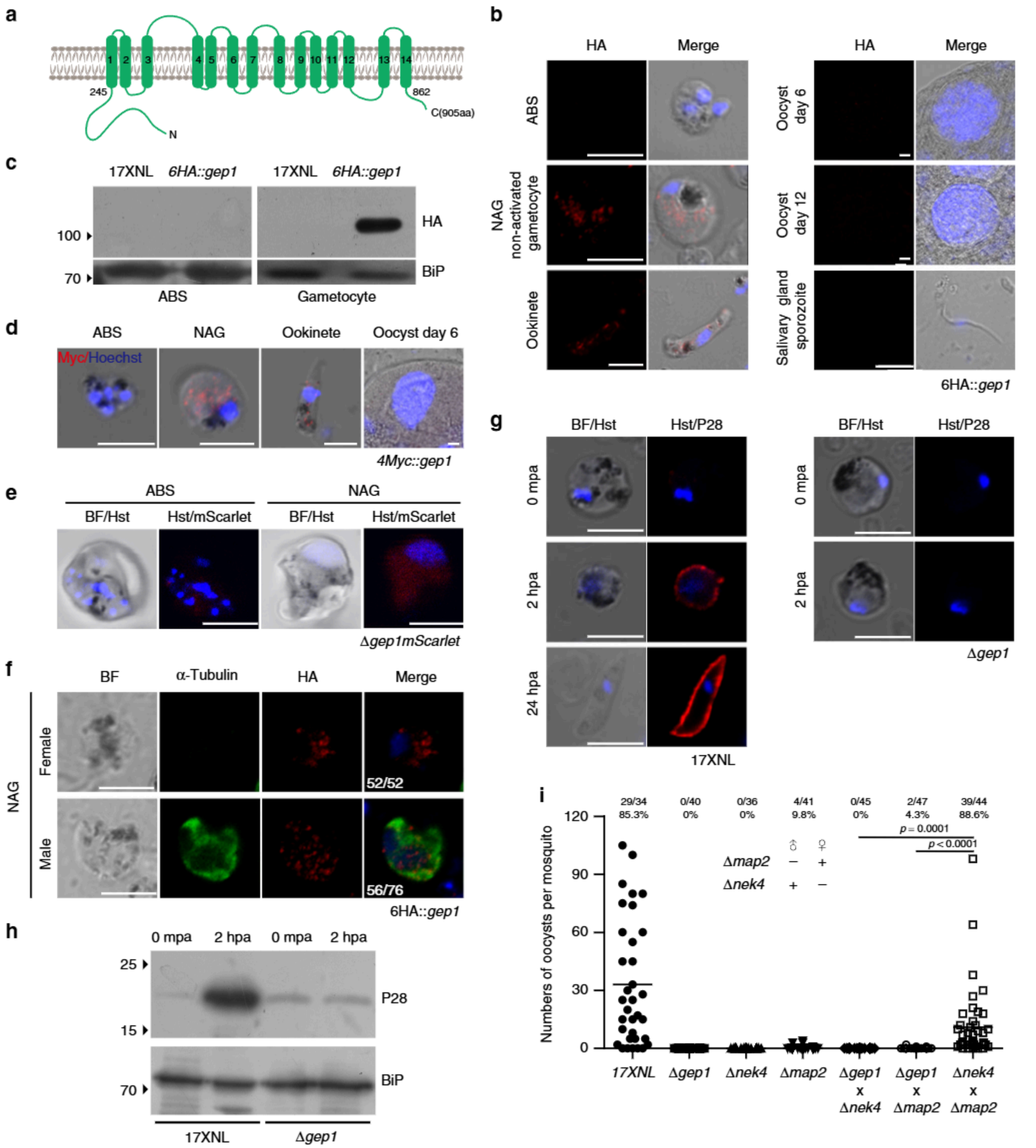

Fig. 2 GEP1 is essential for gametogenesis of both sexes. a Predicted GEP1 protein structure with 14 TM domains (green bar) and cytoplasmic N-termini and C-termini. **b** IFA analysis of GEP1 expression in asexual blood stages (ABS), gametocytes, ookinetes, oocysts, and sporozoites of the *6HA::gep1* parasite using anti-HA antibody. Hoechst 33342 (Blue) is used for nuclear acid stain for all images in this figure. **c** Western blot analysis of GEP1 in ABS and gametocytes of the *6HA::gep1* parasite. BiP as loading control. **d** IFA analysis of GEP1 in the *4Myc::gep1* parasite using anti-Myc antibody. **e** mScarlet fluorescence protein expression driven by the endogenous *gep1* promoter in ABS and gametocytes of the Δ*gep1mScarlet* parasite. **f** Co-staining of GEP1 and α-Tubulin (male gametocyte specific) in the non-activated (NAG) *6HA::gep1* gametocytes. *x/y* in the figure is the number of cell displaying signal/the number of cell tested. **g** and **h**, P28 expression during in vitro gametocyte to ookinete differentiation. P28 expression is detected in female gametes, fertilized zygotes, and ookinetes in IFA (**g**) and western blot (**h**). mpa: minute post activation; hpa, hour post activation. **i** Day 7 midgut oocyst counts from mosquitoes infected with parasites, including 17XNL, Δ*gep1*, Δ*nek4*, or Δ*map2* parasite alone, as well as mixtures of Δ*gep1*/Δ*nek4*, Δ*gep1*/Δ*map2*, or Δ*map2*/Δ*nek4* parasites. Δ*nek4* and Δ*map2* are female and male gamete-defect parasites, respectively. *x/y* on the top is the number of mosquito containing oocyst/the number of mosquito dissected; Mosquito infection prevalence is shown above. Scale bar = 5 μm for all images in this figure. Experiments were independently repeated three times in **b**, **c**, **d**, **e**, **f**, **g**, and two times in **i**. Two-tailed unpaired Student's *t* test in **i**.

gametocytes, but not in asexual blood stages of the Δ*gep1mScarlet* parasite (Fig. 2e). Co-staining *6HA::gep1* gametocytes with anti-α-Tubulin (male gametocyte specific) and anti-HA antibody showed that GEP1 was expressed in both male and female gametocytes (Fig. 2f). Interestingly, GEP1 is not expressed in plasma membrane, but in punctate dots in the cytoplasm of gametocytes and ookinetes (Fig. 2b, d, f).

GEP1 regulates both male and female gametogenesis. Because GEP1 is expressed in both male and female gametocytes, we asked whether GEP1 also regulates the gametogenesis of female gametocytes. P28 protein, a marker for female gamete[21], is expressed in female gametes, fertilized zygotes, and ookinetes of 17XNL parasite, but not in the Δ*gep1* parasite 2 h after XA-stimulation (Fig. 2g, h), indicating that GEP1 depletion also cause defect in female gametogenesis. We next performed genetic crosses between Δ*gep1* and Δ*map2* (male gamete-deficient) or Δ*nek4* (female gamete-deficient) parasites[22,23] (Supplementary Fig. 1j, k). No midgut oocyst was observed in mosquitoes from the Δ*gep1* × Δ*map2* or Δ*gep1* × Δ*nek4* cross day 7 post infection (pi), whereas the Δ*map2* × Δ*nek4* cross produced slightly fewer oocysts than the WT parasite (Fig. 2i), suggesting no functional male and female gametes in the Δ*gep1* parasite. Together, these results demonstrate that GEP1 is essential for both male and female gametogenesis.

The purified Δ*gep1* gametocytes had morphology indistinguishable from that of WT 17XNL parasite (Supplementary Fig. 6a); however, whether GEP1 depletion causes gametocyte death or affects the fitness of gametocytes remains to be determined. We analyzed cell viability by Trypan blue exclusion assay. No gametocyte of WT or Δ*gep1* parasites were stained by Trypan blue (Supplementary Fig. 6b). As a control, both gametocytes were stained after heating the parasites at 60 °C for 5 min. In addition, staining with propidium iodide (PI) also indicated that the Δ*gep1* gametocytes are viable (Supplementary Fig. 6c). To further confirm the observations, we disrupted the endogenous *gep1* in a *P. yoelii* reporter strain *DFsc7* that expressed GFP and mCherry in male and female gametocytes, respectively[24] (Supplementary Fig. 1j, Supplementary Fig. 6d, e). The expressions of fluorescent proteins in both male and female gametocytes were comparable with those of the parental parasite (Supplementary Fig. 6f, g). These results suggest that GEP1-depleted gametocytes are viable, but lost the ability to produce functional male and female gametes.

GEP1 depletion blocks PKG-mediated signaling. Upon stimulation, male gametocytes undergo tubulin polymerization into microtubules and three rounds of genome replication, resulting in release of eight flagellated gametes within 10–15 min[25]. The lack of exflagellation suggests defect in either axoneme assembly or egress from erythrocyte of the Δ*gep1* male gametes. Typical cytosolic distribution of α-Tubulin was observed in male gametocytes of WT, Δ*gep1*, and Δ*map2* parasites before XA stimulation (Fig. 3a). Assembled axonemes were formed and coiled around the nucleus of WT and Δ*map2* gametocytes 8 min post XA stimulation, but axoneme formation was not observed in the Δ*gep1* parasite (Fig. 3a). By 15 min, WT gametocytes released flagellated male gametes, but not Δ*map2* and Δ*gep1* gametocytes (Fig. 3a). Strikingly, α-Tubulin remained in cytosol of the Δ*gep1* male gametocytes (Fig. 3a). We also analyzed the genome replication in stimulated male gametocytes. Flow cytometry analysis of DNA content in Hoechst-stained gametocytes showed that fluorescence increased (from 8.4% to 28.5%) in WT, but not in the Δ*gep1* parasites (from 8.4% to 7.6%) after XA stimulation (Fig. 3b). As reported for *P. berghei*[13,22], no genome replication occurs in the Δ*cdpk4* parasite (Fig. 3b, Supplementary Fig. 1j, k). These results show no axoneme assembly or mitotic division in the stimulated Δ*gep1* male gametocytes.

Differentiation of male and female gametes result in sequential rupture of PVM and EM for escaping from erythrocytes[2,26]. TER119 is a plasma membrane protein of mouse erythrocytes[27,28], and anti-TER119 antibody showed no EM staining for stimulated WT male and female gametocytes (Fig. 3c). In contrast, intact EM was observed for the Δ*gep1* gametocytes 30 min post stimulation (Fig. 3c), indicating that GEP1 depletion affects EM lysis.

XA triggers a cytosolic Ca^{2+} mobilization event within 10–15 s post stimulation of gametocytes[13], which is essential for gametes formation and EM rupture[11,13]. We next examined XA-stimulated Ca^{2+} mobilization in the Δ*gep1* gametocytes using Fluo-8 probe as described[29–31]. Fluo-8 did not affect the gametogenesis since WT gametocytes pre-loaded with Fluo-8 could form XA-stimulated ECs (Supplementary Fig. 7a) and responded to A23187, a Ca^{2+} ionophore[13], in a dose-dependent manner using flow cytometry (Supplementary Fig. 7b). As expected, XA triggered a sharp increase in cytosolic Ca^{2+} signal in WT gametocytes, reaching maximal levels 10–15 s post stimulation, which resembled the observations in *P. berghei* using luminescence-based GFP::Aequorin sensor[13,15]. However, no Ca^{2+} response was detected in XA stimulated Δ*gep1* gametocytes (Fig. 3d). Ca^{2+} mobilization occurred in the Δ*map2* gametocytes as MAP2 functions downstream of Ca^{2+} signal[18,22] (Fig. 3d).

Different from Ca^{2+}-dependent EM rupture, PVM rupture is controlled by a Ca^{2+}-independent mechanism[2]. To study PVM lysis, a parasite line *sep1::4Myc* was generated by C-terminally tagging a PVM protein SEP1 with 4Myc[27,28] (Supplementary Fig. 1j). This parasite line developed normally throughout the life cycle (Supplementary Fig. 5e), indicating intact protein function of SEP1::4Myc. We next deleted the *gep1* gene in the *sep1::4Myc* parasite, generating *sep1::4Myc*/Δ*gep1* mutant (Supplementary Fig. 1j). IFA showed lysis of Sep1::4Myc-labeled PVM in the *sep1::4Myc* gametocytes (Fig. 3e), while intact PVM was maintained in the *sep1::4Myc*/Δ*gep1* gametocytes 8 min post XA stimulation (Fig. 3e), indicating no PVM lysis in stimulated Δ*gep1* gametocytes. Together, these results suggest that GEP1 functions upstream of PKG in XA-stimulated signaling cascade (Fig. 3f).

Impaired cGMP synthesis in GEP1 deficient parasite. Because cGMP is the direct upstream signal activating PKG in XA-stimulated gametogenesis[7,11,13,15], we examined intracellular cGMP synthesis during gametogenesis. Purified gametocytes were stimulated with XA for 2 min, and cGMP levels were measured using an enzyme immunoassay[7,32]. Strikingly, XA induced a significant increase in cGMP level in WT gametocytes (Fig. 4a), consistent with previous observation in *P. falciparum*[7]. In contrast, the Δ*gep1* gametocytes failed to increase cGMP in response to XA stimulation (Fig. 4a). As a control, cGMP response occurred in Δ*map2* gametocytes because MAP2 functions downstream of both cGMP and Ca^{2+} signaling[18,22]. These results indicate that GEP1 regulates cGMP level, the most upstream intracellular signal known in *Plasmodium* gametogenesis.

cGMP level is tightly regulated by the opposing actions of cGMP-synthesizing GC and cGMP-hydrolyzing phosphodiesterase (PDE)[10,11,33]. Inhibition of PDE activity by specific inhibitor Zaprinast (Zap) has been shown to trigger *P. falciparum* gametogenesis in the absence of XA[11,33]. Indeed, treatment of WT gametocytes with 100 μM Zap also induced EC counts comparable to those induced by 50 μM XA (Fig. 4b), and gametogenesis stimulated by either XA or Zap could be blocked

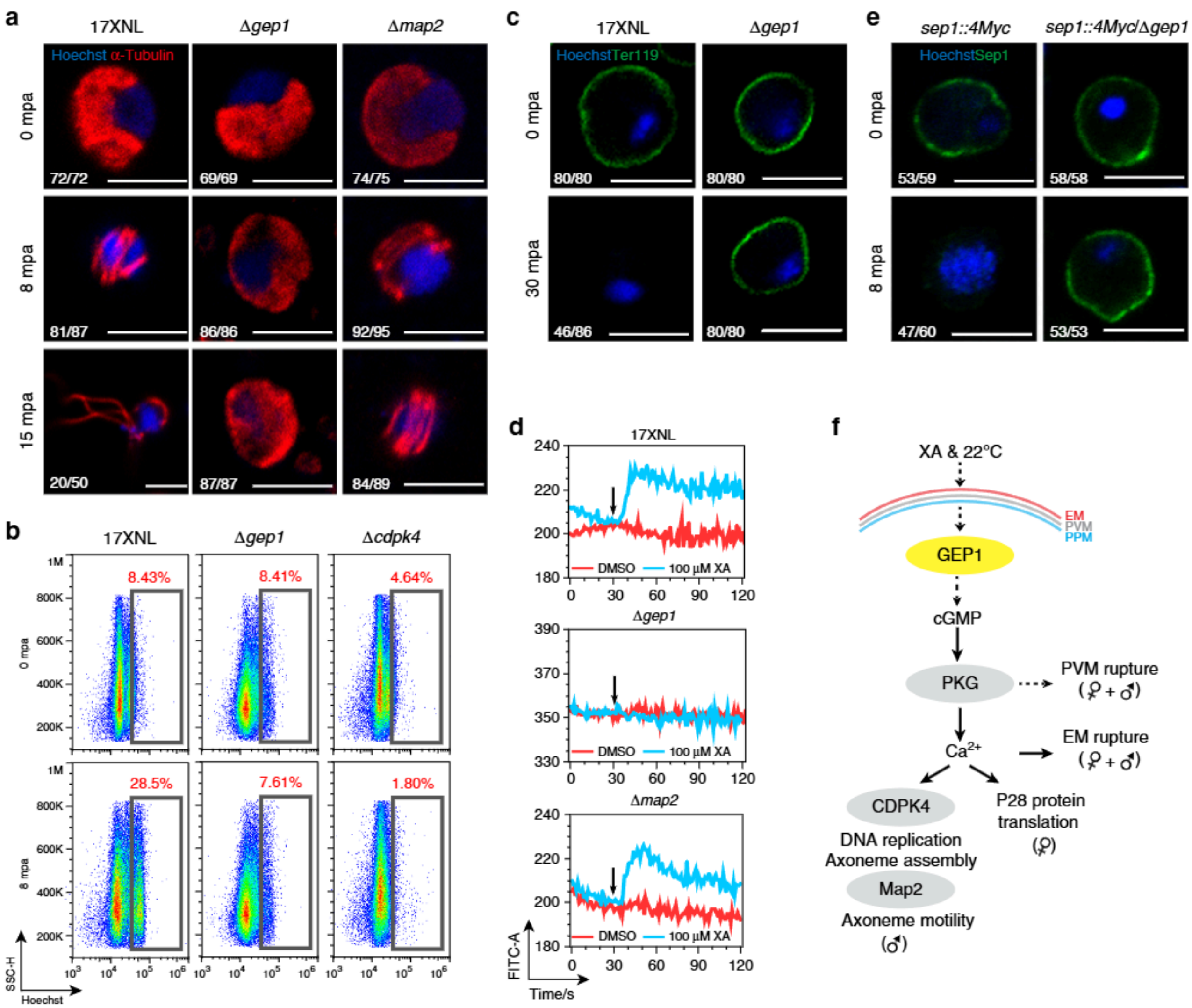

Fig. 3 GEP1 acts upstream of PKG in the cGMP-PKG-Ca^{2+} signaling cascade. a α-Tubulin expression and distribution in differentiating male gametocytes from 17XNL, Δ*gep1* and Δ*map2* parasites after XA stimulation. mpa: minute post XA activation. **b** Flow cytometry analysis of genomic DNA content in XA-stimulated male gametocytes of 17XNL, Δ*gep1* and Δ*cdpk4* parasites. The parasites were fixed with 4% paraformaldehyde at indicated time and stained with Hoechst. **c** Representative images of gametocytes stained by anti-mouse TER119 antibody 0 and 30 min post XA stimulation (mpa). **d** Flow cytometry detection of cytosolic Ca^{2+} in gametocytes using Fluo-8 probe. Purified gametocytes were preloaded with Fluo-8, and signals were collected 30 s before addition of XA or DSMO. Black arrows indicate the time for DMSO or XA addition. **e** Representative IFA images of the *sep1::4Myc* and *sep1::4Myc/*Δ*gep1* gametocytes stained by anti-Myc antibody. **f** Proposed location of GEP1 in the XA-PKG-Ca^{2+} signal cascade of gametogenesis. GEP1 depletion causes defect in both Ca^{2+}-dependent and Ca^{2+}-independent cellular events of gametogenesis. EM: erythrocyte membrane, PVM: parasitophorus vacuole membrane, PPM: parasite plasma membrane. *x*/*y* in **a**, **c**, and **e** are the number of cell displaying representative signal/the number of cell analyzed. Scale bar = 5 μm for all images in this figure. All experiments in this figure were repeated three times independently with similar results.

by a *Plasmodium* PKG protein inhibitor C2 (Fig. 4b), consistent with the established cGMP-PKG signal cascade of gametogenesis[14,15]. In contrast, the Δ*gep1* gametocytes failed to form ECs after treatment with Zap (Fig. 4b). No EC were observed in the control Δ*map2* gametocytes treated in either XA or Zap (Fig. 4b). Consistently, we examined the intracellular cGMP level in gametocytes treated with Zap for 2 min and detected significant increase in both WT and Δ*map2* gametocytes, but not in the Δ*gep1* gametocytes (Fig. 4c). Together, these results suggest that the GC activity for cGMP synthesis is impaired, and therefore no elevation of cGMP in the Δ*gep1* gametocytes after XA stimulation or Zap inhibition of PDE activity. In addition to XA and Zap, increasing pH from 7.4 to 8.0 has been reported to induce gametogenesis although the underlying mechanism is not clear[2,4]. Treating WT gametocytes with pH 8.0 at 22 °C indeed induced comparable number of ECs to those induced by XA or Zap (Fig. 4b), and gametogenesis could be blocked by C2 treatment (Fig. 4b)[15], indicating that the signaling stimulated by pH 8.0 is also cGMP/PKG-dependent. However, pH 8.0 treatment could not induce gametogenesis of the Δ*gep1* gametocytes, further suggesting impaired activity of cGMP synthesis in GEP1 deficient parasite (Fig. 4d).

GEP1 interacts and co-localizes with GCα. We next carried out immunoprecipitation and mass spectrometry experiments to identify molecules that may interact with GEP1 in gametocytes. By comparison of peptide signals (hits) between WT and *6HA::gep1* gametocyte samples from three biological replicates, we obtained 308 proteins that might interact with GEP1 (Supplementary Table 2), including GCα protein that is the enzyme

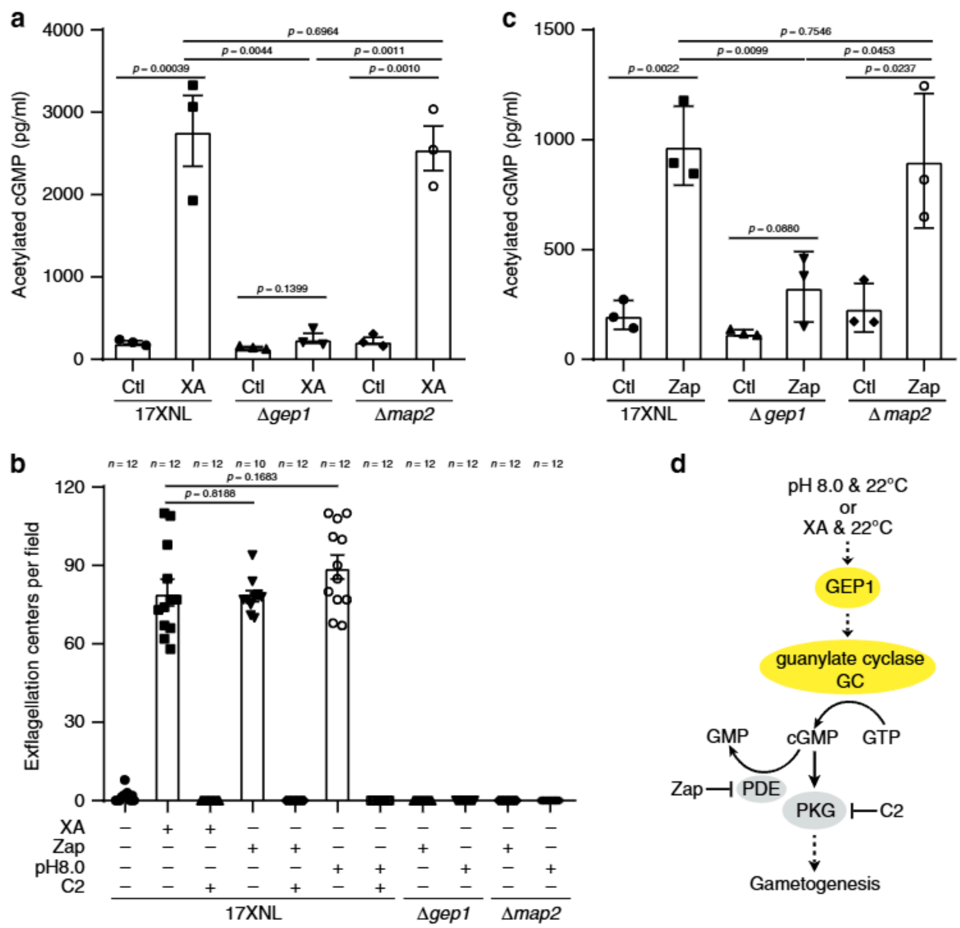

Fig. 4 Impaired activity of cGMP synthesis in GEP1 deficient gametocytes. **a** Enzyme immunoassay detecting intracellular cGMP level in XA-stimulated gametocytes of the 17XNL, Δ*gep1*, and Δ*map2* parasites. Cells were incubated with 100 µM XA at 22 °C for 2 min before assay. Ctl are control groups without XA stimulation. **b** Exflagellation center counts of 17XNL, Δ*gep1*, and Δ*map2* parasites after treatment with XA (100 µM), Zaprinast (Zap, 100 µM), or pH 8.0 alone at 22 °C, or at the presence of compound 2 (C2, 5 µM). *n* is the numbers of microscopic fields counted (40×). **c** Enzyme immunoassay detecting intracellular cGMP level in Zap-treated gametocytes of the 17XNL, Δ*gep1*, and Δ*map2* parasites. Cells were incubated with 100 µM Zap at 22 °C for 2 min before assay. Ctl are control groups without Zap stimulation. **d** Proposed role of GEP1 in regulating cGMP synthesis activity of guanylyl cyclase in gametogenesis. All source data are provided as a Source Data file. Experiments in **a**, **b**, and **c** were repeated three times independently. Data are shown as mean ± SD; two-tailed unpaired Student's *t* test.

presumably responsible for cGMP synthesis during gametogenesis (Fig. 5a, b)[8–10]. The *P. yoelii* GCα is a large protein (3850 amino acids) with 22 TMs distributed in an N-terminal P4-ATPase-like domain (ALD) and a C-terminal guanylate cyclase domain (GCD)[34,35]. To study the expression of GCα in gametocytes, we generated two parasite lines (*gcα::6HA* and *gcα::4Myc*) with endogenous GCα C-terminally tagged with 6HA and 4Myc, respectively (Supplementary Fig. 1j). These parasites developed normally in mouse and mosquito hosts (Supplementary Fig. 5c, d). Similar to GEP1, GCα was also expressed as cytoplasmic puncta in both male and female gametocytes of the *gcα::6HA* and *gcα::4Myc* parasites (Supplementary Fig. 8a). To further confirm the interaction between GEP1 and GCα, we generated a doubly tagged parasite line, *4Myc::gep1/gcα::6HA* (*DTS1*), by tagging the endogenous GEP1 with 4Myc in the *gcα::6HA* parasite (Supplementary Fig. 1j, Supplementary Fig. 5f–h). Results from immunoprecipitation using anti-Myc antibody indicated that GCα interacted with GEP1 in cell lysate of the *DTS1* gametocytes (Fig. 5c). We next generated another independent doubly tagged parasite, *6HA::gep1/gcα::4Myc* (*DTS2*) by tagging GCα with 4Myc in the *6HA::gep1* parasite (Supplementary Fig. 1j, Supplementary Fig. 5f–h) and detected similar interaction between GEP1 and GCα (Fig. 5d). As a control, no interaction between GEP1 and GCβ was detected in gametocytes of the *4Myc::gep1/gcβ::6HA* (*DTS3*) parasite (Supplementary Fig. 8b). These data demonstrate that GEP1 interacts with GCα in gametocytes. In addition, IFA results from the *DTS1* parasite showed that GEP1 and GCα are co-localized at cytosolic puncta in non-activated gametocytes (Fig. 5e, f). Together, these data suggest that GEP1 co-localizes and binds to GCα in gametocytes.

GCα depletion causes defect in XA-stimulated gametogenesis. GCα has been implicated in cGMP synthesis during gametogenesis[8–10]; however, there has been no direct evidence to support the speculation. We attempted to disrupt the *gcα* gene but failed to obtain a GCα mutant parasite, indicating an essential function in asexual blood stage development, as reported in *P. falciparum* and *P. berghei* previously[10]. We used a promoter swap method described previously[36] to replace 1322 bp of endogenous *gcα* promoter region with that (1626 bp) of *sera1* gene (PY17X_0305700) (Fig. 6a, Supplementary Fig. 1h), whose transcripts are expressed in asexual stages, but absent in gametocytes and mosquito stages[37]. In this editing, a 6HA tag was inserted in frame at the N-terminus of the GCα coding sequence. Correct modification in two parasite clones of the resulting mutant

a

Top 10 GEP1 interacting proteins detected via IP-Mass spectrum

Gene_ID	Unique peptide	Description
PY17X_1347900	21	Conserved plasmodium protein, unknown function
PY17X_1226000	19	Tyrosine--tRNA ligase, putative
PY17X_0911700	15	Guanylyl cyclase alpha
PY17X_1109100	15	Conserved protein, unknown function
PY17X_0404000	13	HAD superfamily protein, putative
PY17X_1114400	10	Deoxyribodipyrimidine photo-lyase, putative
PY17X_0807500	10	Conserved plasmodium protein, unknown function
PY17X_0922400	9	Conserved plasmodium protein, unknown function
PY17X_0706700	9	Conserved plasmodium protein, unknown function
PY17X_1221300	9	Oocyst capsule protein cap380, putative

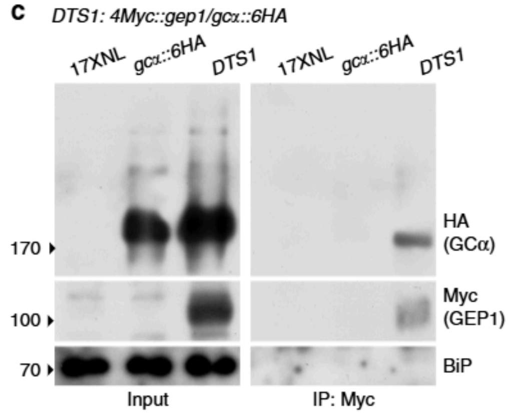

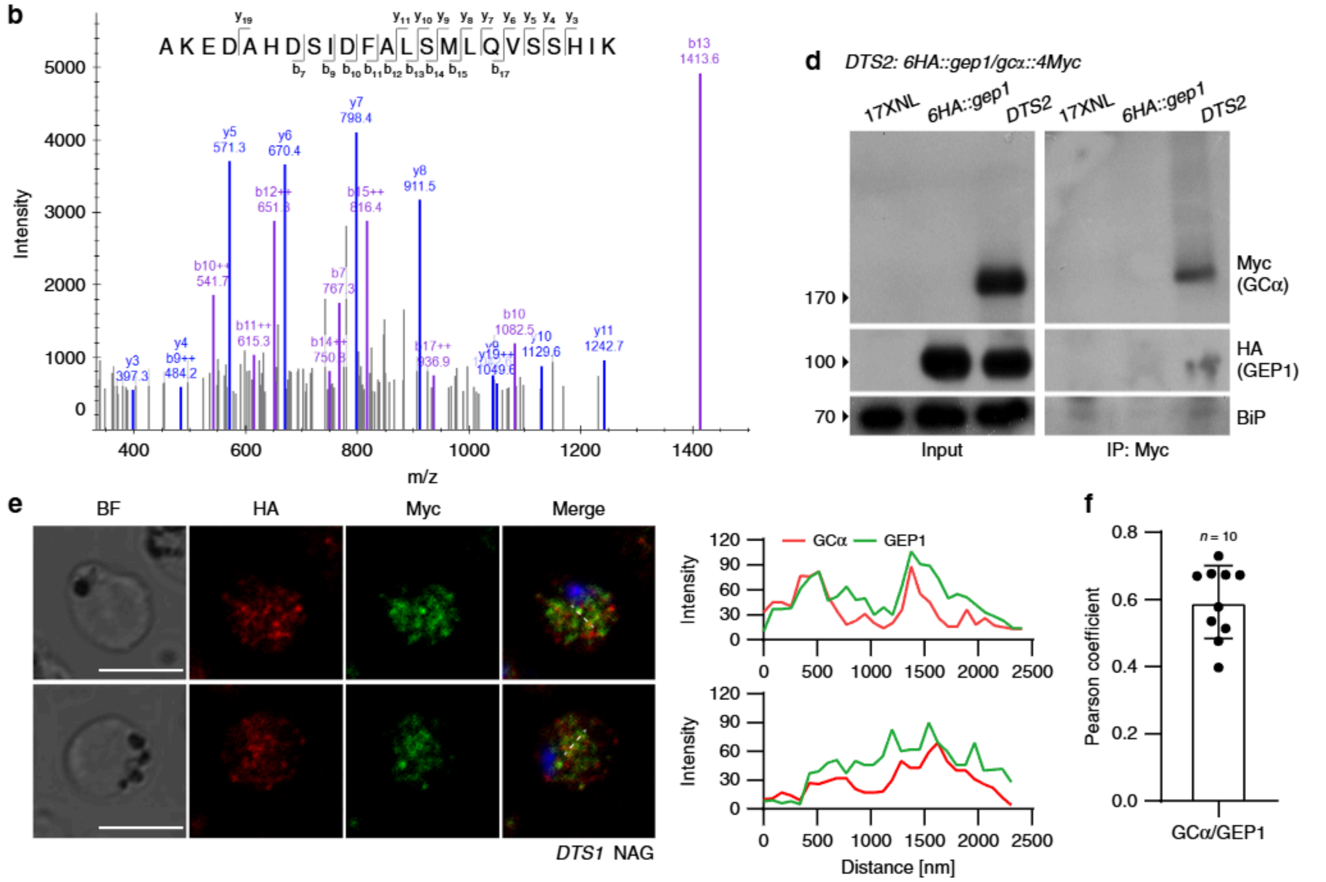

Fig. 5 GEP1 interacts with GCα in gametocytes. a Top 10 GEP1 interacting proteins in the gametocytes of the *6HA::gep1* parasite detected by immunoprecipitation and mass spectrometry (MS), including guanylyl cyclase α (GCα) with 15 peptides detected. **b** MS2 spectrum of a representative peptide of the GCα protein. **c** Co-immunoprecipitation of Myc::GEP1 and GCα::HA proteins in gametocytes of the double tagged parasite *4Myc::gep1/gcα::6HA* (*DTS1*). IP-Myc, anti-Myc antibody was used. **d** Co-immunoprecipitation of HA::GEP1 and GCα::Myc proteins in gametocytes of the double tagged parasite *6HA::gep1/gcα:: 4Myc* (*DTS2*). IP-Myc, anti-Myc antibody was used. **e** Two-colored IFA of GEP1 and GCα proteins in the *DTS1* gametocytes using anti-HA (GCα) and anti-Myc (GEP1) antibodies (left panel). Cross sections (white dash line) of the cells show the co-localization of GEP1 and GCα (right panel). Scale bar = 5 μm. **f** Pearson coefficient analysis for GEP1 and GCα co-localization shown in **e**, data are shown as mean ± SD from $n = 10$ cells measured. Experiments in **c**, **d**, and **e** were repeated three times independently with similar results.

parasite *gcαkd* was confirmed by PCR (Supplementary Fig. 1j). The promoter replacement allowed expression of the GCα protein in asexual blood stages at a level comparable with that of another parallelly modified parasite *6HA::gcα* (Supplementary Fig. 1j), but significantly reduced GCα protein expression in gametocytes (Fig. 6b, c). Notably, the *gcαkd* parasite completely lost the ability to synthesize cGMP and form ECs after XA stimulation in vitro (Fig. 6d, e). In mosquitos fed with *gcαkd* parasite-infected mouse blood, no oocyst was detected in mosquito midgut (Fig. 6f). These results support that GCα is the GC responsible for XA-stimulated cGMP synthesis in gametogenesis (Fig. 6g). In addition, the phenotype caused by GCα knockdown in gametocytes resembles that of GEP1 defect.

Compared to the expression of GCα in both male and female gametocytes, GCβ expression was detected in *gcβ::6HA* female gametocytes only[8] (Supplementary Fig. 8a, lower panel). In

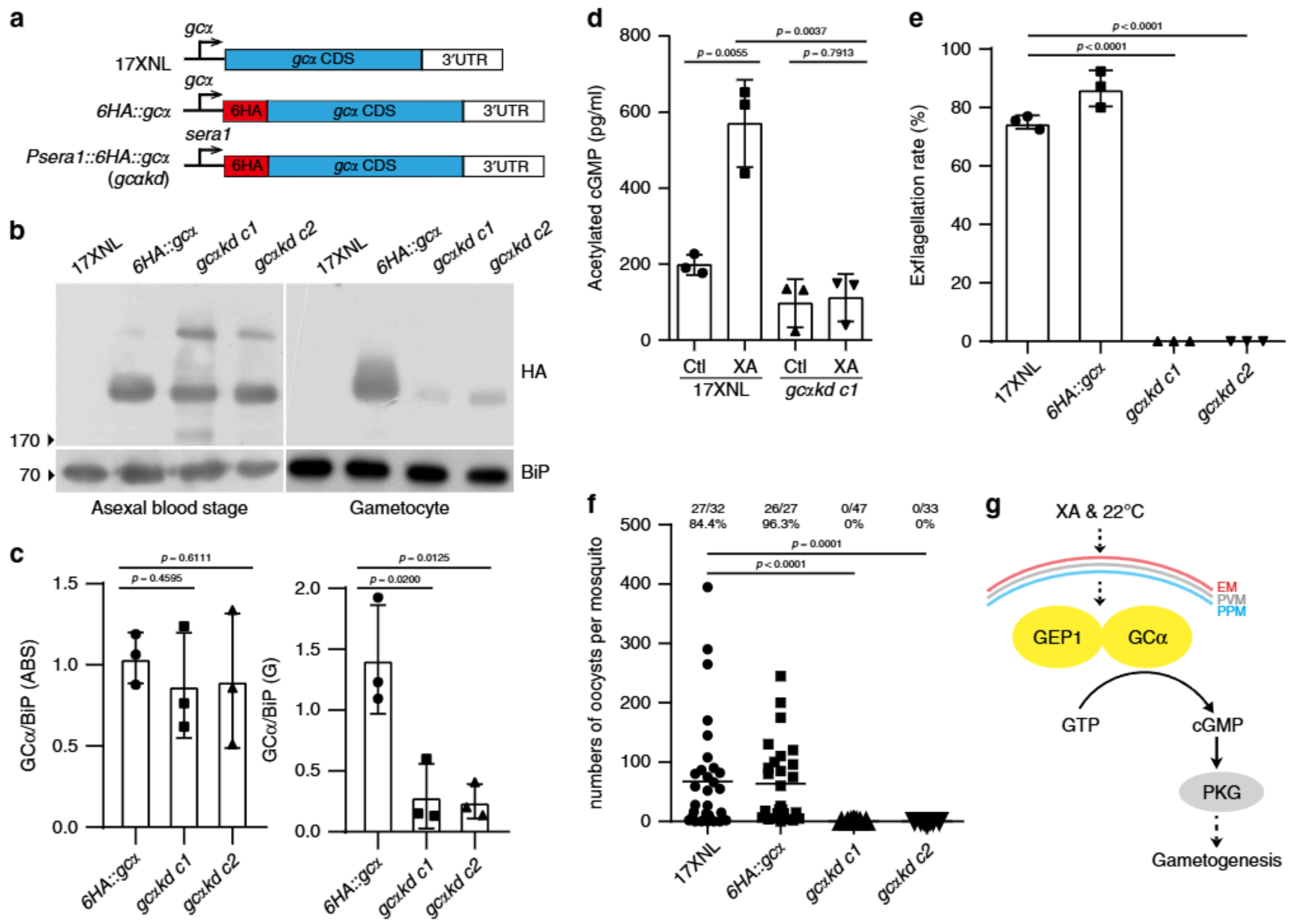

Fig. 6 GCα knockdown in gametocytes results in gametogenesis defect. a Diagram showing a promoter swap strategy to knockdown *gcα* expression in gametocytes, generating HA-tagged *gcαkd* mutant with endogenous *gcα* promoter replaced with the *sera1* promoter. **b** Western blotting of GCα expression in asexual blood stages and gametocytes of the *gcαkd* parasite. The *6HA::gcα* as a control. **c** Quantitative analysis of GCα protein expression in **b**. **d** Intracellular cGMP level in XA-stimulated gametocytes of the 17XNL and *gcαkd* parasites. Cells were incubated with 100 μM XA at 22 °C for 2 min before assay. Ctl are control groups without XA stimulation. **e** In vitro exflagellation rates for 17XNL, *6HA::gcα*, and two clones of the *gcαkd* parasite after XA stimulation. **f** Day 7 midgut oocyst counts in mosquitos infected with 17XNL, *6HA::gcα*, and two clones of the *gcαkd* parasites. Mosquito infection prevalence is shown above. **g** A proposed model of GEP1/GCα interaction essential for XA-stimulated cGMP synthesis and gametogenesis. Experiments were independently repeated three times in **b**, **d**, **e**, and **f**. Data are shown as mean ± SD in **c**, **d**, and **e**. Two-tailed unpaired Student's *t* test in **c**, **d**, **e**, and **f**. Source data of **c**, **d**, **e**, and **f** are provided as a Source Data file.

addition, GCβ depletion had no effect on XA-stimulated elevation of cGMP (Supplementary Fig. 8c) and in vitro EC formation (Supplementary Fig. 8d) in gametocytes of the Δ*gcβ* parasite[8], in agreement with previous reports in *P. falciparum* and *P. berghei*[9,33]. These results exclude the involvement of GCβ in XA-stimulated cGMP signaling and gametogenesis.

GEP1 depletion has no effect on GCα expression and localization. As GCα and GEP1 interacted with each other and functioned upstream of cGMP signaling, we investigated whether GEP1 depletion would affect the expression and cellular localization of GCα in gametocytes. We deleted *gep1* gene in the *gcα::6HA* parasite, generating a *gcα::6HA/Δgep1* mutant parasite (Supplementary Fig. 1j, Supplementary Fig. 5i, j). GEP1 depletion had no effect on *gcα* mRNA level or GCα protein abundance in gametocytes of the *gcα::6HA/Δgep1* parasite compared to the parental parasite (Fig. 7a, b). As a control, depletion of CDPK4 had no effect on both mRNA and protein level of GCα either because CDPK4 functions downstream of cGMP signal (Fig. 7a, b). In addition, XA stimulation had no effect on protein abundance of both GEP1 and GCα in gametocytes of the *DTS1* parasite (Fig. 7c).

Next, we investigated the effect of XA stimulation in cellular localization of GEP1 and GCα proteins in gametocytes of the *6HA::gep1* or *gcα::6HA* parasite, respectively. Two minutes post XA stimulation, both GEP1 and GCα were expressed as cytoplasmic puncta in activated female gametocytes (Fig. 7d, e). Even 8 min post XA stimulation, both GEP1 and GCα still maintained in cytoplasmic puncta in activated female gametocytes (Supplementary Fig. 9a, b). Strikingly, both proteins were redistributed from cytoplasm to the cell periphery of activated male gametocytes 2 min post XA stimulation (Fig. 7d, e). We further investigated the localization of both GEP1 and GCα in activated gametocytes of the *DTS1* parasite. Two color IFA results indicate that GEP1 and GCα were co-localized in cytoplasm of activated female gametocytes but in cell periphery of activated male gametocytes 2 min post XA stimulation (Supplementary Fig. 9c, d), repeating the results from single color IFA. In activated male gametocytes, eight axonemes are assembled in the cytoplasm and coiled around the enlarged nucleus containing octaploid genome, likely pushing the cytosolic puncta to cell periphery. However, no redistribution of GCα was detected from cytoplasm to cell periphery in the stimulated *gcα::6HA/Δgep1* male gametocytes (Fig. 7e), which could be explained by no

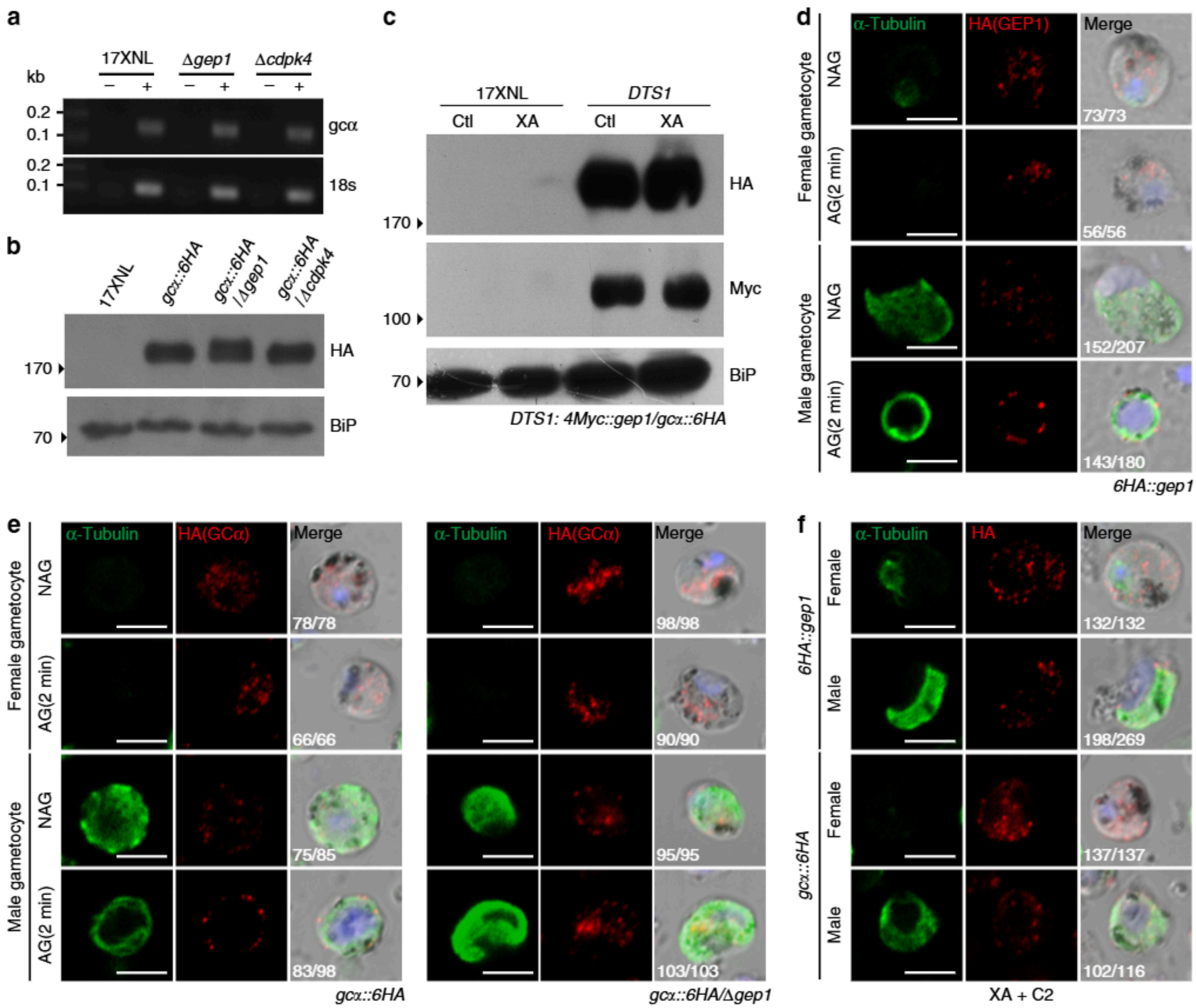

Fig. 7 GCα expression and localization in the GEP1-depleted gametocytes. a RT-PCR analysis of *gcα* transcript in gametocytes of the 17XNL, Δ*gep1*, and Δ*cdpk4* parasites. **b** Western blotting detecting GCα protein in gametocytes of the 17XNL, *gcα::6HA*, *gcα::6HA/*Δ*gep1*, and *gcα::6HA/*Δ*cdpk4* parasites. **c** Western blotting detecting GEP1 (Myc) and GCα (HA) proteins expression in gametocytes of *DTS1* parasite 2 min post XA stimulation. Ctl are control groups without XA stimulation. **d** Co-staining of GEP1 and α-Tubulin expressions in gametocytes of the *6HA::gep1* parasite 2 min post XA stimulation. NAG: non-activated, AG: XA stimulation. **e** Co-staining of GCα and α-Tubulin expressions in the *gcα::6HA* and *6HA::gcα/*Δ*gep1* gametocytes 2 min post XA stimulation. NAG: non-activated, AG: XA stimulation. **f** Co-staining of α-Tubulin and HA-tagged GEP1 or GCα expressions in the *6HA::gep1* (upper panel) and *gcα::6HA* (lower panel) gametocytes 2 min post XA stimulation plus C2 treatment. *x/y* in **d**, **e**, and **f** are the number of cell displaying representative signal/the number of cell analyzed. Scale bar = 5 μm for all images in this figure. All experiments in this figure were repeated three times independently.

initiation of gametogenesis caused by GEP1 depletion. To further confirm the observations above, we treated the gametocytes with PKG inhibitor C2 to block the initiation of XA-stimulated gametogenesis. Indeed, no redistribution of either GEP1 or GCα was observed from cytoplasm to the cell periphery in the stimulated male gametocytes of the *6HA::gep1* and *gcα::6HA* parasite respectively (Fig. 7f). Together, these results indicate that GEP1 does not regulate the expression level and localization of GCα in non-activated male and female gametocytes, but affects the localizations of GCα in XA activated male gametocytes.

XA stimulation likely enhances the GEP1/GCα interaction. Lastly we asked whether XA stimulation could enhance the interaction between GEP1 and GCα in gametocytes. Proximity Ligation Assay (PLA) is a homogeneous immunohistochemical tool that couples the specificity of ELISA with the sensitivity of PCR, which allows in situ detection of endogenous proteins interaction with high specificity and sensitivity[38,39]. We performed the PLA to investigate the protein interaction in both non-activated gametocytes and activated gametocytes 2 min post XA stimulation. Robust PLA signals were detected in cytoplasm of the non-activated gametocytes of *DTS1* parasite when both anti-Myc and anti-HA primary antibodies were present (Fig. 8a), indicative of GEP1 and GCα interaction. As a control, no PLA signal was detected in gametocytes of the single tagged *gcα::6HA* parasite. 2 min post XA stimulation, the PLA signals were detected in cytoplasm of activated female gametocytes but in cell periphery of activated male gametocytes (Fig. 8a), which is consistent with the protein localization in IFA analysis (Fig. 7d, e, Supplementary Fig. 9c). Quantifying the number of PLA signal dots in each cells of gametocytes showed no difference between non-activated and activated gametocytes (Fig. 8b). However, the fluorescence intensity of PLA signal in the XA-activated

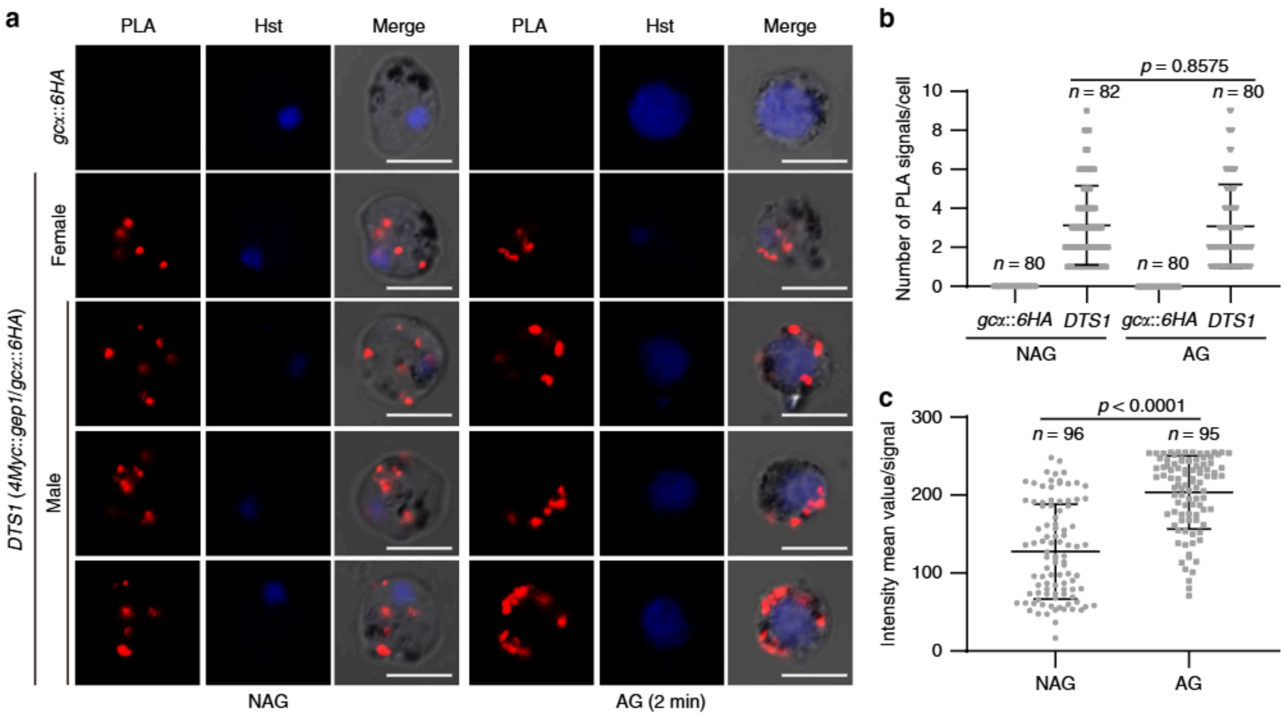

Fig. 8 XA stimulation likely enhances the interaction between GEP1 and GCα. a Proximity Ligation Assay (PLA) detecting protein interaction between GEP1 and GCα in *DTS1* gametocytes. NAG: non-activated, AG: 2 min after XA stimulation. Activated male gametocytes were observed with enlarged nucleus containing replicated genome. Scale bar = 5 µm. **b** Number of PLA signal dot in each cell shown in **a**, *n* is the number of cells counted. **c** Fluorescence intensity value for each PLA signal dot shown in **a**. *n* is the number of PLA signal dot measured. Source data are provided as a Source Data file. Experiment was repeated three times independently. Data are shown as mean ± SD; two-tailed unpaired Student's *t* test.

gametocytes is significantly higher than that of the non-activated gametocytes (Fig. 8c), suggesting possible enhanced interaction between GEP1 and GCα in gametocytes after XA stimulation. We performed the PLA experiment in another independent doubly tagged parasite *DTS2* and observed the same results (Supplementary Fig. 10a–c).

Discussion

It has been well-established that the XA-cGMP-PKG-Ca^{2+} signaling drives gametogenesis of *Plasmodium* parasites[7,11,13] since the discovery of mosquito-derived XA as an inducer for gametogenesis more than two decades ago[5,6]. However, how the parasite senses external stimuli such as XA and reduction in environmental temperature to activate the cGMP signaling pathway remains unknown. In this study, we identified a membrane protein (GEP1) that responds to XA stimulation and binds to GCα, leading to activation of cGMP-PKG-Ca^{2+} signaling pathway and gametogenesis after functional screening 59 genes encoding integral membrane proteins expressed in gametocytes. Using CRISPR/Cas9 method, we successfully obtained gene deletion mutant parasites for 45 out of 59 candidate genes. To the best of our knowledge, our study is the first CRISPR/Cas9-based gene functional screening performed in malaria parasites, and the results from our CRISPR/Cas9-based screen largely matched the outcomes of a recent gene disruption screening using conventional homologous recombination in *P. berghei*[40]. Of the 45 genes, 25 orthologs of *P. berghei* were shown to be dispensable for asexual blood stage proliferation, 8 orthologs were resistant for disruption, and 12 orthologs were not tested in the screening of *P. berghei* (Supplementary Table 1)[40]. For the 14 disruption-resistant genes in our hands, all of the *P. berghei* orthologs also failed deletion attempts[40].

After establishing the causative relationship of GEP1 deletion and gametogenesis defect, we investigated the position where GEP1 exerts its function in the XA-stimulated signaling cascade during gametogenesis. Previous studies have shown that cGMP enhances exflagellation of *P. berghei* and *P. falciparum*[41,42]. In addition, XA was shown to increase cGMP synthesis by GC from isolated membrane preparations of *P. falciparum* gametocytes[7], suggesting that XA-stimulated gametogenesis is mediated by elevated GC activity and cGMP synthesis. Consistent with these observations, we detected significant increases in cytosolic cGMP level in WT gametocytes 2 min after XA stimulation, but not in Δ*gep1* gametocytes. GEP1 depletion resulted in impaired cGMP production in response to XA, indicating that GEP1 locates upstream of cGMP in the XA-cGMP-PKG-Ca^{2+} cascade. Compared with the 10–15 min required for whole process of gametogenesis, XA rapidly triggers a cytosolic Ca^{2+} mobilization within 10–15 s post stimulation, which was also observed in other studies[13]. These results suggest that GEP1 functions at an early or initiating step of gametogenesis. Consistently, disruption of *gep1* causes defects in all PKG-downstream cellular and signaling events during gametogenesis, including Tubulin polymerization for axoneme assembly, genome replication in male gametocytes, release of P28 translational repression in female gametocytes, PVM and EM rupture for egressing of both male and female gametes from erythrocytes, and Ca^{2+} mobilization. These results suggest that GEP1 functions upstream of cGMP-PKG-Ca^{2+} cascade in XA-stimulated gametogenesis.

The cytosolic cGMP level is balanced by the activities of cGMP-synthesizing GC and cGMP-hydrolyzing PDE[10,11,33]. That inhibition of PDE activity by inhibitor Zap could trigger gametogenesis in the absence of XA suggests the existence of low and sub-threshold endogenous cGMP level precluding PKG activation in gametocytes[11,33]. Strikingly, the Δ*gep1* gametocytes not only failed to initiate XA-stimulated gametogenesis, but also could not undergo Zap-induced gametogenesis. Consistently, we detected no significant Zap-induced elevation of cytosolic cGMP level in the Δ*gep1* gametocytes as seen in WT gametocytes. These results suggest that GEP1 is an essential component of the GC synthesis machinery, and its depletion completely impairs parasite ability to synthesize cGMP, resulting in no accumulation of basal level cGMP in gametocytes.

Two large guanylyl cyclases (GCα and GCβ) for cGMP synthesis are found in *Plasmodium* parasites[34]. GCα and GCβ in *P. yoelii* consist of 3850 and 3015 amino acids, respectively, and both proteins are predicted to have 22 TMs distributed in an N-terminal P4-ATPase-like domain (ALD) and a C-terminal guanylate cyclase domain (GCD). GC enzymes possessing the ALD/GCD structure are observed in many protozoan species[34,43]. Whereas the GCD is responsible for cGMP synthesis, the function of the ALD is still obscure. Both *P. berghei* and *P. falciparum* parasites without GCβ can produce functional male gametes[9,10]. Consistent with these reports, our study also showed deletion of *gcβ* did not affect XA-stimulated cGMP elevation and male gamete formation, confirming that GCβ is not the enzyme for cGMP synthesis during gametogenesis. Using unbiased immunoprecipitation and mass spectrometry analysis, we found that GEP1 interacted with GCα and this interaction was confirmed by co-immunoprecipitation and co-localization analyses. Furthermore, we attempted to disrupt the *gcα* gene, but were not able to obtain a viable mutant parasite, consistent with previous reports in other *Plasmodium* species[10]. Alternatively, we generated a mutant parasite with decreased GCα expression in gametocytes. Specific knockdown of GCα in gametocytes blocked XA-stimulated cGMP elevation and the consequent gametogenesis, mimicking the defect of GEP1 disruption. These results indicate that GCα is the enzyme for cGMP synthesis in gametogenesis.

Interestingly, GEP1 and GCα proteins were expressed as cytoplasmic puncta in female gametocytes either before or after XA stimulation. In the contrast, both proteins were redistributed from cytoplasm to the cell periphery of male gametocytes post XA stimulation. Once gametogenesis is initiated after XA stimulation, eight axonemes are assembled and coiled around the enlarged nucleus containing octaploid genome[18,22], possibly occupying most cytoplasmic space and pushing cytoplasmic vesicles, including the GEP1/GCα residing puncta or possible membrane vesicle, to the periphery of the stimulated male gametocytes. Consistent with our observations, Carucci et al. also revealed that GCα displayed a peripheral localization in the *P. falciparum* stimulated gametocytes using immunoelectron microscopy[34]. In addition, these results also suggest that GEP1 likely exerts its function in controlling cGMP synthesis by directly binding GCα and regulating GCα conformation because GEP1 depletion had no effect in the expression and cellular localization of GCα in gametocytes.

GEP1 possesses 14 predicted TM domains, encoding a possible sodium-neurotransmitter symporter or amino acid transporter family protein. Three independent studies recently revealed that the *Toxoplasma gondii*, another Apicomplexan parasite, regulates natural egress of tachyzoites from host cell via a guanylate cyclase receptor platform[44–46]. Similar to *Plasmodium* GCα and GCβ, *T. gondii* guanylate cyclase (TgGC) also possesses the atypical ALD/GCD structure. By crosslinking experiment coupled to immunoprecipitation and mass spectrometry, 55 TgGC-interacting proteins were identified[44], including a top 5th hit (TGGT1_208420) encoding a putative sodium-neurotransmitter symporter family protein. Notably, TGGT1_208420 displays some similarity in protein sequence with GEP1. These results suggest the interaction between GC and sodium-neurotransmitter symporter family protein is conserved in *Plasmodium* and *T. gondii*. Similar to *P. yoelii* GEP1, depletion of this protein does not cause tachyzoite growth defect[44], suggesting a dispensable role in asexual lytic cycle of *T. gondii* although its function in sexual cycle is unknown. In addition, these studies also identified another *T. gondii* GC-interacting protein UGO that is believed to act as a chaperone[44]. Whether the *Plasmodium* UGO ortholog protein (PY17X_1204500) plays a similar role in the GC machinery remains to be determined.

Based on our results, we proposed a model for GEP1/GCα mediated cGMP signaling in XA-stimulated gametogenesis. The membrane protein GEP1 acts as a binding partner of GCα. In the absence of XA, GEP1 supports a functional conformation of GCα that maintains its basal catalytic activity and synthesizes low and sub-threshold endogenous cGMP level precluding PKG activation. In the presence of XA, the stimulation enhances the interaction of GEP1/GCα, leading to enhanced GC activity of GCα and increased cGMP level for PKG activation. In the GEP1-deficient gametocytes, GCα loses catalytic activity of cGMP synthesis and therefore fails to elevate cGMP level in response to XA, Zap treatment, or environmental pH. Currently, we could not exclude the possibility that there is an unknown molecule as the XA sensor residing in cytoplasm or plasma membrane and functioning upstream of GEP1/GCα complex. XA-stimulated gametocyte to gamete differentiation in the midgut is the first and essential step for mosquito transmission of malaria parasites, and elucidating the mechanisms involved may facilitate development of measures to block disease transmission.

Methods

Animal usage and ethics statement. Animal experiments were performed in accordance with the approved protocols (XMULAC20140004) by the Committee for Care and Use of Laboratory Animals of Xiamen University. ICR mice (female, 5 to 6 weeks old) were purchased and housed in the Animal Care Center of Xiamen University and kept at room temperature under a 12 h light/dark cycle at a constant relative humidity of 45%.

Mosquito maintenance. The *Anopheles stephensi* mosquito (strain Hor) was reared at 28 °C, 80% relative humidity and at a 12 h light/dark cycle. Mosquitoes were fed on a 10% sucrose solution.

Plasmid construction and parasite transfection. CRISPR/Cas9 plasmid pYCm was used for all the genetic modifications. For gene deleting, 5'-genomic and 3'-genomic segments (400 to 700 bp) of the target genes were amplified as left and right homologous arms, respectively, using gene specific primers (Supplementary Table 3). The PCR products were digested with appropriate restriction enzymes, and the digested products were inserted into matched restriction sites of pYCm. Oligonucleotides for sgRNAs were annealed and ligated into pYCm[17]. For each deletion modification, two sgRNAs were designed to disrupt the coding region of a target gene (Supplementary Table 3) using the online program ZiFit[47]. For gene tagging, a 400 to 800 bp segment from N-terminal or C-terminal of the coding region and 400 to 800 bp sequences from 5'UTR or 3'UTR of a target gene were amplified and fused with a DNA fragment encoding 6HA or 4Myc in frame at N-terminal or C-terminal of the gene. For each tagging modification, two sgRNAs were designed to target sites close to the C-terminal or N-terminal of the gene coding region. Infected red blood cells (iRBC) were electroporated with 5 μg circular plasmid DNA using Lonza Nucleofector. Transfected parasites were immediately injected *i.v.* into a naive mouse and treated with pyrimethamine (6 μg/ml) in drinking water. Parasites with transfected plasmids usually appear 5 to 7 days post drug selection.

Genotype analysis of transgenic parasites. All transgenic parasites were generated from *P. yoelii* 17XNL strain or *P. berghei* ANKA strain. The schematic for different genetic modifications and the results of parasite transfection, single cloning and genetic verification of modified strains are summarized in Supplementary Fig. 1. Blood samples from infected mice were collected from the orbital sinus, and blood cells were lysed using 1% saponin in PBS. Parasite genomic DNAs were isolated from blood stage parasites using DNeasy Blood kits (QIAGEN). For each parasite, both 5' and 3' homologous recombination events were detected using specific PCR primers (Supplementary Fig. 1). PCR products from some modified parasites were DNA sequenced. All the primers used in this study are listed in Supplementary Table 3. Parasite clones with targeted modifications were obtained after limiting dilution. At least two clones for each gene-modified parasite were used for phenotype analysis. Parasite growth characteristics in mouse and in mosquito for the modified parasite strains are shown in Supplementary Fig. 5.

Negative selection with 5-fluorouracil. Parasites subjected to sequential modifications were negatively selected with 5-Fluorouracil (5FC, Sigma, F6627) to remove episomal plasmid. 5FC (2 mg/ml) in drinking water was provided to mice in a dark bottle for 8 days with a change of drug on day 4. Clearance of episomal plasmid in parasites after negative selection was confirmed by checking the parasite survival after reapplying pyrimethamine pressure (6 μg/ml) in new infected mice.

Gametocyte induction. ICR mice were treated with phenylhydrazine (80 μg/g mouse body weight) through intraperitoneal injection. Three days post treatment, the mice were infected with 3.0×10^6 parasites through tail vein injection. Gametocytemia usually peaks at day 3 post infection. Male and female gametocytes were counted via Giemsa staining of thin blood smears. Gametocytemia was calculated as the ratio of male or female gametocyte over parasitized erythrocytes. All experiments were repeated three times independently.

Male gametocyte exflagellation assay. Two and a half microliters of mouse tail blood with 4–6% gametocytemia were added to 100 μl exflagellation medium (RPMI 1640 supplemented with 10% fetal calf serum and 50 μM XA, pH 7.4) containing 1 μl of 200 units/ml heparin. After 10 min of incubation at 22 °C, the numbers of EC and RBC were counted in a hemocytometer under a light microscope. The percentage of RBCs containing male gametocytes was calculated from Giemsa-stained smears, and the number of ECs per 100 male gametocytes was then calculated as exflagellation rate. Compound 2 (5 μM) and Zaprinast (100 μM) were added to exflagellation medium with or without XA (for Zaprinast) to evaluate their effects on exflagellation.

In vitro ookinete differentiation. In vitro culture for ookinete differentiation was prepared as described previously[13]. Briefly, mouse blood with 4–6% gametocytemia was collected in heparin tubes and immediately added to ookinete culture medium (RPMI 1640 medium containing 25 mM HEPES, 10% fetal calf serum, 100 μM XA, and pH 8.0) in a blood/medium volume ratio of 1:10. The cultures were incubated at 22 °C for 12 h to allow gametogenesis, fertilization, and ookinete differentiation. Ookinete formation was monitored by Giemsa-staining of culture smears. Ookinete conversion rate was calculated as the number of ookinetes (including mature and immature) per 100 female gametocytes.

Mosquito feeding and transmission assay. Thirty female mosquitoes were allowed to feed on an anaesthetized mouse with 4–6% gametocytemia for 30 min. Mosquito midguts were dissected on day 7 post blood-feeding and stained with 0.1% mercurochrome for detection of oocyst. Salivary glands from 20–30 mosquitoes were dissected on day 14 post blood-feeding, and the number of sporozoites per mosquito was calculated.

Parasite genetic cross. Genetic crosses between two different parasite lines were performed by infecting phenylhydrazine pre-treated mice with equal numbers of both parasites. Day 3 pi, 30 female mosquitoes were allowed to feed on mice carrying gametocytes for 30 min. Mosquito midguts were dissected on day 7 post blood-feeding and stained with 0.1% mercurochrome for oocyst counting.

Gametocyte purification. Gametocytes were purified using the method described previously[48]. Briefly, mice were treated with phenylhydrazine 3 days before parasite infection. From day 3 pi, infected mouse were treated with sulfadiazine at 20 mg/l in drinking water to eliminate asexual blood stage parasites. After 48 h treatment with sulfadiazine, mouse blood containing gametocytes was collected from orbital sinus into a heparin tube. Gametocytes were separated from the uninfected erythrocyte by centrifugation using 48% Nycodenz solution (27.6% w/v Nycodenz in 5 mM Tris-HCl, 3 mM KCl, 0.3 mM EDTA, pH 7.2,) and prepared in gametocyte maintenance buffer (GMB, 137 mM NaCl, 4 mM KCl, 1 mM $CaCl_2$, 20 mM glucose, 20 mM HEPES, 4 mM $NaHCO_3$, pH 7.24–7.29, 0.1% BSA)[48]. Gametocytes were harvested from the interphase and washed three times in the GMB buffer. All the operations were performed at 19–22 °C.

Trypan blue staining. Purified gametocytes were prepared in PBS and mixed with 0.4% trypan blue solution at a 1:9 volume ratio. The mixtures were incubated at room temperature for 5 min and examined under a light microscope.

Propidium iodide staining. Purified gametocytes were prepared in PBS and stained with Propidium iodide (PI) at a final concentration of 50 μg/ml. The mixtures were incubated at room temperature for 10 min, washed with PBS twice, and then examined under a fluorescencec microscope.

Flow cytometry analysis. For measuring DNA content in gametocytes, half of purified gametocytes were immediately fixed and half were transferred to exflagellation medium for gametogenesis for 8 min before fixation. Cells were fixed in 4% paraformaldehyde (PFA) for 20 min, washed in PBS and stained with Hoechst 33342 (0.5 μg/ml) for 30 min. Hoechst fluorescence signal of gametocytes was collected using Novocyte 3130 flow cytometer. For detecting GFP and mCherry in gametocytes, the gametocytes were stained with Hoechst 33342 and washed with PBS twice, GFP and mCherry fluorescence signal of gametocytes was collected using BD LSR Fortessa flow cytometer. Cell gating strategies are provided in Supplementary Fig. 11.

Ca^{2+} mobilization assay using flow cytometry. Purified gametocytes were washed three times with Ca^{2+} free buffer (CFB, 137 mM NaCl, 4 mM KCl, 20 mM glucose, 20 mM HEPES, 4 mM NaHCO3, pH 7.2–7.3, 0.1% BSA) and then incubated in CFB containing 5 μM Fluo-8 at 37 °C for 20 min. Fluo-8 loaded gametocytes were washed twice with CFB and suspended in RPMI 1640 for flow cytometer analysis. Fluo-8 fluorescence signal reflecting cellular Ca^{2+} content in gametocytes were collected using BD LSR Fortessa flow cytometer. Signals were consecutively collected at 30 s before until 90 s post addition of XA (100 μM) or A23187 (0.1 and 1 μM). Cell gating strategies are provided in Supplementary Fig. 11.

Detection of cellular cGMP. The assay for measuring cGMP levels in gametocytes was performed using a cyclic cGMP enzyme immunoassay kit (Cayman Chemical, #581021). For each test, more than 1.5×10^7 gametocytes were collected and maintained in GMB buffer on ice. After treatment with 100 μM XA or 100 μM Zap for 2 min, cells were immediately lysed by 0.2 M cold hydrochloric acid on ice for 10 min, vortexed, and passed through a 22-gauge needle. For each replicate, three equal volumes of cell extract from each parasite preparation were parallel tested according to manufacturer's instructions.

Antibodies and antiserum. The primary antibodies used were: rabbit anti-HA (Western blot, 1:1000 dilution, IFA, 1:500 dilution) and rabbit anti-Myc (Western blot, 1:1000 dilution, IFA, 1:500 dilution) from Cell Signaling Technology; mouse anti-HA (IFA, 1:200) and mouse anti-Myc (IFA, 1:200) from Santa Cruz; mouse anti-α-Tubulin II from Sigma-Aldrich (IFA, 1:1000). The secondary antibodies used were: goat anti-rabbit IgG HRP-conjugated and goat anti-mouse IgG HRP-conjugated secondary antibodies from Abcam (1:5000); the Alexa 555 labeled goat anti-rabbit IgG, Alexa 555 labeled goat anti-mouse IgG, and Alexa 488 labeled goat anti-mouse IgG secondary antibodies from Thermo Fisher Scientific (1:500); Alexa 488 labeled anti-mouse TER-119 IgG antibody from BioLegend (IFA, 1:1000), biotinylated anti-rabbit IgG (H+L) antibody from Cell Signaling Technology (IFA, 1:1000); Streptavidin-ACP from Bioscience (IFA, 1:500). The anti-sera, including rabbit anti-Hep17 (Western blot, 1:1000), rabbit anti-P28 (Western blot, 1:1000, IFA, 1:1000), rabbit anti-BiP (Western blot, 1:1000) were prepared by immunization of synthetic peptides or recombinant protein as described previously[8].

Immunofluorescence assays. Purified parasites or chemical-treated parasites were fixed in 4% PFA and transferred onto a poly-L-Lysine pre-treated coverslip. The fixed cells were permeabilized with 0.1% Triton X-100 PBS solution for 7 min, blocked in 5% BSA solution for 60 min at room temperature or 4 °C overnight, and incubated with the primary antibodies diluted in PBS with 3% BSA at 4 °C for 12 h. The coverslip was incubated with fluorescently conjugated secondary antibodies. Cells were stained with Hoechst 33342, mounted in 90% glycerol solution, and sealed with nail polish. All images were captured and processed using identical settings on a Zeiss LSM 780 confocal microscope.

Proximity ligtaion assay. The PLA assay detecting in situ protein interaction was performed using the kit (Sigma-Aldrich: DUO92008, DUO92001, DUO92005, and DUO82049). Non-activated and activated gametocytes were fixed with 4% PFA for 30 min, permeabilized with 0.1% Triton X-100 for 10 min, and blocked with a blocking solution overnight at 4 °C. The primary antibodies were diluted in the Duolink Antibody Diluent, added to the cells and then incubated in a humidity chamber overnight at 4 °C. The primary antibodies were removed and the slides were washed with Wash Buffer A twice. The PLUS and MINUS PLA probe were diluted in Duolink Antibody Diluent, added to the cells and incubated in a pre-heated humidity chamber for 1 h at 37 °C. Next, cells were washed with Wash Buffer A and incubated with the ligation solution for 30 min at 37 °C. Then, cells were washed with Wash Buffer A twice and incubated with the amplification solution for 100 min at 37 °C in the dark. Cells were washed with 1× Wash Buffer B twice and 0.01× Wash Buffer B once. Finally, cells were incubated with Hoechst 33342 and washed with PBS. Images were captured and processed using identical settings on a Zeiss LSM 780 confocal microscope.

Protein extraction and western blotting. Proteins were extracted from asexual blood parasites and gametocytes using buffer A (0.1% SDS, 1 mM DTT, 50 mM NaCl, 20 mM Tris-HCl, pH 8.0) containing protease inhibitor cocktail and PMSF. After ultrasonication, the protein solution was kept on ice for 15 min before centrifugation at 14,000 × *g* for 10 min at 4 °C. The supernatant was lysed in Laemmli sample buffer. GEP1 protein was separated in 9% SDS-PAGE and transferred to PVDF membrane (Millipore, IPVH00010). GCα and GCβ proteins were separated in 4.5% SDS-PAGE.

The membrane was blocked with TBST buffer (0.3 M NaCl, 20 mM Tris-HCl, 0.1% Tween 20, pH 8.0) containing 5% skim milk and incubated with primary antibodies. After incubation, the membrane was washed three times with TBST and incubated with HRP-conjugated secondary antibodies. The membrane was washed five times in TBST before enhanced chemiluminescence detection.

Immunoprecipitation. For immunoprecipitation analysis, 6.0×10^7 gametocytes were lysed in 1 ml protein extraction buffer A plus (0.01% SDS, 1 mM DTT, 50 mM NaCl, 20 mM Tris-HCl; pH8.0). After ultrasonication, the protein solution was incubated on ice for 15 min before centrifugation at $14,000 \times g$ at 4 °C for 10 min. Rabbit anti-Myc antibody (1 µg, CST, #2272 s) or Rabbit anti-HA antibody (1 µg, CST, #3724 s) was added to the supernatant, and the solution was incubated on a vertical mixer at 4 °C for 15 h. After incubation, 20 µl buffer A plus pre-balanced protein A/G beads (Pierce, #20423) was added and incubated for 5 h. The beads were washed three times with buffer A plus before elution with Laemmli buffer.

Mass spectrometry. After immunoprecipitation as described above, proteins were eluted twice with 0.3% SDS in 20 mM Tris-HCl (pH 8.0). Eluted proteins were precipitated using 20% trichloroacetic acid (TCA), washed twice with 1 ml cold acetone, and dried in centrifugation vacuum. The protein pellets were dissolved in buffer containing 1% SDC, 10 mM TCEP, 40 mM CAA, Tris-HCl pH 8.5 and were digested with trypsin (1:100 ratio) at 37 °C for 12–16 h after dilution with water to reduce SDS content to 0.5%. Peptides were desalted using SDB-RPS StageTips. For timsTOF Pro, an ultra-high pression nano-flow chromatography system (Elute UHPLC, Bruker) was coupled. Liquid chromatography was performed on a reversed-phase column (40 cm × 75 µm i.d.) at 50 °C packed with Magic C18 AQ 3-µm 200-Å resin with a pulled emitter tip. The timsTOF Pro was operated in PASEF mode[49]. Bruker.tdf raw files were converted to mgf files with the vendor provided software. The mgf files were searched against *P. yoelii* 17X genome database (downloaded from Uniprot) using PEAKS Studio X (BSI, Canada). Candidate peptides of targeted proteins were systematically validated by manual inspection of spectra.

Bioinformatics analysis and tools. The genomic sequences of *Plasmodium* genes were downloaded from the *Plasmodium* database of PlasmoDB (http://plasmodb.org). Transmembrane domains of proteins were identified using the TMHMM Server (http://www.cbs.dtu.dk/services/TMHMM/). Multiple sequence alignments were performed by ClustalW in MEGA7.0 [41]. Flow cytometry data were analyzed using FlowJo v10.

Quantification and statistical analysis. Statistical analysis was performed using GraphPad Software 8.0. Two-tailed Student's *t*-test or Whiney Mann test was used to compare differences between treated groups. *P*-value in each statistical analysis was indicated within the figures.

Reporting summary. Further information on research design is available in the Nature Research Reporting Summary linked to this article.

Data availability

The data supporting the findings of this study are available within the paper and its Supplementary Information files or are available from the corresponding author on reasonable request. The source data underlying Figs. 1a, e, f, 2i, 4a–c, 5e–f, 6c–f, 8b-c and Supplementary Figs. 2a, 3a–c, f, 5a–j, 6d-e, 8c-d, 9c-d, and 10b-c are provided as a Source Data file.

Received: 1 August 2019; Accepted: 14 March 2020;
Published online: 09 April 2020

References

1. Guttery, D. S., Roques, M., Holder, A. A. & Tewari, R. Commit and transmit: molecular players in Plasmodium sexual development and zygote differentiation. *Trends Parasitol.* **31**, 676–685 (2015).
2. Sologub, L. et al. Malaria proteases mediate inside-out egress of gametocytes from red blood cells following parasite transmission to the mosquito. *Cell Microbiol.* **13**, 897–912 (2011).
3. Sinden, R. E. & Croll, N. A. Cytology and kinetics of microgametogenesis and fertilization in Plasmodium yoelii nigeriensis. *Parasitology* **70**, 53–65 (1975).
4. Sinden, R. E. Sexual development of malarial parasites. *Adv. Parasitol.* **22**, 153–216 (1983).
5. Billker, O. et al. Identification of xanthurenic acid as the putative inducer of malaria development in the mosquito. *Nature* **392**, 289–292 (1998).
6. Garcia, G. E., Wirtz, R. A., Barr, J. R., Woolfitt, A. & Rosenberg, R. Xanthurenic acid induces gametogenesis in Plasmodium, the malaria parasite. *J. Biol. Chem.* **273**, 12003–12005 (1998).
7. Muhia, D. K., Swales, C. A., Deng, W., Kelly, J. M. & Baker, D. A. The gametocyte-activating factor xanthurenic acid stimulates an increase in membrane-associated guanylyl cyclase activity in the human malaria parasite Plasmodium falciparum. *Mol. Microbiol* **42**, 553–560 (2001).
8. Gao, H. et al. ISP1-anchored polarization of GCbeta/CDC50A complex initiates malaria ookinete gliding motility. *Curr. Biol.* **28**, 2763–2776 e2766 (2018).
9. Hirai, M., Arai, M., Kawai, S. & Matsuoka, H. PbGCbeta is essential for Plasmodium ookinete motility to invade midgut cell and for successful completion of parasite life cycle in mosquitoes. *J. Biochem.* **140**, 747–757 (2006).
10. Moon, R. W. et al. A cyclic GMP signalling module that regulates gliding motility in a malaria parasite. *PLoS Pathog.* **5**, e1000599 (2009).
11. McRobert, L. et al. Gametogenesis in malaria parasites is mediated by the cGMP-dependent protein kinase. *PLoS Biol.* **6**, e139 (2008).
12. Taylor, H. M. et al. The malaria parasite cyclic GMP-dependent protein kinase plays a central role in blood-stage schizogony. *Eukaryot. Cell* **9**, 37–45 (2010).
13. Billker, O. et al. Calcium and a calcium-dependent protein kinase regulate gamete formation and mosquito transmission in a malaria parasite. *Cell* **117**, 503–514 (2004).
14. Bennink, S., Kiesow, M. J. & Pradel, G. The development of malaria parasites in the mosquito midgut. *Cell Microbiol.* **18**, 905–918 (2016).
15. Brochet, M. et al. Phosphoinositide metabolism links cGMP-dependent protein kinase G to essential Ca(2)(+) signals at key decision points in the life cycle of malaria parasites. *PLoS Biol.* **12**, e1001806 (2014).
16. Zhang, C. et al. Efficient editing of malaria parasite genome using the CRISPR/Cas9 system. *MBio* **5**, e01414–e01414 (2014).
17. Zhang C., *et al.* CRISPR/Cas9 mediated sequential editing of genes critical for ookinete motility in Plasmodium yoelii. *Mol. Biochem. Parasitol.* (2016).
18. Rangarajan, R. et al. A mitogen-activated protein kinase regulates male gametogenesis and transmission of the malaria parasite Plasmodium berghei. *EMBO Rep.* **6**, 464–469 (2005).
19. Lopez-Barragan, M. J. et al. Directional gene expression and antisense transcripts in sexual and asexual stages of Plasmodium falciparum. *BMC Genomics* **12**, 587 (2011).
20. Yeoh, L. M., Goodman, C. D., Mollard, V., McFadden, G. I. & Ralph, S. A. Comparative transcriptomics of female and male gametocytes in Plasmodium berghei and the evolution of sex in alveolates. *BMC Genomics* **18**, 734 (2017).
21. Grotendorst, C. A., Kumar, N., Carter, R. & Kaushal, D. C. A surface protein expressed during the transformation of zygotes of Plasmodium gallinaceum is a target of transmission-blocking antibodies. *Infect. Immun.* **45**, 775–777 (1984).
22. Tewari, R., Dorin, D., Moon, R., Doerig, C. & Billker, O. An atypical mitogen-activated protein kinase controls cytokinesis and flagellar motility during male gamete formation in a malaria parasite. *Mol. Microbiol.* **58**, 1253–1263 (2005).
23. Reininger, L. et al. A NIMA-related protein kinase is essential for completion of the sexual cycle of malaria parasites. *J. Biol. Chem.* **280**, 31957–31964 (2005).
24. Liu, C., Li, Z., Jiang, Y., Cui, H. & Yuan, J. Generation of Plasmodium yoelii malaria parasite carrying double fluorescence reporters in gametocytes. *Mol. Biochem. Parasitol.* **224**, 37–43 (2018).
25. Sinden, R. E., Butcher, G. A., Billker, O. & Fleck, S. L. Regulation of infectivity of Plasmodium to the mosquito vector. *Adv. Parasitol.* **38**, 53–117 (1996).
26. Rupp, I. et al. Malaria parasites form filamentous cell-to-cell connections during reproduction in the mosquito midgut. *Cell Res.* **21**, 683–696 (2011).
27. Deligianni, E. et al. A perforin-like protein mediates disruption of the erythrocyte membrane during egress of Plasmodium berghei male gametocytes. *Cell Microbiol.* **15**, 1438–1455 (2013).
28. Kehrer, J. et al. A putative small solute transporter is responsible for the secretion of G377 and TRAP-containing secretory vesicles during Plasmodium Gamete Egress and sporozoite motility. *PLoS Pathog.* **12**, e1005734 (2016).
29. Zipprer, E. M., Neggers, M., Kushwaha, A., Rayavara, K. & Desai, S. A. A kinetic fluorescence assay reveals unusual features of Ca(+)(+) uptake in Plasmodium falciparum-infected erythrocytes. *Malar. J.* **13**, 184 (2014).
30. Gao, X., Gunalan, K., Yap, S. S. & Preiser, P. R. Triggers of key calcium signals during erythrocyte invasion by Plasmodium falciparum. *Nat. Commun.* **4**, 2862 (2013).
31. Singh, S., Alam, M. M., Pal-Bhowmick, I., Brzostowski, J. A. & Chitnis, C. E. Distinct external signals trigger sequential release of apical organelles during erythrocyte invasion by malaria parasites. *PLoS Pathog.* **6**, e1000746 (2010).
32. Lakshmanan, V. et al. Cyclic GMP balance is critical for malaria parasite transmission from the mosquito to the mammalian host. *MBio* **6**, e02330 (2015).
33. Taylor, C. J., McRobert, L. & Baker, D. A. Disruption of a Plasmodium falciparum cyclic nucleotide phosphodiesterase gene causes aberrant gametogenesis. *Mol. Microbiol.* **69**, 110–118 (2008).

34. Carucci, D. J. et al. Guanylyl cyclase activity associated with putative bifunctional integral membrane proteins in Plasmodium falciparum. *J. Biol. Chem.* **275**, 22147–22156 (2000).
35. Baker, D. A. et al. Cyclic nucleotide signalling in malaria parasites. *Open Biol* **7**, 331–339 (2017).
36. Sebastian, S. et al. A Plasmodium calcium-dependent protein kinase controls zygote development and transmission by translationally activating repressed mRNAs. *Cell Host Microbe* **12**, 9–19 (2012).
37. Qian, P. et al. A Cas9 transgenic Plasmodium yoelii parasite for efficient gene editing. *Mol. Biochem. Parasitol.* **222**, 21–28 (2018).
38. Bagchi, S., Fredriksson, R. & Wallen-Mackenzie, A. In Situ Proximity Ligation Assay (PLA). *Methods Mol. Biol.* **1318**, 149–159 (2015).
39. Alam, M. S. Proximity Ligation Assay (PLA). *Curr. Protoc. Immunol.* **123**, e58 (2018).
40. Bushell, E. et al. Functional profiling of a Plasmodium genome reveals an abundance of essential genes. *Cell* **170**, 260–272 e268 (2017).
41. Kawamoto, F., Alejo-Blanco, R., Fleck, S. L., Kawamoto, Y. & Sinden, R. E. Possible roles of Ca2+ and cGMP as mediators of the exflagellation of Plasmodium berghei and Plasmodium falciparum. *Mol. Biochem. Parasitol.* **42**, 101–108 (1990).
42. Kawamoto, F. et al. The roles of Ca^{2+}/calmodulin- and cGMP-dependent pathways in gametogenesis of a rodent malaria parasite, Plasmodium berghei. *Eur. J. Cell Biol.* **60**, 101–107 (1993).
43. Linder, J. U. et al. Guanylyl cyclases with the topology of mammalian adenylyl cyclases and an N-terminal P-type ATPase-like domain in paramecium, tetrahymena and plasmodium. *EMBO J.* **18**, 4222–4232 (1999).
44. Bisio, H., Lunghi, M., Brochet, M. & Soldati-Favre, D. Phosphatidic acid governs natural egress in Toxoplasma gondii via a guanylate cyclase receptor platform. *Nat. Microbiol.* **4**, 420–428 (2019).
45. Brown, K. M. & Sibley, L. D. Essential cGMP signaling in toxoplasma is initiated by a Hybrid P-type ATPase-guanylate cyclase. *Cell Host Microbe* **24**, 804–816 e806 (2018).
46. Yang, L. et al. An apically located hybrid guanylate cyclase-ATPase is critical for the initiation of Ca(2+) signaling and motility in Toxoplasma gondii. *J. Biol. Chem.* **294**, 8959–8972 (2019).
47. Wright, D. A. et al. Standardized reagents and protocols for engineering zinc finger nucleases by modular assembly. *Nat. Protoc.* **1**, 1637–1652 (2006).
48. Raabe, A. C., Wengelnik, K., Billker, O. & Vial, H. J. Multiple roles for Plasmodium berghei phosphoinositide-specific phospholipase C in regulating gametocyte activation and differentiation. *Cell Microbiol.* **13**, 955–966 (2011).
49. Meier, F. et al. Online parallel accumulation-serial fragmentation (PASEF) with a novel trapped ion mobility mass spectrometer. *Mol. Cell Proteom.* **17**, 2534–2545 (2018).

Acknowledgements
This work was supported by the National Natural Science Foundation of China (31772443, 31872214, 31970387), the Natural Science Foundation of Fujian Province (2019J05010), the 111 Project sponsored by the State Bureau of Foreign Experts and Ministry of Education of China (BP2018017), and the Division of Intramural Research, National Institute of Allergy and Infectious Diseases (NIAID), National Institutes of Health (NIH, X-z.S.). The authors thank Bradley Otterson (NIH Library Writing Center) for manuscript editing assistance.

Author contributions
J.Y.Y., C.H.T., W.J., L.C.Y., Z.Y., J.Z.Z., L.Z.K., L.S.N., Y.Z.K., W.X., and Q.P.G. generated the modified parasites, J.Y.Y. conducted the phenotype analysis, IFA assay, image analysis, mosquito experiments, and performed the biochemical experiments. Z.C. performed the Ca^{2+} mobilization, Z.CQ. analyzed the MS results, J.Y.Y., C.H.T., and Y.J. analyzed the data. Y.J. and C.H.T. supervised the work. X.-z.S. and Y.J. wrote the manuscript.

Competing interests
The authors declare no competing interests.

Additional information
Supplementary information is available for this paper at https://doi.org/10.1038/s41467-020-15479-3.

Correspondence and requests for materials should be addressed to J.Y.

Peer review information Nature Communications thanks David Baker, Gabriele Pradel and the other, anonymous, reviewer(s) for their contribution to the peer review of this work.

Reprints and permission information is available at http://www.nature.com/reprints

Publisher's note Springer Nature remains neutral with regard to jurisdictional claims in published maps and institutional affiliations.

Open Access This article is licensed under a Creative Commons Attribution 4.0 International License, which permits use, sharing, adaptation, distribution and reproduction in any medium or format, as long as you give appropriate credit to the original author(s) and the source, provide a link to the Creative Commons license, and indicate if changes were made. The images or other third party material in this article are included in the article's Creative Commons license, unless indicated otherwise in a credit line to the material. If material is not included in the article's Creative Commons license and your intended use is not permitted by statutory regulation or exceeds the permitted use, you will need to obtain permission directly from the copyright holder. To view a copy of this license, visit http://creativecommons.org/licenses/by/4.0/.

© The Author(s) 2020

Supplementary Information

An intracellular membrane protein GEP1 regulates xanthurenic acid induced gametogenesis of malaria parasites

Jiang et al.

1. Supplementary Figures 1-11 and figure legends

2. Supplementary Table 1. List of candidate gene for screening in this study

3. Supplementary Table 2. GEP1 interacted proteins detected by Mass spectrum

4. Supplementary Table 3. Primers and oligonucleotides used in this study

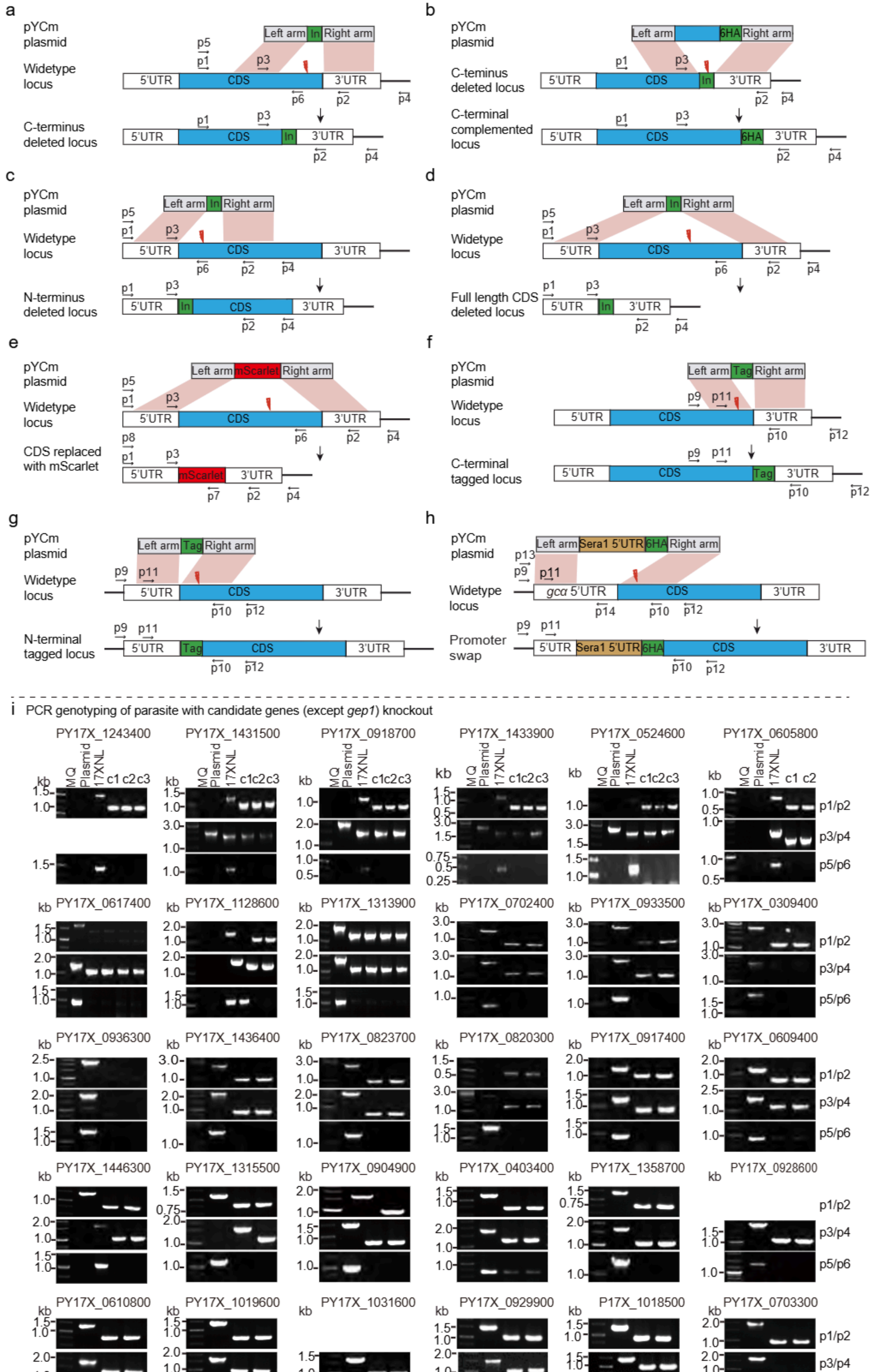
a
pYCm plasmid
Left arm
In
Right arm
Widetype locus
5'UTR
CDS
3'UTR
p5
p1
p3
p6
p2
p4
C-terminus deleted locus
b
C-teminus deleted locus
6HA
C-terminal complemented locus
c
N-terminus deleted locus
d
Full length CDS deleted locus
e
mScarlet
CDS replaced with mScarlet
p7
p8
f
Tag
p9
p11
p10
p12
C-terminal tagged locus
g
N-terminal tagged locus
h
Sera1 5'UTR
p13
p14
gca 5'UTR
Promoter swap
i PCR genotyping of parasite with candidate genes (except gep1) knockout
MQ
Plasmid
17XNL
c1
c2
c3
kb
p1/p2
p3/p4
p5/p6
PY17X_1243400
PY17X_1431500
PY17X_0918700
PY17X_1433900
PY17X_0524600
PY17X_0605800
PY17X_0617400
PY17X_1128600
PY17X_1313900
PY17X_0702400
PY17X_0933500
PY17X_0309400
PY17X_0936300
PY17X_1436400
PY17X_0823700
PY17X_0820300
PY17X_0917400
PY17X_0609400
PY17X_1446300
PY17X_1315500
PY17X_0904900
PY17X_0403400
PY17X_1358700
PY17X_0928600
PY17X_0610800
PY17X_1019600
PY17X_1031600
PY17X_0929900
P17X_1018500
PY17X_0703300

Supplementary Fig. 1. Genotyping and DNA sequencing of modified parasites.

(a to h) Schematic for CRISPR/Cas9-mediated gene modification, including gene deletion in the C-terminus **(a)**, gene re-constitution in the C-terminal **(b)**, gene deletion in the N-terminus **(c)**, deletion of full length CDS **(d),** CDS replaced with mScarlet **(e)**, N-terminal **(f)** or C-terminal **(g)** tagging of genes with epitope tag, and promoter swap **(h)** via double cross homologous recombination. **(i to j** and **l)** For each modification, both 5' and 3' homologous recombination was detected using gene specific PCR pair (Supplementary Table 3) to confirm correct integration of the homologous template. At least two parasite clones (sc) for each modification were obtained after limiting dilution and phenotype analysis. **(k and m)** DNA sequencing to confirm correct modifications in some mutant parasites. Experiments in this figure were performed one time to ensure the correct genotype of the modified parasites.

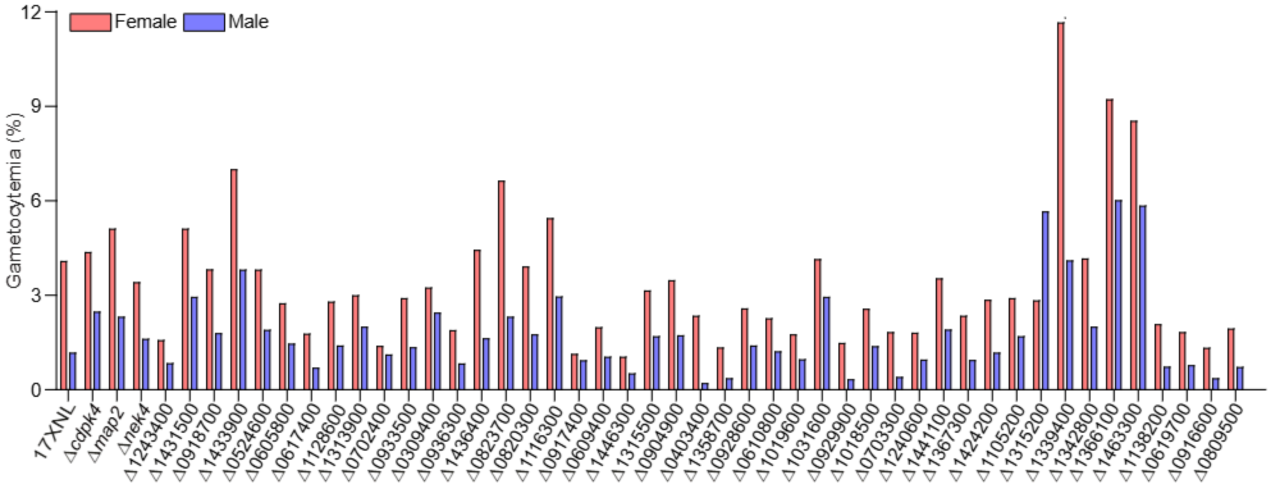

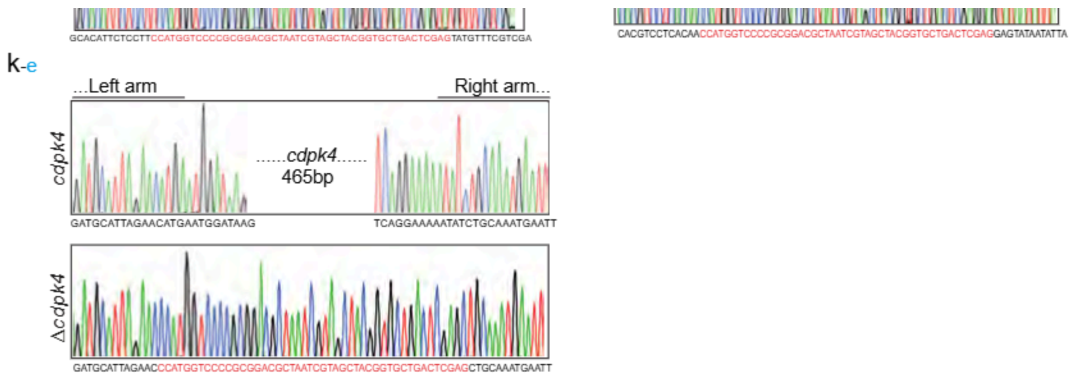

l PCR genotyping of parasite clones with modification in *gep1* and *map2 of P.berghei*

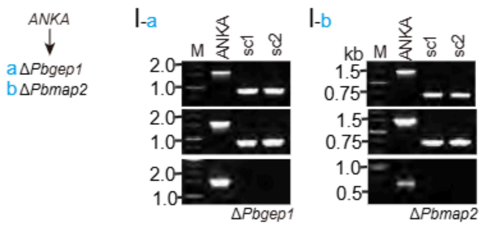

m DNA sequencing confirming right modification in *gep1* and *map2 of P.berghei*

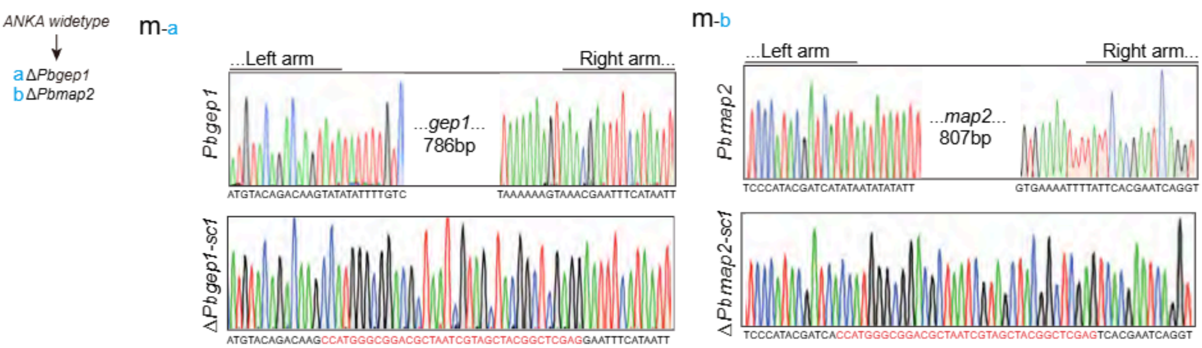

Supplementary Fig. 2. Gametocyte formation in the mice.

The male and female gametocytemia in mice infected with 17XNL and 45 mutant parasites with candidate gene disrupted. The numbers shown in X axis are gene names (gene IDs) derived from the PlasmoDB database. Experiment was performed one time to ensure the formation of gametocyte in the mutants tested.

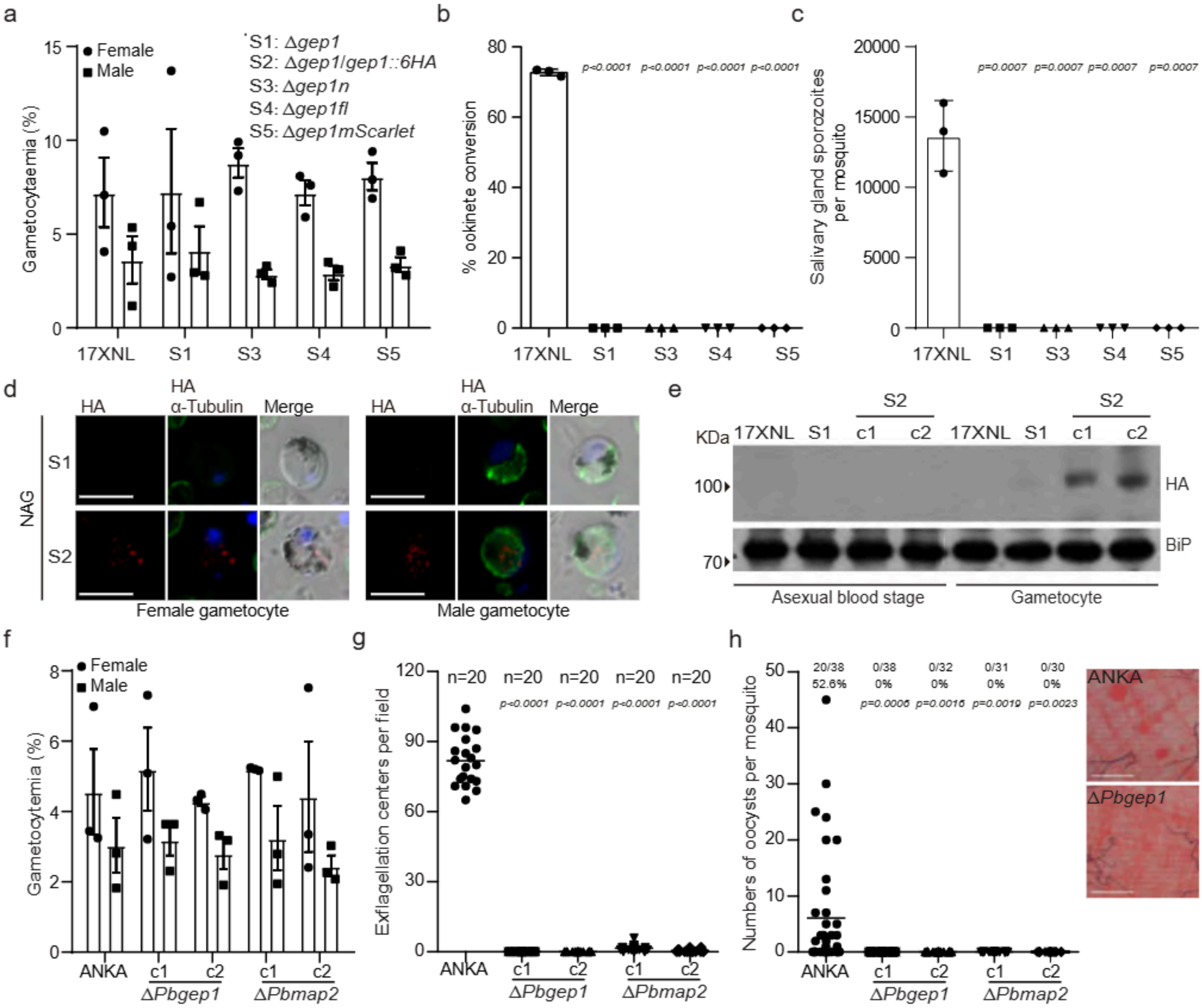

a
Female
Male
S1: Δgep1
S2: Δgep1/gep1::6HA
S3: Δgep1n
S4: Δgep1fl
S5: Δgep1mScarlet
Gametocytaemia (%)
17XNL S1 S3 S4 S5
b
% ookinete conversion
p<0.0001 p<0.0001 p<0.0001 p<0.0001
17XNL S1 S3 S4 S5
c
Salivary gland sporozoites per mosquito
p=0.0007 p=0.0007 p=0.0007 p=0.0007
17XNL S1 S3 S4 S5
d
HA
HA α-Tubulin
Merge
NAG
S1
S2
Female gametocyte
Male gametocyte
e
KDa
17XNL S1 S2 c1 c2 17XNL S1 S2 c1 c2
100
70
HA
BiP
Asexual blood stage
Gametocyte
f
Female
Male
Gametocytemia (%)
ANKA c1 c2 c1 c2
ΔPbgep1
ΔPbmap2
g
Exflagellation centers per field
n=20 n=20 n=20 n=20 n=20
p<0.0001 p<0.0001 p<0.0001 p<0.0001
ANKA c1 c2 c1 c2
ΔPbgep1
ΔPbmap2
h
Numbers of oocysts per mosquito
20/38 52.6%
0/38 0%
0/32 0%
0/31 0%
0/30 0%
p=0.0006 p=0.0016 p=0.0019 p=0.0023
ANKA c1 c2 c1 c2
ΔPbgep1
ΔPbmap2
ANKA
ΔPbgep1

Supplementary Fig. 3. GEP1 disruption causes defect in gametogenesis.

a, Gametocytemia in mice infected with 17XNL or *gep1* mutant parasites: S1 (Δ*gep1*), deletion in C-terminus; S3 (Δ*gep1n*), deletion in N-terminus; S4 (Δ*gep1fl*), deletion of the full coding region; S5 (Δ*gep1mScarlet*), coding region replaced with *mScarlet* gene. **b**, *In vitro* ookinete conversion rates for 17XNL and the *gep1* mutants. **c**, Numbers of salivary gland sporozoites in mosquitoes 14 day after feeding on mice infected with the parasites. **d**, Co-staining of GEP1 and α-Tubulin (male gametocyte specific) in the non-activated gametocytes (NAG) of S1 and S2 parasites. Scale bar = 5 μm. **e**, Western blot of GEP1 in ABS and gametocytes of S1 and S2 parasites. c1/c2: two independent clones of S2 parasite. **f**, Gametocytemia in mice infected with *P. berghei* ANKA and parasite with disrupted *Pbgep1* (Δ*Pbgep1*) or *Pbmap2* (Δ*Pbmap2*). **g**, Numbers of exflagellation centers (ECs) per microscopic field (40X) for the parasites in **f**. n is the numbers of microscopic fields counted (40X). **h,** Day 7 midgut oocyst counts in mosquitoes infected with the parasites in **f**. x/y on the top are the number of mosquito containing oocyst / the number of mosquito dissected; the percentage number indicates the mosquito infection prevalence. two-tailed unpaired Student's t test. Experiments were independently repeated three times in **a**, **b**, **c**, **d**, **f**, **g**, and two times in **e** and **h** with similar results. Data are shown as mean ± SD; two-tailed unpaired Student's t test in **b**, **c**, **g** and **h**.

```
P.yoelii      1   ---------- ---------M ETSN---KEI ISSKLK---- -DDKMIKNKK  23
P.berghei     1   ---------- ---------M ETTN---KEI ISSKLK---- -DDKMIKNKK  23
P.chabaudi    1   ---------- ---------M EIPN---KEI IFSKLK---- -DDKIIQNKK  23
P.vivax       1   ---------- ---------M EDTP------ ---------- ----------  5
P.falciparum  1   MSRETSKDDF YKTNKYGHSI EESKNIYKES YESDLNNELE EKENKMKNRK  50

P.yoelii      24  KYLHKFSQYN ---------- --NNYSKIFR NKHTLG---- ----FRSVGR  53
P.berghei     24  KYLHKISQYN ---------- --NNYSKMFR NKHTLG---- ----FRSIGK  53
P.chabaudi    24  KPLHKIGQYH ---------- --NNYSKIFR NKHTLG---- ----FRSIGR  53
P.vivax       5   ---GASAQKS ---------- ---------- ---------- -----KFFGR  17
P.falciparum  51  RRNASSSFHN SFNRRNISIN KDNGYNNIRK IKNKYGDDYF PFRFYKNINN  100

P.yoelii      54  TKSSIIKKNK NKS-----LG IITK------ ---------- ---ENIINLI  79
P.berghei     54  TKSSIVKKNK NKS-----LG IITK------ ---------- ---ENIINLI  79
P.chabaudi    54  TKSSIIKKNK SKS-----LG IITK------ ---------- ---ENIINLI  79
P.vivax       18  SASPERSKST YES------- ---------- ---------- -----VIGCV  35
P.falciparum  101 YKCSNVNKYN YKDKYKYEKG YTSKNTKICN FRNNRIKTYK NTYHNIINFI  150

P.yoelii      80  RHNKSDVRKI RSILFLKAYE HSELFHKKKQ DRVEKLKLN- ----KYNKCV  124
P.berghei     80  RHNNSDIRKI RSILFLKAYE HSELFHKKKQ DRVEKLKLN- ----EYNKCI  124
P.chabaudi    80  RHNKSDVRKI RSILFLKAYE HSELFHKKKQ DRLEKLKLN- ----KYNKCI  124
P.vivax       36  RENKNDRRRI RYSLFLKAYE NAELVQMERQ NKREKLKLRM NEWSKWNTCI  85
P.falciparum  151 KENRNDMKKV RYFLFLRAYE NSELFQINKQ NKKEKHNLR- ----KHNKCI  195

P.yoelii      125 EIKDAKEKER LKLLKLLKSY NIKYEGYTNL YDLCDYSIYF SEQNYKNGEE  174
P.berghei     125 EIKDAKEKER LKLLKLLKSY NIKYEGYTNL YDLCDYSIYF SEQNYKNGEE  174
P.chabaudi    125 EVKDAKEKER LKLLKLLKSY NIKYEGYTNL YDLCDYSIYF SEQNNKNGKE  174
P.vivax       86  HMKGAKEKQR LKLLNMLKNY QIKYQTYSNL KDLCDYSVYF DKPS------  129
P.falciparum  196 DIKDAKEKER LKLLKLLKSY DIKYEGYTDL YTLCNYSIYY EDK-------  238

P.yoelii      175 IKDKQLCKIN EKNQKKKYDC DNFLYYLVSI GISYNDIIEM ASVFENMKYL  224
P.berghei     175 TKGNKICKIN EKNQKKKYDC DNFLYYLVSI GISYNDIIEM ASVFENMKYL  224
P.chabaudi    175 VTDIQMYKIN EKNKKKKDDN DNFLYYLVSI GISYNDIIEM ASVFENMKYL  224
P.vivax       129 ---IGTVPKE SKSILEEAQR DNFFFHLVSM GVSYNDIILV SSVFQNREHL  176
P.falciparum  238 -------KLV EELLNKQ-NC NNFFYYLVSI GISYNDIIHM ASVFENMEYL  280

P.yoelii      225 KYCNLYMLPW IYKKVNEFHN YDVNTFVLYC VVYSITTLSS SLYLFIKYKT  274
P.berghei     225 KYCNLYMLPW IYKKVNEFHN YDVNTFVLYC VVYSITTLSS SLYLFIKYKT  274
P.chabaudi    225 KYCNLYMLPW IYKKVNEFHN YDVNTFVLHC VVYSITTLSS SLYLFIKYKT  274
P.vivax       177 KNCNLFMLPW IYRKLNDFHS MDVITFLIHC VGYSLSTFPS SLFLFLQYRS  226
P.falciparum  281 KYGNLYMLPW IYKKLNKFYN FDVTTFILHC IIYSISTLNS SLFLFIKYKT  330
                                                   TM1

P.yoelii      275 IAIIFPLFIT YIFFSAPFLL QEINGGRFVL DGCISFFNSI NTCHLPIAIS  324
P.berghei     275 IAIIFPLFIT YVFFSAPFLL QEINGGRFVL DGCISFFNSI NTCHLPIAIS  324
P.chabaudi    275 IAIIFPLFIT YMFFSAPFLL QEINGGRFVL DGCISFFNSI NSYHLPIAIS  324
P.vivax       227 LAIVFPLFFT YMCLSLPFLF QEINCGRFVL DGCLSFFVSL DYYHLPIGII  276
P.falciparum  331 FAIIFPLFIT YLLLSTPLVL QEINSGRFVL DGCISFFWSI NNYHLPIGII  380
                            TM2                                  TM3

P.yoelii      325 LIISYILSII KCIDSICLHL HYFSYYFLDK NPWVYKNLNN KICSKFNGNK  374
P.berghei     325 LIISYILSII KCIDSICLHL HYFSYYFLEK NPWVYKNLNN KICSKFNGNK  374
P.chabaudi    325 LLISYILSII KCIDSICLHL HYFSYYFIDK NPWVYKNLNN KICSKFNGNK  374
P.vivax       277 LIISYVLSII NCVDIICLQV IYFSFYLAPN NPWVYRNVDA KICSKFNASR  326
P.falciparum  381 LIISYILSII KCIDFISLHL LYLSSYLFEN NPWIYKNIDS KICSKFNGSK  430
                      TM3

P.yoelii      375 NICNISRNIC SYNIADGKCE INTMKLSMKM YDTLLRKYTE PKTKNFGEDI  424
P.berghei     375 NICNISRNIC SYNIADGKCE INTMKLSMKM YDTLLRKYTE PKTKNFGGSI  424
P.chabaudi    375 NICNIGRNIC SYNITDGKCE INTMKLSMKM YDTLLRKYTE PKTINFGGNV  424
P.vivax       327 SICDFARNIC FYNEATAVCE LNRVKLGTKI YDTLLSKYAE PKSEKFAAST  376
P.falciparum  431 NICDFSRNIC YYNDQTNICE INKIKLGTKI YDMLLNKYIP PKSEKFPILV  480

P.yoelii      425 VLYSFLFLFI YNSFSKYKSS NKLIKLFTFL IIFIFTIDII SLRDFSLIEL  474
P.berghei     425 VLYSFLFLFL YNSFSKYKSS NKLIKLFAFL IIFIFTIDII SLRDFSLIEL  474
P.chabaudi    425 VLYSFLFLFL YNSFSKYKSS NKLIKLFTFL IIFIFTIDII SLRDFSLLEL  474
P.vivax       377 VLLSFGLLIL YNAFSKFKTS HKVLKIHLSI LILVFASFII TMRDFSLLEF  426
P.falciparum  481 ILASFLSLIL YNAFSKYKTS HKFLKIFLFL LISLFLMNII TVWDFTLFEF  530
                            TM4                   TM5

P.yoelii      475 LSADLNISKI FNILSNHEVW ISCMIHCIVN MSFHSGIYFY TSKGLRLGIN  524
P.berghei     475 LSVDLNISKI FNILSNHEVW ISCMMHCIVN MSFHSGIYFY TSKGLRLGIN  524
P.chabaudi    475 LSVDLNVSKI FSILSNHEVW ISCMIHCIVN MSFHSGIYFY TSKGLRLGID  524
P.vivax       427 LLADFGWERV RGVLLDHEVW IACMMHCALS MSLHSGMYFY TAKGLRLGVN  476
P.falciparum  531 LLSDFNFNKI VDIILNYEVW ILCMLHCIVN LSIHSGLYFY TSKGLRLGIN  580
                                           TM6

P.yoelii      525 IIYCTYLIVM CCFLFDILIF ITFSVIIGNN LKNIENNYYF LLKLIKRNFY  574
P.berghei     525 IIYCTYLIVM CCFLFDILIF ITFSVIIGKN LKNIENNYYF LLKLIKRNFY  574
P.chabaudi    525 IIYCTYLIVM CCFLFDILIF ITFSVIIGKN LKNIENNYYF LLKLIKRNFY  574
P.vivax       477 VVRCACLTAL CCFLLDMLLF VTFSNIIGTH IKDIAKNYAY LVKLVKRNVF  526
P.falciparum  581 VVKSTYIITL SCFLVDMLIF VAFSNIIGKY LKDINRNYSF LLKLIKKNIF  630
                                 TM7

P.yoelii      575 YILVPVAHNY YNKFTLFLSI IFAFIYLTFM LISASKRIDV LFLSLNDIFH  624
P.berghei     575 YILVPVAHNY YNKFTLFLSI IFAFIYLNFM LISASKRIDI LFLSLNDIFH  624
P.chabaudi    575 YILVPVAHNY YNKFTLFLSI IFAFIYLTFM LISASKRIDI LFLSLNDIFH  624
P.vivax       527 YILLPVGNNC FSKFSFFLGI NISVVFLAFM LLAASKRVEI LFLSFDDVNF  576
P.falciparum  631 YILIPVGNNL YNKFTLFLGI YLGIIFLTFL LLSASKRIDI LFLSINDMYP  680
                                      TM8

P.yoelii      625 FRGNTQNKII TLGWIFIFCL YYIYKSININ YLDICITQLS HIIILLILFY  674
P.berghei     625 FRGNTKKKII ALGWIFIFCL YYIYKSININ YLDICITQLS HIIILLILFY  674
P.chabaudi    625 FRGPTKQKMI TLGWIFIFCL YYIYRSININ YLDICITQLS HIIILLILFY  674
P.vivax       577 FK--PKSRWF DVRWVFLFLL YYLYSSVDIT FLDLFFTEMS QIVTLLILFY  624
P.falciparum  681 LN---SKKHI TIVWIVIFFI YINYIFLDNE IRYILCQYVY QLITLLILFY  727
                                 TM9                            TM10

P.yoelii      675 INFNFFWIRG IKKTAQKIGL FPLSLNMILI FLNEFIFMYC EIRLKLQNRV  724
P.berghei     675 INFNFFWIRG INKTTKKIGL FPLALNMILI FLNEFIFMYF EILLKLQNRV  724
P.chabaudi    675 INFNFFWIRG IKKTAKKIGL FPLALNMILI FLNEFTFMYF EIFLKLQNRV  724
P.vivax       625 INFNFFWVRG FNKTMDKFGM CPLLCQVVLT ALNLFLFFYF EIIFRLPNRV  674
P.falciparum  728 INFNFFWLSG IKETVNKLGK LPLISKFFFT FLNEFSLLYL EIIYNVKYRI  777
                  TM10                        TM11

P.yoelii      725 LLYFIRQFIN IFIIPLFSIF TYSVFQWISC RSPHS---LL KEITK-IYLL  770
P.berghei     725 LLYFIRQFIN IFIIPLFSIL IYSTLQWISY RNSNSTLFGL KEIAK-INLL  773
P.chabaudi    725 LLYFIRQFIN IFIIPLCSIF TYSVFQCIAC RNPGSAPFGL KEMTK-SYLL  773
P.vivax       675 PLYLVRQLVN ICVIPLVSVL LSRCASFGGP KQPRGG--GL RQILADAYEL  722
P.falciparum  778 SFFFIRQFIN ILIIPLLSML ISSYLSNMRK KRKTKVKKGI KYILQNSYSL  827
                                 TM12

P.yoelii      771 IIGNIDKSKH IQLEFNKNSK YIDWFNIYLI IFFRYFAMDL IFMCFLHLWN  820
P.berghei     774 IIGNIDKSKH IQIEFNKNSK YMNWYNIYLI IFFRYFAMDL IFMCFLHLWN  823
P.chabaudi    774 IVGDIDKSKH IQLEFKNNSK YMKWFNLYMV IFFRYFAMDL IFMCFLHLWN  823
P.vivax       723 ATECADKSKN IQLEPSQTS- --KWFNIYLI LFCKYLGIDL IFMCFVHVGS  769
P.falciparum  828 AIEYTSKNKN IQLEYIQKMK YTKWFNIYII FFLKYIGLDI ILMCIVYVGN  877
                                                      TM13

P.yoelii      821 EFLIKNEAFF NLENIIWGID PYLFFFLLYV IYVYICYLHV PLLILIKKKN  870
P.berghei     824 EFLIKNEAFF NLKNIIWGID PYFFFFLLYV IYVYICYLHV PLLILIKKKN  873
P.chabaudi    824 EFLIKNEAFF NLENIIFGID PYLFFFLLYV IYVYICYLHV PLLILIKKKK  873
P.vivax       770 SIFSIKENFF KKKNVHLQTD PYLLFFLLFL CYVYVAYVNV PLLQLIKRRK  819
P.falciparum  878 KLCSQNEIYL KKRNINILLS QY-FLFIIFL LYVYISYINI PLLHIIKRKL  926
                                                 TM14

P.yoelii      871 IFKINNFNIL DYHIPFDKIK RNQKNSFYGE FSIRG----- - 905
P.berghei     874 IFKVNNFNIL DYHIPFDKIK RNKKNSFYGE FSLRG----- - 908
P.chabaudi    874 IFKVNNFNIL DYPIPFDQIK QNKKSSFYGE FSIRG----- - 908
P.vivax       820 LFPVNKFSIL DYPVCPEEPR RPRRGLLFEE FKRGRLKKSA S 860
P.falciparum  927 FFKPNNFNVL DYPVSFEKIK HQKKNSLFSE FINM------ - 960
```

Supplementary Fig. 4. GEP1 sequence alignment among *Plasmodium* parasites.

Aligned GEP1 amino acid sequences from *P. falciparum*, *P. vivax*, *P. chabaudi*, *P. berghei*, and *P. yoelii* (GeneID in PlasmoDB: PF3D7_0515500, PVP01_1018400, PCHAS_1114700, PBANKA_1115100, PY17X_1116300). Fourteen predicted transmembrane domains (TM1- TM14) are underlined.

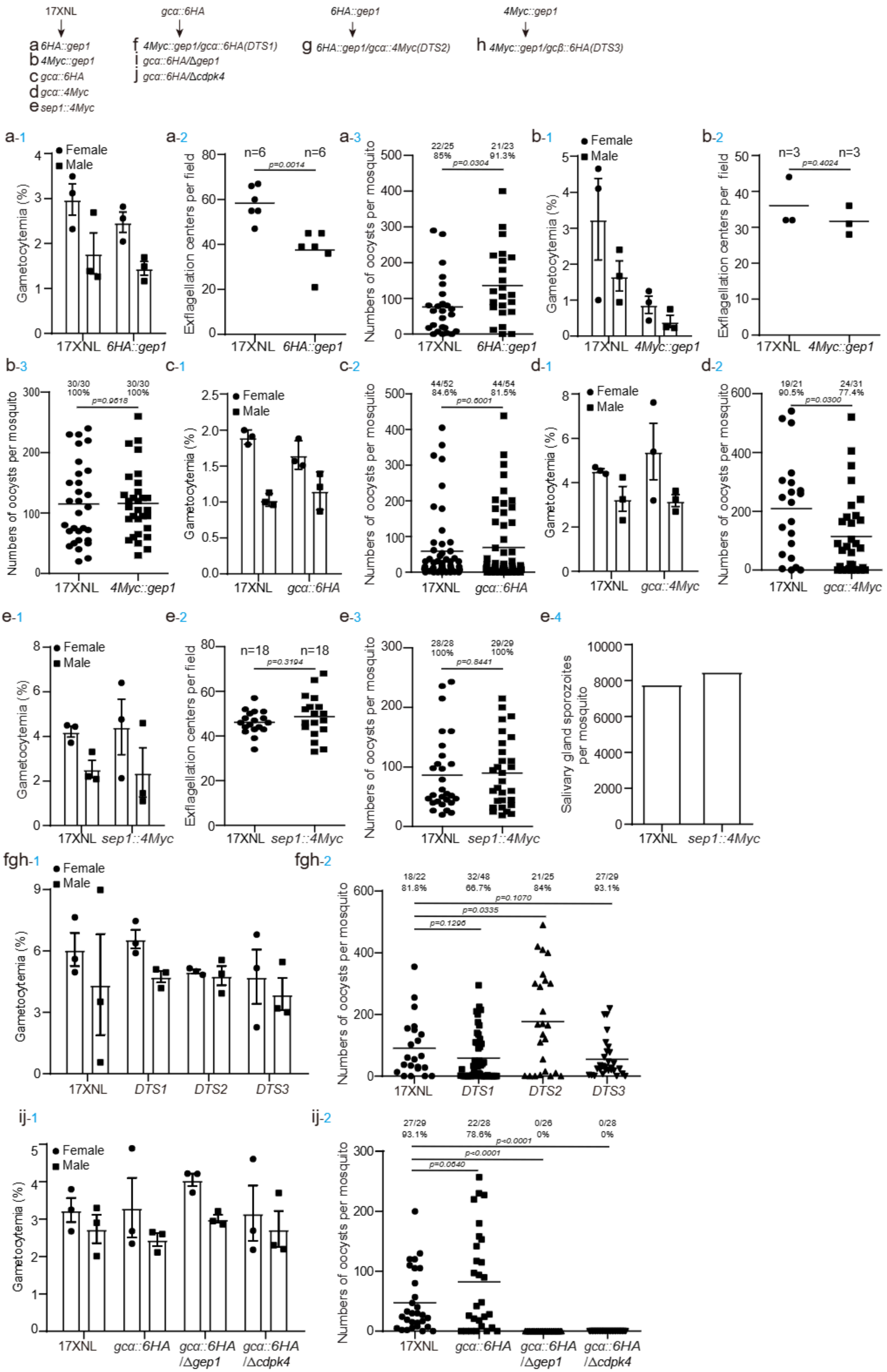

17XNL
a 6HA::gep1
b 4Myc::gep1
c gcα::6HA
d gcα::4Myc
e sep1::4Myc
gcα::6HA
f 4Myc::gep1/gcα::6HA(DTS1)
i gcα::6HA/Δgep1
j gcα::6HA/Δcdpk4
6HA::gep1
g 6HA::gep1/gcα::4Myc(DTS2)
4Myc::gep1
h 4Myc::gep1/gcβ::6HA(DTS3)
a-1
Female
Male
Gametocytemia (%)
17XNL
6HA::gep1
a-2
Exflagellation centers per field
n=6
p=0.0014
a-3
Numbers of oocysts per mosquito
22/25
85%
21/23
91.3%
p=0.0304
b-1
4Myc::gep1
b-2
n=3
p=0.4024
b-3
30/30
100%
p=0.9618
c-1
gcα::6HA
c-2
44/52
84.6%
44/54
81.5%
p=0.6001
d-1
gcα::4Myc
d-2
19/21
90.5%
24/31
77.4%
p=0.0300
e-1
sep1::4Myc
e-2
n=18
p=0.3194
e-3
28/28
100%
29/29
100%
p=0.8441
e-4
Salivary gland sporozoites per mosquito
fgh-1
DTS1
DTS2
DTS3
fgh-2
18/22
81.8%
32/48
66.7%
21/25
84%
27/29
93.1%
p=0.1070
p=0.0335
p=0.1296
ij-1
gcα::6HA /Δgep1
gcα::6HA /Δcdpk4
ij-2
27/29
93.1%
22/28
78.6%
0/26
0%
0/28
0%
p<0.0001
p<0.0001
p=0.0640

Supplementary Fig. 5. Parasite growth in mouse and mosquito of some strains. Male and female gametocytes in mouse, *in vitro* exflagellation of male gametocytes, midgut oocyst formation and salivary gland sporozoite formation in mosquito of the modified parasites, including the *6HA::gep1* (**a**), *4Myc::gep1* (**b**), *gcα::6HA* (**c**), *gcα::4Myc* (**d**), *sep1::4Myc* (**e**), *DTS1* (**f**), *DTS2* (**g**), *DTS3* (**h**), and *gcα::6HA/Δgep1* (**i**, GEP1 disruption in the *gcα::6HA*) and *gcα::6HA/Δcdpk1* (**j**, CDPK1 disruption in the *gcα::6HA*). Gametocytemia count was repeated three times, exflagellation and mosquito infection was performed one time to ensure the normal life cycle progression of these parasites. n in the exflagellation experiments is the numbers of microscopic fields counted (40X). x/y on the top of the oocyst count is the number of mosquito containing oocyst / the number of mosquito dissected; the percentage number is the mosquito infection prevalence. Gametocytemia data are shown as mean ± SEM. Two-tailed unpaired Student's t test was used in the exflagellation and oocyst counting.

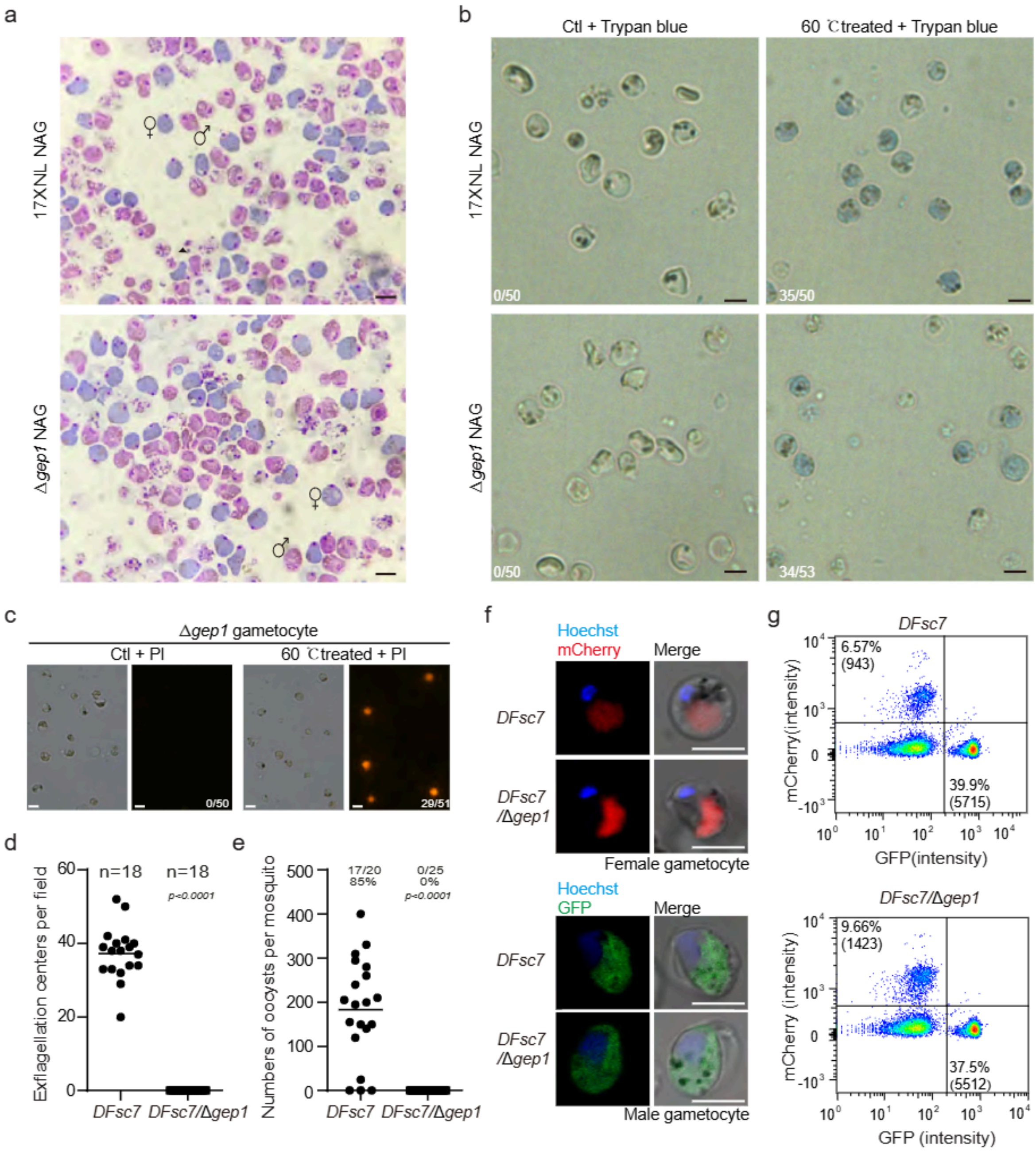
a
b
Ctl + Trypan blue
60 ℃treated + Trypan blue
17XNL NAG
Δgep1 NAG
0/50
35/50
0/50
34/53
c
Δgep1 gametocyte
Ctl + PI
60 ℃treated + PI
0/50
29/51
d
Exflagellation centers per field
n=18
n=18
p<0.0001
DFsc7
DFsc7/Δgep1
e
Numbers of oocysts per mosquito
17/20
85%
0/25
0%
p<0.0001
DFsc7
DFsc7/Δgep1
f
Hoechst
mCherry
Merge
DFsc7
DFsc7
/Δgep1
Female gametocyte
Hoechst
GFP
Merge
DFsc7
DFsc7
/Δgep1
Male gametocyte
g
DFsc7
6.57%
(943)
39.9%
(5715)
mCherry(intensity)
GFP(intensity)
DFsc7/Δgep1
9.66%
(1423)
37.5%
(5512)
mCherry (intensity)
GFP (intensity)

Supplementary Fig. 6. Gametocytes without GEP1 are viable.

a, Giemsa staining of the purified non-activated gametocytes (NAG). **b,** Cell viability analysis of the gametocytes by Trypan blue staining. **c,** Cell viability analysis of the Δ*gep1* gametocytes by propidium iodide (PI) staining. x/y in the **b** and **c** are the number of cell displaying signal / the number of cell counted. **d**, EC formation of the *DFsc7* and *DFsc7*/Δ*gep1* parasites after XA stimulation *in vitro*. n is the numbers of microscopic fields counted. **e,** Day 7 midgut oocysts counts from mosquitoes infected with *DFsc7* or *DFsc7*/Δ*gep1* parasites. Mosquito infection prevalence is shown above. **f,** GFP expression in male gametocytes and mCherry expression in female gametocytes of the *DFsc7* and *DFsc7*/Δ*gep1* parasites. **g,** Flow cytometry detection of GFP and mCherry fluorescence in male and female gametocytes of the *DFsc7* and *DFsc7*/Δ*gep1* parasites. Cell number and percentage are shown in the quadrants of the FACS plots. Scale bar = 5 μm for all images in this figure. Experiments in this figure were independently repeated three times with similar results. Two-tailed unpaired Student's t test in **d** and **e**.

a

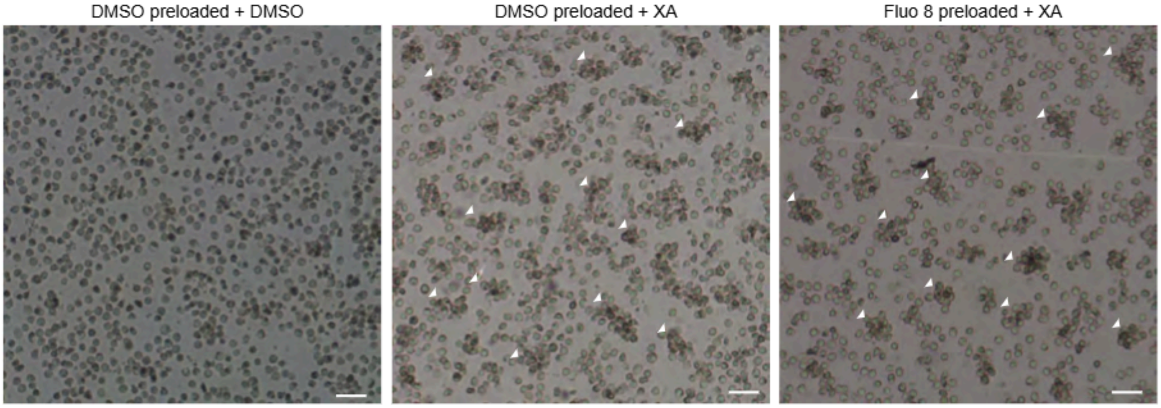
DMSO preloaded + DMSO
DMSO preloaded + XA
Fluo 8 preloaded + XA

b

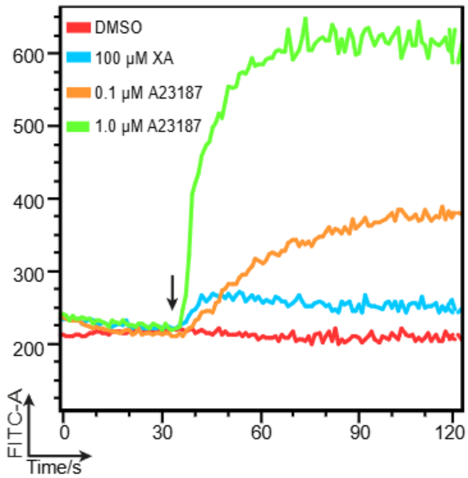
DMSO
100 μM XA
0.1 μM A23187
1.0 μM A23187
600
500
400
300
200
FITC-A
0
30
60
90
120
Time/s

Supplementary Fig. 7. Cellular Ca^{2+} mobilization in activated gametocytes.

a, WT gametocytes pre-loaded with Fluo-8 are capable of forming XA-stimulated ECs (white arrows) *in vitro*. Scale bar = 20 μm. **b,** Cellular Ca^{2+} signals in Fluo-8 pre-loaded WT gametocytes in response to A23187 (Ca^{2+} ionophore) and XA stimulation using flow cytometry analysis. Purified gametocytes were preloaded with Ca^{2+} probe Fluo-8, and signals were collected 30 seconds before addition of A23187, XA, or DSMO. Black arrows indicate the time for chemical addition. Experiments in this figure were independently repeated three times with similar results.

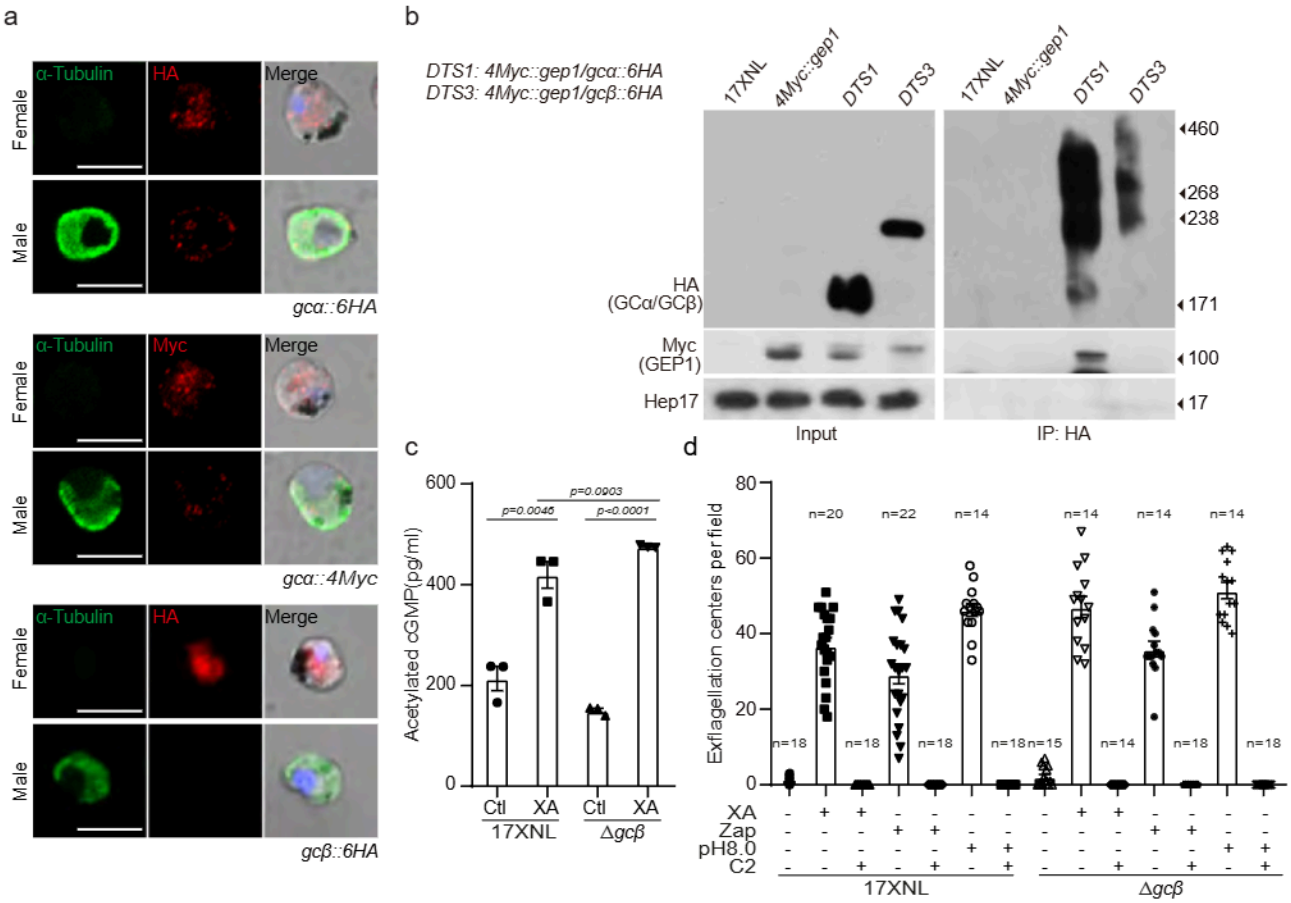
a
α-Tubulin
HA
Merge
Female
Male
gcα::6HA
α-Tubulin
Myc
Merge
Female
Male
gcα::4Myc
α-Tubulin
HA
Merge
Female
Male
gcβ::6HA
b
DTS1: 4Myc::gep1/gcα::6HA
DTS3: 4Myc::gep1/gcβ::6HA
17XNL
4Myc::gep1
DTS1
DTS3
HA (GCα/GCβ)
Myc (GEP1)
Hep17
Input
IP: HA
460
268
238
171
100
17
c
Acetylated cGMP(pg/ml)
p=0.0046
p=0.0903
p<0.0001
Ctl
XA
17XNL
Δgcβ
d
Exflagellation centers per field
n=18
n=20
n=22
n=14
n=15
XA
Zap
pH8.0
C2
17XNL
Δgcβ

Supplementary Fig. 8. GCβ is not involved in cGMP signaling of gametogenesis.

a, IFA of GCα and GCβ expression in female and male gametocytes of the *gcα::6HA*, *gcα::4Myc*, and *gcβ::6HA* parasites. α-Tubulin is a male gametocyte specific protein. Scale bar = 5 μm. **b,** Co-immunoprecipitation of GEP1 and GCβ in gametocyte extract of the *4Myc::gep1/gcβ::6HA* parasites (Double Tagged Strain 3, *DTS3*). IP-HA, anti-HA antibody was used in pulldown. **c**, Enzyme immunoassay detecting intracellular cGMP level in XA-stimulated gametocytes of the 17XNL and △*gcβ* parasites. Cells were incubated with 100 μM XA at 22°C for 2 min before assay. Ctl is control group without XA stimulation. **d**, *In vitro* EC formation of the 17XNL and △*gcβ* parasites after stimulation with XA (100 μM), Zaprinast (Zap, 100 μM), or pH 8.0 alone at 22°C, or conjugated with compound 2 (C2, 5 μM). Experiments in this figure were independently repeated three times. Data are represented as mean ± SEM in **c** and **d**, two-tailed unpaired Student's t test in **c**.

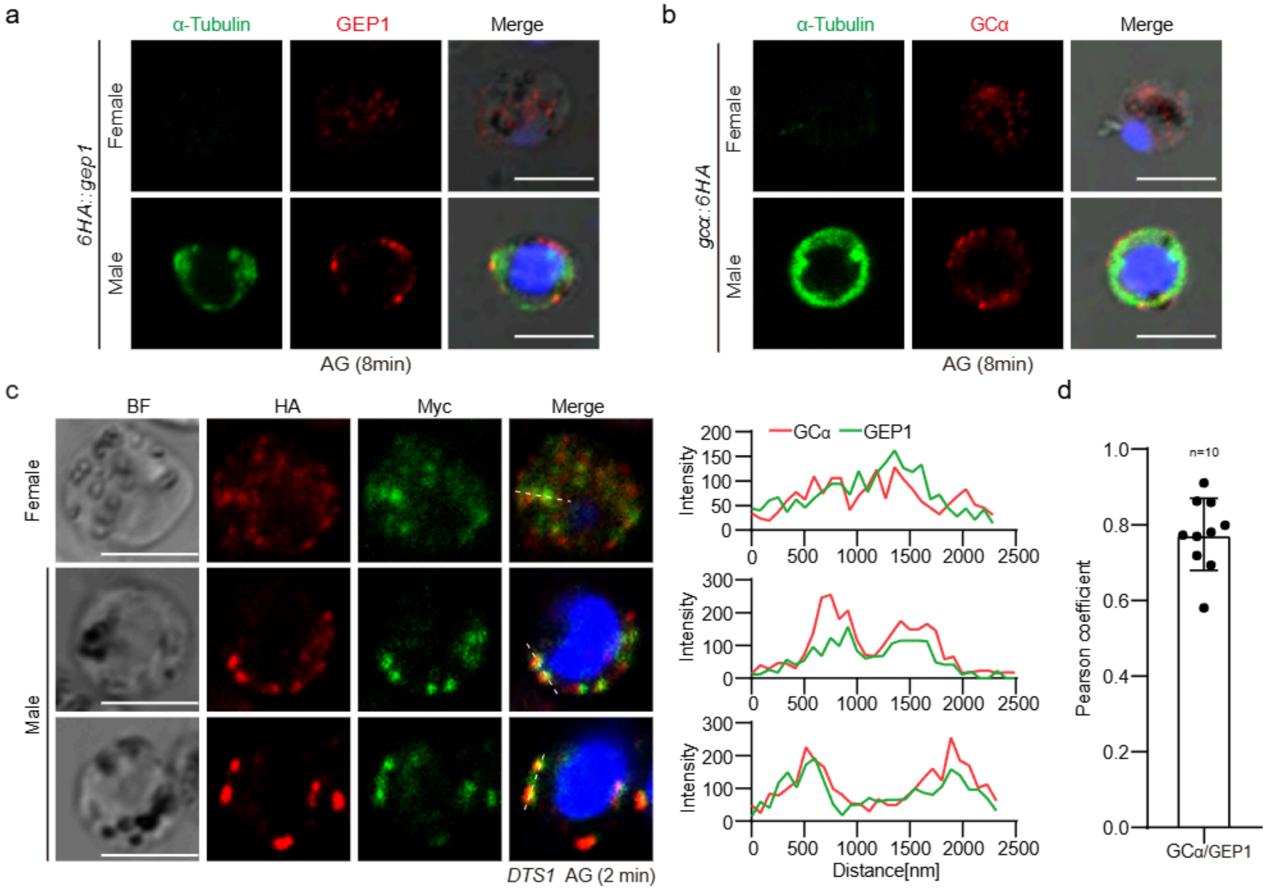

a
α-Tubulin
GEP1
Merge
6HA::gep1
Female
Male
AG (8min)
b
α-Tubulin
GCα
Merge
gcα::6HA
Female
Male
AG (8min)
c
BF
HA
Myc
Merge
Female
Male
DTS1 AG (2 min)
GCα
GEP1
Intensity
Distance[nm]
d
n=10
Pearson coefficient
GCα/GEP1

Supplementary Fig. 9. GEP1 co-localizes with GCα in activated gametocytes.

a, Co-staining of GEP1 and α-Tubulin expressions in the activated gametocytes (AG) of the *6HA::gep1* parasite 8 min post XA stimulation. **b**, Co-staining GCα and α-Tubulin in the *gcα::6HA* gametocytes 8 min post XA stimulation. **c**, Co-staining of GEP1 and GCα in the *DTS1* gametocytes 2 min post XA stimulation using anti-HA (GCα) and anti-Myc (GEP1) antibodies (left panel). Activated male gametocytes were observed with enlarged nucleus. Cross sections (white dash line) of the cells show the co-localization of GEP1 and GCα (right panel). Scale bar = 5 μm. **d**, Pearson coefficient analysis for GEP1 and GCα co-localization shown in **c**, data are shown as mean ± SD from n=10 cells measured. Scale bar = 5 μm for all image in this figure. Experiments in this figure were independently repeated three times with similar results.

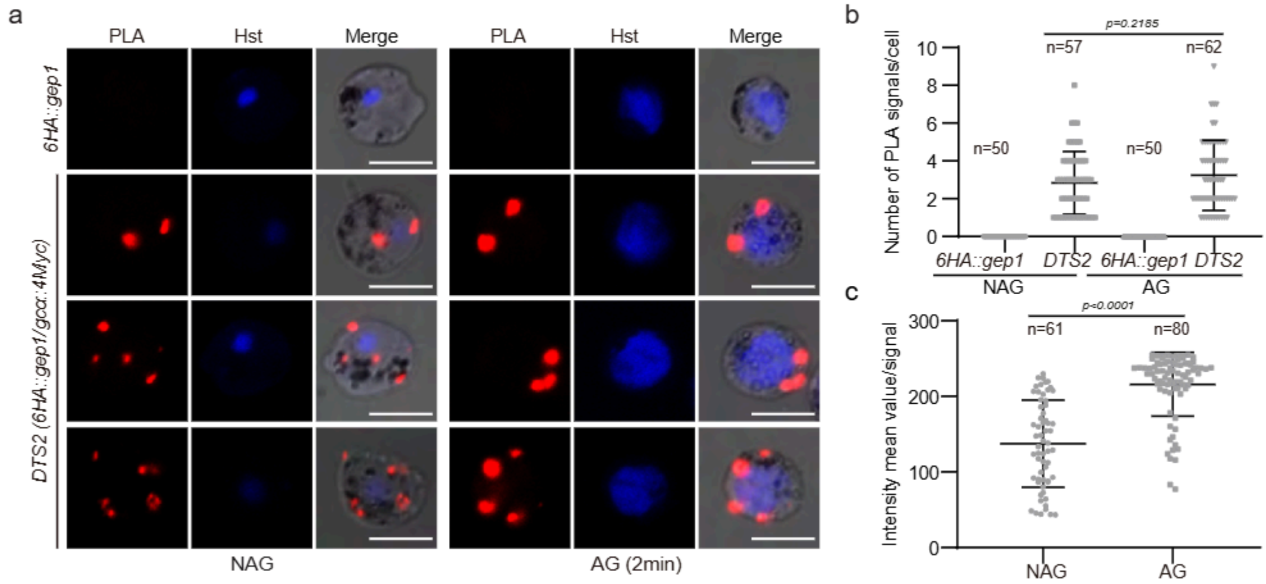
a
PLA
Hst
Merge
PLA
Hst
Merge
6HA::gep1
DTS2 (6HA::gep1/gcα::4Myc)
NAG
AG (2min)
b
p=0.2185
n=57
n=62
n=50
n=50
Number of PLA signals/cell
10
8
6
4
2
0
6HA::gep1
DTS2
6HA::gep1
DTS2
NAG
AG
c
p<0.0001
n=61
n=80
Intensity mean value/signal
300
200
100
0
NAG
AG

Supplementary Fig. 10. XA stimulation likely enhances GEP1/GCα interaction.

a, Proximity Ligation Assay (PLA) detecting protein interaction between GEP1 and GCα in *DTS2* gametocytes. NAG: non-activated, AG: 2 min after XA stimulation. Activated male gametocytes were observed with enlarged nucleus. Scale bar = 5 μm. **b**, Number of PLA signal dot in each cell shown in **a**, n is the number of cells counted. **c**, Fluorescence intensity value for each PLA signal dot shown in **a**. n is the number of PLA signal dot measured. Experiment was repeated three times independently with similar results. Data are represented as mean ± SD; two-tailed unpaired Student's t test in **b** and **c**.

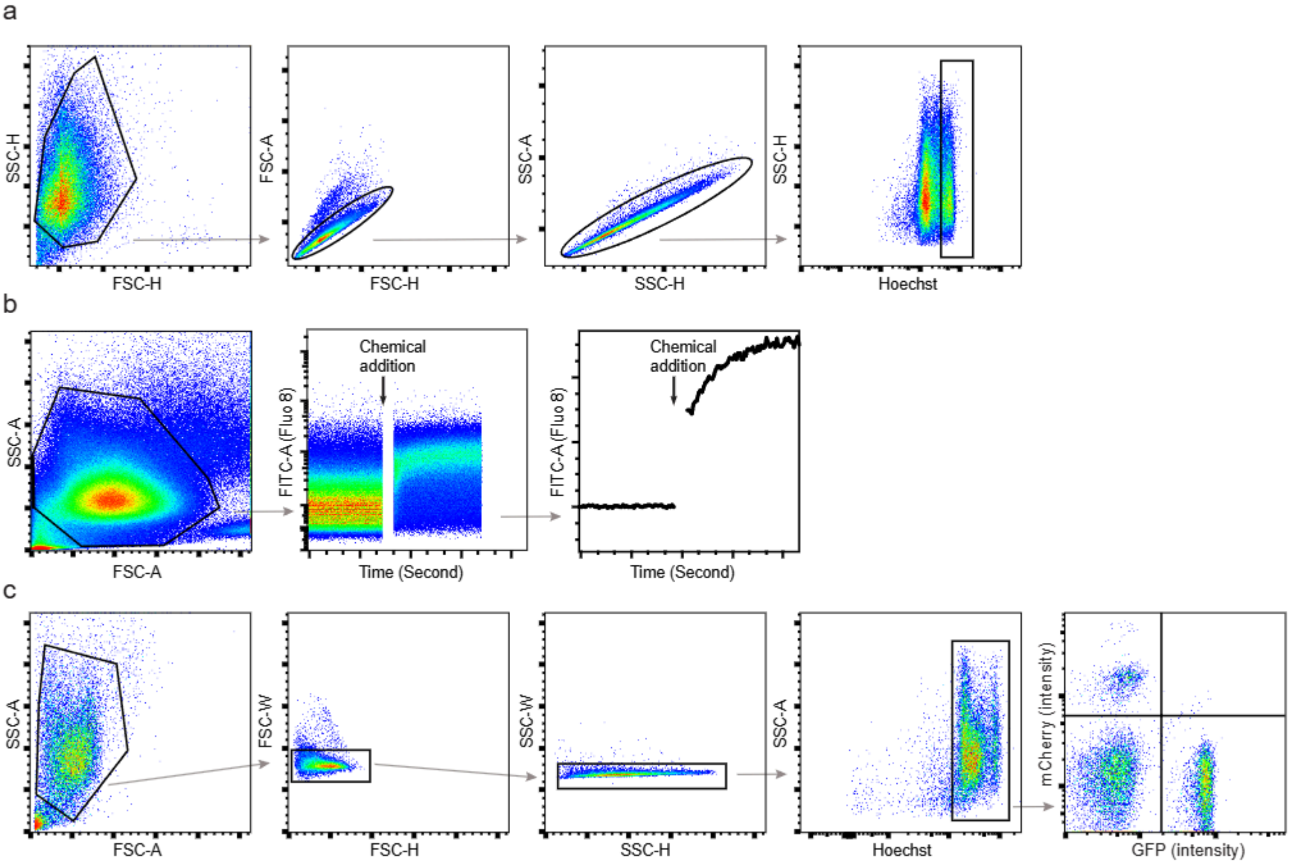

a
SSC-H
FSC-H
FSC-A
FSC-H
SSC-A
SSC-H
SSC-H
Hoechst
b
SSC-A
FSC-A
FITC-A (Fluo 8)
Chemical addition
Time (Second)
FITC-A (Fluo 8)
Chemical addition
Time (Second)
c
SSC-A
FSC-A
FSC-W
FSC-H
SSC-W
SSC-H
SSC-A
Hoechst
mCherry (intensity)
GFP (intensity)

Supplementary Fig. 11. Gating strategies used for cell sorting in flow cytometry.

a, Gating strategy to sort activated male gametocytes with rounds of genome duplication from the purified gametocytes (including male and female) pre-stained with Hoechst 33342 presented on Figure. 3b. **b**, Gating strategy to sort gametocyte preloaded with Fluo-8 presented on Figure. 3d and Supplementary Figure. 7b. Black arrows indicate the time for A23187, XA or DMSO addition. Signals were collected at 30 sec before until 90 sec post addition. **c**, Gating strategy to sort male (GFP+) and female (mCherry+) gametocytes from Hoechst 33342 pre-stained parasites containing gametocytes and asexual blood stage parasites presented on Supplementary Figure. 6g. Infected mice were phenylhydrazine treated for inducing gametocytes and sulfadiazine treated to reduce asexual blood stage parasites. Parasites were further purified via nycodenz centrifugation before flow cytometry analysis.

Supplementary Table 1. List of candidate gene for screening in this study.

Gene ID	Description	Ortholog in *P.falciparum*	Ortholog in *P.beighei*	Number of TM predicted	Blood-stage phenotype in *P.berghei* from *PlasmoGEM* database	Blood-stage phenotype in this study
PY17X_1243400	7-helix-1 protein, putative	PF3D7_0525400	PBANKA_1240200	3	Dispensable	Dispensable
PY17X_1431500	integral membrane protein GPR180, putative	PF3D7_1213500	PBANKA_1429300	7	Dispensable	Dispensable
PY17X_0918700	serpentine receptor, putative	PF3D7_1131100	PBANKA_0917100	7	Slow	Dispensable
PY17X_1433900	serpentine receptor, putative	PF3D7_1215900	PBANKA_1431600	8	Not tested	Dispensable
PY17X_0524600	serpentine receptor, putative	PF3D7_0422800	PBANKA_0523200	8	Dispensable	Dispensable
PY17X_1421700	GPCR-like receptor SR25, putative	PF3D7_0713400	PBANKA_1420000	8	Essential	Essential
PY17X_0605800	sexual stage-specific protein G37, putative	PF3D7_1204400	PBANKA_0603300	7	Not tested	Dispensable
PY17X_0617400	conserved Plasmodium membrane protein, unknown function	PF3D7_0717000	PBANKA_0614700	7	Not tested	Dispensable
PY17X_0914700	conserved Plasmodium membrane protein, unknown function	PF3D7_1135300	PBANKA_0913200	7	Essential	Essential
PY17X_1128600	protease, putative	PF3D7_0628400	PBANKA_1127100	8	Dispensable	Dispensable
PY17X_1313900	conserved Plasmodium protein, unknown function	PF3D7_1446300	PBANKA_1310000	8	Not tested	Dispensable
PY17X_0702400	folate transporter 1, putative	PF3D7_0828600	PBANKA_0702100	12	Dispensable	Dispensable
PY17X_0933500	folate transporter 2, putative	PF3D7_1116500	PBANKA_0931500	11	Dispensable	Dispensable
PY17X_0309400	GDP-fructose; GMP antiporter, putative	PF3D7_0212000	PBANKA_0308800	8	Not tested	Dispensable
PY17X_0936300	UDP-galactose transporter, putative	PF3D7_1113300	PBANKA_0934300	8	Essential	Dispensable
PY17X_1436400	phosphate translocator, putative	PF3D7_1218400	PBANKA_1434000	10	Dispensable	Dispensable
PY17X_0823700	major facilitator superfamily domain-containing protein, putative	PF3D7_0919500	PBANKA_0820400	12	Dispensable	Dispensable
PY17X_0820300	major facilitator superfamily domain-containing protein, putative	PF3D7_0916000	PBANKA_0817000	11	Dispensable	Dispensable
PY17X_1116300	amino acid transporter, putative	PF3D7_0515500	PBANKA_1115100	14	Dispensable	Dispensable
PY17X_0307300	transporter, putative	PF3D7_0209600	PBANKA_0306700	13	Essential	Essential
PY17X_0917400	amino acid transporter	PF3D7_1132500	PBANKA_0915900	15	Not tested	Dispensable
PY17X_0609400	amino acid transporter, putative	PF3D7_1208400	PBANKA_0606900	10	Dispensable	Dispensable
PY17X_1448600	amino acid transporter, putative	PF3D7_1231400	PBANKA_1446100	10	Essential	Essential
PY17X_1241000	multidrug resistance protein 1, putative	PF3D7_0523000	PBANKA_1237800	11	Essential	Essential
PY17X_1446300	multidrug resistance-associated protein 2, putative	PF3D7_1229100	PBANKA_1443800	11	Slow	Dispensable
PY17X_1315500	multidrug resistance protein 2, putative	PF3D7_1447900	PBANKA_1311700	10	Slow	Dispensable
PY17X_0904900	ABC transporter B family member 3, putative	PF3D7_1145500	PBANKA_0903500	6	Not tested	Dispensable
PY17X_0403400	ABC transporter B family member 4, putative	PF3D7_0302600	PBANKA_0401200	3	Dispensable	Dispensable
PY17X_1358700	ABC transporter B family member 5, putative	PF3D7_1339900	PBANKA_1353300	4	Slow	Dispensable
PY17X_0928600	protein GCN20, putative	PF3D7_1121700	PBANKA_0926600	0	Dispensable	Dispensable
PY17X_1370600	ABC transporter B family member 6, putative	PF3D7_1352100	PBANKA_1364800	4	Essential	Essential
PY17X_0610800	ABC transporter B family member 7, putative	PF3D7_1209900	PBANKA_0608300	6	Not tested	Dispensable
PY17X_1145400	ABC transporter E family member 1, putative	PF3D7_1368200	PBANKA_1144100	0	Essential	Essential
PY17X_1019600	ABC transporter G family member 2, putative	PF3D7_1426600	PBANKA_1018000	5	Slow	Dispensable
PY17X_1425800	ABC transporter F family member 1, putative	PF3D7_0813700	PBANKA_1423800	0	Essential	Essential
PY17X_1222000	ABC transporter I family member 1, putative	PF3D7_0319700	PBANKA_1218800	13	Essential	Essential
PY17X_1031600	FeS assembly ATPase SufC, putative	PF3D7_1413500	PBANKA_1029200	1	Essential	Dispensable
PY17X_0407300	ER membrane protein complex subunit 5, putative	PF3D7_0306700	PBANKA_0405100	2	Essential	Essential
PY17X_0929900	CorA-like Mg2+ transporter protein, putative	PF3D7_1120300	PBANKA_0927900	2	Not tested	Dispensable
PY17X_1018500	CorA-like Mg2+ transporter protein, putative	PF3D7_1427600	PBANKA_1017000	2	Dispensable	Dispensable
PY17X_0703300	magnesium transporter, putative	PF3D7_0827700	PBANKA_0703000	9	Not tested	Dispensable
PY17X_1240600	inner membrane complex protein, putative	PF3D7_0522600	PBANKA_1237300	8	Dispensable	Dispensable
PY17X_1441100	vacuolar iron transporter, putative	PF3D7_1223700	PBANKA_1438600	5	Dispensable	Dispensable
PY17X_1367300	E1-E2 ATPase, putative	PF3D7_1348800	PBANKA_1361600	10	Not tested	Dispensable
PY17X_0109300	zinc transporter ZIP1, putative	PF3D7_0609100	PBANKA_0107700	8	slow	Essential
PY17X_1424200	cation diffusion facilitator family protein, putative	PF3D7_0715900	PBANKA_1422200	4	Dispensable	Dispensable
PY17X_1105200	MOLO1 domain-containing protein, putative	PF3D7_0504500	PBANKA_1104100	2	Dispensable	Dispensable
PY17X_1315200	conserved protein, unknown function	PF3D7_1447600	PBANKA_1311400	1	Dispensable	Dispensable
PY17X_1339400	transmembrane protein 43, putative	PF3D7_1471500	PBANKA_1334700	4	Dispensable	Dispensable
PY17X_1342800	conserved protein, unknown function	PF3D7_1322900	PBANKA_1338100	2	Dispensable	Dispensable
PY17X_1366100	conserved protein, unknown function	PF3D7_1347600	PBANKA_1360400	1	Dispensable	Dispensable
PY17X_1463300	dipeptidyl aminopeptidase 2, putative	PF3D7_1247800	PBANKA_1460700	1	Dispensable	Dispensable
PY17X_0911700	guanylyl cyclase, putative	PF3D7_1138400	PBANKA_0910300	19	slow	Essential
PY17X_1138200	guanylyl cyclase beta	PF3D7_1360500	PBANKA_1136700	22	slow	Dispensable
PY17X_0619700	LEM3/CDC50 family protein	PF3D7_0719500	PBANKA_0617000	2	Not tested	Dispensable
PY17X_0916600	LEM3/CDC50 family protein, putative	PF3D7_1133300	PBANKA_0915100	2	Dispensable	Dispensable
PY17X_0809500	P-type ATPase, putative	PF3D7_0319000	PBANKA_0806300	10	Dispensable	Dispensable
PY17X_1437200	aminophospholipid-transporting P-ATPase, putative	PF3D7_1219600	PBANKA_1434800	9	Essential	Essential
PY17X_1440800	phospholipid-ansporting ATPase, putative	PF3D7_1223400	PBANKA_1438300	10	slow	Essential

Supplementary Table 2. GEP1 interacted proteins detected by Mass spectrum.

Protein	Probability	Unique peptides	Gene_ID	Description	Protein size/aa
tr|V7PTB0|V7PTB0_9APIC	1	21	PY17X_1347900	conserved Plasmodium protein, unknown function	2308
tr|V7PT05|V7PT05_9APIC	1	19	PY17X_1226000	tyrosine--tRNA ligase, putative	372
tr|V7PFK1|V7PFK1_9APIC	**1**	**15**	**PY17X_0911700**	**guanylyl cyclase, putative**	**3850**
tr|V7PBU4|V7PBU4_9APIC	1	15	PY17X_1109100	conserved protein, unknown function	390
tr|V7PHN7|V7PHN7_9APIC	1	13	PY17X_0404000	HAD superfamily protein, putative	1115
tr|V7PBN0|V7PBN0_9APIC	1	10	PY17X_1114400	deoxyribodipyrimidine photo-lyase, putative	849
tr|V7PNU6|V7PNU6_9APIC	1	10	PY17X_0807500	conserved Plasmodium protein, unknown function	1878
tr|V7PDR5|V7PDR5_9APIC	1	9	PY17X_0922400	conserved Plasmodium protein, unknown function	1961
tr|V7PGJ3|V7PGJ3_9APIC	1	9	PY17X_0706700	conserved Plasmodium protein, unknown function	1108
tr|V7PVM5|V7PVM5_9APIC	1	9	PY17X_1221300	oocyst capsule protein Cap380, putative	3290
tr|V7PV53|V7PV53_9APIC	1	8	PY17X_0113800	myosin E, putative	2403
tr|V7PDP7|V7PDP7_9APIC	1	7	PY17X_0501900	reticulocyte binding protein, putative	2748
tr|V7PGA5|V7PGA5_9APIC	1	6	PY17X_0623600	conserved Plasmodium protein, unknown function	1140
tr|V7PJ59|V7PJ59_9APIC	1	6	PY17X_0520600	conserved Plasmodium protein, unknown function	225
tr|V7PU86|V7PU86_9APIC	1	6	PY17X_1322800	conserved protein, unknown function	800
tr|V7PYL5|V7PYL5_9APIC	1	6	PY17X_0103000	SAC3 domain-containing protein, putative	1203
tr|V7PAS9|V7PAS9_9APIC	1	5	PY17X_0710300	2-oxoglutarate dehydrogenase E1 component, putative	1038
tr|V7PBN8|V7PBN8_9APIC	1	5	PY17X_1370200	inner membrane complex protein 1f, putative	1122
tr|V7PI71|V7PI71_9APIC	1	5	PY17X_0526500	reticulocyte binding protein, putative	2757
tr|V7PN10|V7PN10_9APIC	1	5	PY17X_1016800	rRNA (adenosine-2'-O-)-methyltransferase, putative	2379
tr|V7PNJ6|V7PNJ6_9APIC	1	5	PY17X_1135900	Sas10 domain-containing protein, putative	761
tr|V7PP62|V7PP62_9APIC	1	5	PY17X_0216200	Plasmodium exported protein, unknown function	278
tr|V7PRL1|V7PRL1_9APIC	1	5	PY17X_1223000	Cg2 protein, putative	2439
tr|V7PDA4|V7PDA4_9APIC	1	4	PY17X_1102000	fam-a protein	609
tr|V7PIB6|V7PIB6_9APIC	1	4	PY17X_0411100	eukaryotic translation initiation factor 3 subunit K,	235
tr|V7PMC7|V7PMC7_9APIC	1	4	PY17X_1032900	mini-chromosome maintenance complex-binding protein, putative	910
tr|V7PQH8|V7PQH8_9APIC	1	4	PY17X_1452400	CCR4-NOT transcription complex subunit 4, putative	1408
tr|V7PSJ6|V7PSJ6_9APIC	1	4	PY17X_1430600	glycerol-3-phosphate 1-O-acyltransferase, putative	583
tr|V7PXA8|V7PXA8_9APIC	1	4	PY17X_0103400	conserved Plasmodium protein, unknown function	499
tr|V7PXF5|V7PXF5_9APIC	1	4	PY17X_0106800	conserved Plasmodium protein, unknown function	1921
tr|V7PD97|V7PD97_9APIC	1	4	PY17X_0911300	WD repeat-containing protein, putative	1647
tr|V7PJS9|V7PJS9_9APIC	1	4	PY17X_0417200	formate-nitrite transporter, putative	311
tr|V7PKF4|V7PKF4_9APIC	1	4	PY17X_0419100	nucleoporin NUP221, putative	2003
tr|V7PUE6|V7PUE6_9APIC	1	4	PY17X_0101221	reticulocyte binding protein, putative	2771
tr|V7PBU9|V7PBU9_9APIC	1	3	PY17X_0301500	repetitive organellar protein, putative	1980
tr|V7PDJ6|V7PDJ6_9APIC	1	3	PY17X_0915300	DNA-directed RNA polymerase I subunit RPA2, putative	1470
tr|V7PDS4|V7PDS4_9APIC	1	3	PY17X_0309500	conserved Plasmodium protein, unknown function	987
tr|V7PFR2|V7PFR2_9APIC	1	3	PY17X_0934500	histone-lysine N-methyltransferase SET7, putative	707
tr|V7PI90|V7PI90_9APIC	1	3	PY17X_0419300	copper-transporting ATPase, putative	1981
tr|V7PIU0|V7PIU0_9APIC	1	3	PY17X_0709200	protein transport protein SEC61 subunit beta, putative	79
tr|V7PNL8|V7PNL8_9APIC	1	3	PY17X_0215800	AP2 domain transcription factor AP2-L, putative	1269
tr|V7PP81|V7PP81_9APIC	1	3	PY17X_0832600	conserved Plasmodium protein, unknown function	131
tr|V7PPU3|V7PPU3_9APIC	1	3	PY17X_1135500	U3 small nucleolar RNA-associated protein 21, putative	1246
tr|V7PQK0|V7PQK0_9APIC	1	3	PY17X_0213300	cation transporting ATPase, putative	1682
tr|V7PR31|V7PR31_9APIC	1	3	PY17X_1453700	p25-alpha family protein, putative	152
tr|V7PRL8|V7PRL8_9APIC	1	3	PY17X_1136300	zinc finger protein, putative	571
tr|V7PRR3|V7PRR3_9APIC	1	3	PY17X_1140100	conserved Plasmodium protein, unknown function	1415
tr|V7PS22|V7PS22_9APIC	1	3	PY17X_1238000	EELM2 domain-containing protein, putative	825
tr|V7PS95|V7PS95_9APIC	1	3	PY17X_1233600	ribonuclease, putative	2677
tr|V7PXT9|V7PXT9_9APIC	1	3	PY17X_1340100	histone deacetylase, putative	1640
tr|V7PU48|V7PU48_9APIC	1	3	PY17X_1331200	fam-a protein	387
tr|V7PBE1|V7PBE1_9APIC	1	2	PY17X_1109300	conserved protein, unknown function	230
tr|V7PE52|V7PE52_9APIC	1	2	PY17X_0923400	protein phosphatase, putative	288
tr|V7PEX6|V7PEX6_9APIC	1	2	PY17X_1205600	WD repeat-containing protein, putative	2513
tr|V7PEY8|V7PEY8_9APIC	1	2	PY17X_1105900	actin-like protein, putative	556
tr|V7PFG6|V7PFG6_9APIC	1	2	PY17X_0910000	conserved Plasmodium protein, unknown function	166
tr|V7PFI0|V7PFI0_9APIC	1	2	PY17X_1213100	conserved protein, unknown function	175
tr|V7PG25|V7PG25_9APIC	1	2	PY17X_0944100	conserved Plasmodium protein, unknown function	708
tr|V7PGV0|V7PGV0_9APIC	1	2	PY17X_0912800	CLPTM1 domain-containing protein, putative	644
tr|V7PGX6|V7PGX6_9APIC	1	2	PY17X_1201900	conserved Plasmodium protein, unknown function	932
tr|V7PI44|V7PI44_9APIC	1	2	PY17X_0404900	inner membrane complex protein 1e, putative	512
tr|V7PI48|V7PI48_9APIC	1	2	PY17X_0405400	circumsporozoite (CS) protein	427
tr|V7PIM7|V7PIM7_9APIC	1	2	PY17X_0704400	ubiquitin conjugation factor E4 B, putative	1240
tr|V7PIX7|V7PIX7_9APIC	1	2	PY17X_0607700	DNA-directed RNA polymerase III subunit RPC2,	1414
tr|V7PJT8|V7PJT8_9APIC	1	2	PY17X_0404100	DNA-directed RNA polymerases I, II, and III subunit RPABC2, putative	152
tr|V7PQ08|V7PQ08_9APIC	1	2	PY17X_1437000	formin 2, putative	2823
tr|V7PQ99|V7PQ99_9APIC	1	2	PY17X_1444900	conserved Plasmodium protein, unknown function	814
tr|V7PRJ4|V7PRJ4_9APIC	1	2	PY17X_1464800	protein phosphatase PPM4, putative	734
tr|V7PS26|V7PS26_9APIC	1	2	PY17X_1238300	protein phosphatase PPM9, putative	712
tr|V7PTL0|V7PTL0_9APIC	1	2	PY17X_1341000	GTPase-activating protein, putative	616
tr|V7PU13|V7PU13_9APIC	1	2	PY17X_0700600	fam-a protein	338
tr|V7PUT1|V7PUT1_9APIC	1	2	PY17X_0109900	palmitoyltransferase DHHC2, putative	284
tr|V7PUW8|V7PUW8_9APIC	1	2	PY17X_1456000	HD superfamily phosphohydrolase protein, putative	782
tr|V7PWB5|V7PWB5_9APIC	1	2	PY17X_1240300	18S rRNA (guanine-N(7))-methyltransferase, putative	274
tr|V7PYZ7|V7PYZ7_9APIC	1	2	PY17X_0111500	basal complex transmembrane protein 1, putative	634
tr|V7PBB3|V7PBB3_9APIC	0.9999	3	PY17X_1111900	stearoyl-CoA desaturase, putative	944
tr|V7PI49|V7PI49_9APIC	0.9999	2	PY17X_0416400	zinc finger protein, putative	271
tr|V7PJQ2|V7PJQ2_9APIC	0.9999	2	PY17X_1022100	peptidyl-prolyl cis-trans isomerase, putative	435
tr|V7PPF6|V7PPF6_9APIC	0.9999	2	PY17X_1424900	conserved protein, unknown function	393
tr|V7PR12|V7PR12_9APIC	0.9999	2	PY17X_1417200	U4/U6.U5 tri-snRNP-associated protein 2, putative	640

tr|V7PVK6|V7PVK6_9APIC	0.9998	4	PY17X_1220100	ATP-dependent RNA helicase DDX42, putative	720
tr|V7PKI5|V7PKI5_9APIC	0.9998	4	PY17X_0421700	reticulocyte binding protein, putative	2730
tr|V7PQ59|V7PQ59_9APIC	0.9998	2	PY17X_1429100	protein phosphatase PPM7, putative	305
tr|V7PTE3|V7PTE3_9APIC	0.9998	2	PY17X_1347700	ribose-phosphate pyrophosphokinase, putative	541
tr|V7PAT4|V7PAT4_9APIC	0.9997	3	PY17X_0720800	RNA-binding protein NOB1, putative	491
tr|V7PCA3|V7PCA3_9APIC	0.9997	3	PY17X_0717500	cdc2-related protein kinase 3	1263
tr|V7PQS3|V7PQS3_9APIC	0.9997	3	PY17X_1445600	conserved Plasmodium protein, unknown function	1113
tr|V7PBW3|V7PBW3_9APIC	0.9997	2	PY17X_1107500	transcription factor 25, putative	842
tr|V7PIS2|V7PIS2_9APIC	0.9997	2	PY17X_0707800	RWD domain-containing protein, putative	228
tr|V7PGU6|V7PGU6_9APIC	0.9995	2	PY17X_1215200	conserved Plasmodium protein, unknown function	2140
tr|V7PH62|V7PH62_9APIC	0.9995	2	PY17X_1206500	U3 small nucleolar RNA-associated protein 25, putative	995
tr|V7PWR8|V7PWR8_9APIC	0.9995	2	PY17X_1332700	serine/threonine protein phosphatase UIS2, putative	1339
tr|V7PXB4|V7PXB4_9APIC	0.9995	2	PY17X_0103900	cation/H+ antiporter, putative	440
tr|V7PHN2|V7PHN2_9APIC	0.9994	2	PY17X_0403900	CLP1 P-loop domain-containing protein, putative	1402
tr|V7PF60|V7PF60_9APIC	0.9992	2	PY17X_1204500	conserved protein, unknown function	1075
tr|V7PSZ8|V7PSZ8_9APIC	0.9992	2	PY17X_1354600	conserved oligomeric Golgi complex subunit 3, putative	1329
tr|V7PDY2|V7PDY2_9APIC	0.9991	2	PY17X_0916800	conserved Plasmodium protein, unknown function	1073
tr|V7PJX8|V7PJX8_9APIC	0.999	2	PY17X_1015000	large subunit GTPase 1, putative	763
tr|V7PHA3|V7PHA3_9APIC	0.9989	2	PY17X_0511900	conserved Plasmodium protein, unknown function	1500
tr|V7PR35|V7PR35_9APIC	0.9989	2	PY17X_0503500	serine/threonine protein phosphatase 8, putative	2124
tr|V7PVS2|V7PVS2_9APIC	0.9988	2	PY17X_1356100	1-deoxy-D-xylulose 5-phosphate synthase, putative	1047
tr|V7PSE4|V7PSE4_9APIC	0.9987	2	PY17X_1461300	conserved Plasmodium protein, unknown function	511
tr|V7PT67|V7PT67_9APIC	0.9987	2	PY17X_1351300	conserved Plasmodium protein, unknown function	492
tr|V7PMY2|V7PMY2_9APIC	0.9986	2	PY17X_1133200	histone-lysine N-methyltransferase, putative	511
tr|V7PPG6|V7PPG6_9APIC	0.9986	2	PY17X_0211200	conserved protein, unknown function	713
tr|V7PFE7|V7PFE7_9APIC	0.9985	2	PY17X_1209400	histone deacetylase 2, putative	2032
tr|V7PGT8|V7PGT8_9APIC	0.9983	2	PY17X_0706000	conserved protein, unknown function	1006
tr|V7PCP9|V7PCP9_9APIC	0.9982	2	PY17X_0312800	conserved Plasmodium protein, unknown function	354
tr|V7PVZ3|V7PVZ3_9APIC	0.9981	2	PY17X_1231400	periodic tryptophan protein 2, putative	1040
tr|V7PCA7|V7PCA7_9APIC	0.998	1	PY17X_0303800	DNA-directed RNA polymerase II 16 kDa subunit,	133
tr|V7PCB5|V7PCB5_9APIC	0.998	1	PY17X_0718600	histone acetyltransferase, putative	1028
tr|V7PDC0|V7PDC0_9APIC	0.998	1	PY17X_1120400	ATP synthase-associated protein, putative	128
tr|V7PDN8|V7PDN8_9APIC	0.998	1	PY17X_1109600	conserved Plasmodium protein, unknown function	2719
tr|V7PDY6|V7PDY6_9APIC	0.998	1	PY17X_0715000	ribosome assembly protein RRB1, putative	441
tr|V7PEH6|V7PEH6_9APIC	0.998	1	PY17X_0933900	serine esterase, putative	1470
tr|V7PEZ8|V7PEZ8_9APIC	0.998	1	PY17X_1105400	centrosomal protein CEP120, putative	525
tr|V7PFL4|V7PFL4_9APIC	0.998	1	PY17X_0613900	pantothenate kinase 2	677
tr|V7PH11|V7PH11_9APIC	0.998	1	PY17X_0610000	mago-binding protein, putative	150
tr|V7PKB7|V7PKB7_9APIC	0.998	1	PY17X_1038600	RNA-binding protein 8A, putative	107
tr|V7PL90|V7PL90_9APIC	0.998	1	PY17X_0815500	conserved protein, unknown function	856
tr|V7PMQ8|V7PMQ8_9APIC	0.998	1	PY17X_0204600	bromodomain protein, putative	1337
tr|V7PNQ7|V7PNQ7_9APIC	0.998	1	PY17X_1402800	ATP-dependent RNA helicase DHR1, putative	1557
tr|V7PP89|V7PP89_9APIC	0.998	1	PY17X_0214900	ribosome biogenesis protein BRX1, putative	426
tr|V7PPX4|V7PPX4_9APIC	0.998	1	PY17X_1434600	cell traversal protein for ookinetes and sporozoites	185
tr|V7PPX5|V7PPX5_9APIC	0.998	1	PY17X_1138200	guanylyl cyclase beta	3015
tr|V7PPZ0|V7PPZ0_9APIC	0.998	1	PY17X_0811500	E3 ubiquitin-protein ligase, putative	548
tr|V7PQA0|V7PQA0_9APIC	0.998	1	PY17X_1146600	conserved Plasmodium protein, unknown function	2674
tr|V7PQU3|V7PQU3_9APIC	0.998	1	PY17X_1447700	WD repeat-containing protein, putative	434
tr|V7PR30|V7PR30_9APIC	0.998	1	PY17X_0503800	pre-mRNA-splicing factor RDS3, putative	111
tr|V7PRG6|V7PRG6_9APIC	0.998	1	PY17X_1219600	mRNA-capping enzyme subunit beta, putative	613
tr|V7PRY1|V7PRY1_9APIC	0.998	1	PY17X_1233800	zinc finger protein, putative	2333
tr|V7PSC4|V7PSC4_9APIC	0.998	1	PY17X_1237800	zinc finger protein, putative	645
tr|V7PSC6|V7PSC6_9APIC	0.998	1	PY17X_1369000	conserved Plasmodium protein, unknown function	864
tr|V7PSF4|V7PSF4_9APIC	0.998	1	PY17X_1243200	structural maintenance of chromosomes protein 6, putative	1606
tr|V7PT91|V7PT91_9APIC	0.998	1	PY17X_1450800	homocysteine S-methyltransferase, putative	507
tr|V7PTT1|V7PTT1_9APIC	0.998	1	PY17X_1462800	conserved protein, unknown function	178
tr|V7PUX3|V7PUX3_9APIC	0.998	1	PY17X_1456500	DNA gyrase subunit B, putative	930
tr|V7PV18|V7PV18_9APIC	0.998	1	PY17X_1243000	zinc finger protein, putative	674
tr|V7PVD4|V7PVD4_9APIC	0.998	1	PY17X_1368000	conserved Plasmodium protein, unknown function	2660
tr|V7PX98|V7PX98_9APIC	0.998	1	PY17X_0102600	MYND-type zinc finger protein, putative	262
tr|V7PEP9|V7PEP9_9APIC	0.9979	3	PY17X_0939500	conserved Plasmodium protein, unknown function	691
tr|V7P9G4|V7P9G4_9APIC	0.9979	1	PY17X_1320000	syntaxin-6, putative	212
tr|V7PBF4|V7PBF4_9APIC	0.9979	1	PY17X_1308100	zinc finger protein, putative	1223
tr|V7PBN9|V7PBN9_9APIC	0.9979	1	PY17X_1113900	conserved protein, unknown function	251
tr|V7PC70|V7PC70_9APIC	0.9979	1	PY17X_1304100	tubulin epsilon chain, putative	500
tr|V7PCT4|V7PCT4_9APIC	0.9979	1	PY17X_0315400	SUZ domain-containing protein, putative	830
tr|V7PCW5|V7PCW5_9APIC	0.9979	1	PY17X_1319100	LCCL domain-containing protein, putative	879
tr|V7PFV2|V7PFV2_9APIC	0.9979	1	PY17X_0938000	endonuclease/exonuclease/phosphatase family protein, putative	653
tr|V7PGI1|V7PGI1_9APIC	0.9979	1	PY17X_0705600	SAYSvFN domain-containing protein, putative	151
tr|V7PNG3|V7PNG3_9APIC	0.9979	1	PY17X_1133600	splicing factor 3B subunit 5, putative	85
tr|V7PNH1|V7PNH1_9APIC	0.9979	1	PY17X_1005300	gametocyte-specific protein, putative	177
tr|V7PPK0|V7PPK0_9APIC	0.9979	1	PY17X_1412100	M1-family alanyl aminopeptidase, putative	1064
tr|V7PQ92|V7PQ92_9APIC	0.9979	1	PY17X_1129800	amino acid transporter AAT1, putative	626
tr|V7PQP2|V7PQP2_9APIC	0.9979	1	PY17X_1442900	small subunit rRNA processing factor, putative	418
tr|V7PRI3|V7PRI3_9APIC	0.9979	1	PY17X_1463700	pre-mRNA-splicing factor RBM22, putative	393
tr|V7PTE5|V7PTE5_9APIC	0.9979	1	PY17X_1454700	periodic tryptophan protein 1, putative	528
tr|V7PUE5|V7PUE5_9APIC	0.9979	1	PY17X_1225800	AP-3 complex subunit delta, putative	1436
tr|V7PH97|V7PH97_9APIC	0.9978	1	PY17X_0616200	conserved Plasmodium protein, unknown function	367
tr|V7PLF5|V7PLF5_9APIC	0.9978	1	PY17X_0822900	conserved Plasmodium protein, unknown function	585
tr|V7PNE8|V7PNE8_9APIC	0.9978	1	PY17X_1132200	phosphoinositide phosphatase SAC1, putative	814
tr|V7PRS5|V7PRS5_9APIC	0.9978	1	PY17X_1229400	methionine aminopeptidase 1c, putative	680
tr|V7PSD6|V7PSD6_9APIC	0.9978	1	PY17X_1459600	WD repeat-containing protein 82, putative	374
tr|V7PLQ9|V7PLQ9_9APIC	0.9977	2	PY17X_1004000	6-cysteine protein	416
tr|V7PM67|V7PM67_9APIC	0.9977	2	PY17X_0837300	conserved Plasmodium protein, unknown function	743
tr|V7PQ77|V7PQ77_9APIC	0.9977	2	PY17X_1443000	conserved Plasmodium protein, unknown function	782

tr|V7PE13|V7PE13_9APIC	0.9977	1	PY17X_0316800	Plasmodium exported protein, unknown function	248
tr|V7PGY6|V7PGY6_9APIC	0.9977	1	PY17X_0521200	conserved Plasmodium protein, unknown function	710
tr|V7PNC6|V7PNC6_9APIC	0.9977	1	PY17X_0805100	phosphopantetheine adenylyltransferase	1270
tr|V7PNR0|V7PNR0_9APIC	0.9977	1	PY17X_0811600	conserved Plasmodium protein, unknown function	113
tr|V7PPD4|V7PPD4_9APIC	0.9977	1	PY17X_0214200	alpha/beta hydrolase, putative	561
tr|V7PQT0|V7PQT0_9APIC	0.9977	1	PY17X_1457700	ATP-dependent RNA helicase DBP9, putative	867
tr|V7PWV2|V7PWV2_9APIC	0.9977	1	PY17X_1365100	conserved Plasmodium protein, unknown function	562
tr|V7P9J2|V7P9J2_9APIC	0.9976	1	PY17X_1317600	signal recognition particle subunit SRP54, putative	500
tr|V7PFN1|V7PFN1_9APIC	0.9976	1	PY17X_0931900	heat shock protein 90, putative	852
tr|V7PFS2|V7PFS2_9APIC	0.9976	1	PY17X_0914700	conserved Plasmodium membrane protein, unknown function	416
tr|V7PKJ1|V7PKJ1_9APIC	0.9976	1	PY17X_1033700	rhomboid protease ROM8, putative	637
tr|V7PKU7|V7PKU7_9APIC	0.9976	1	PY17X_1027500	conserved Plasmodium protein, unknown function	4192
tr|V7PNX9|V7PNX9_9APIC	0.9976	1	PY17X_1409500	protein phosphatase PPM6, putative	658
tr|V7PQJ8|V7PQJ8_9APIC	0.9976	1	PY17X_1137900	ER membrane protein complex subunit 3, putative	256
tr|V7PBS2|V7PBS2_9APIC	0.9975	1	PY17X_1317500	serine/threonine protein kinase, putative	375
tr|V7PJE2|V7PJE2_9APIC	0.9975	1	PY17X_1028600	NADP-specific glutamate dehydrogenase, putative	470
tr|V7PQY0|V7PQY0_9APIC	0.9975	1	PY17X_1414800	lipoate-protein ligase 1, putative	411
tr|V7PRQ4|V7PRQ4_9APIC	0.9975	1	PY17X_1436000	thrombospondin-related apical membrane protein	349
tr|V7PBZ0|V7PBZ0_9APIC	0.9974	1	PY17X_1312200	eukaryotic translation initiation factor 2-alpha kinase 1, putative	1496
tr|V7PLV1|V7PLV1_9APIC	0.9974	1	PY17X_0812000	GTPase-activating protein, putative	891
tr|V7PLV8|V7PLV8_9APIC	0.9974	1	PY17X_0215700	AP-4 complex subunit beta, putative	892
tr|V7PNS6|V7PNS6_9APIC	0.9974	1	PY17X_0809800	cleavage and polyadenylation specificity factor, putative	954
tr|V7PQ90|V7PQ90_9APIC	0.9974	1	PY17X_1145600	ribosomal protein L1, putative	312
tr|V7PS98|V7PS98_9APIC	0.9974	1	PY17X_1234000	conserved oligomeric Golgi complex subunit 4, putative	1058
tr|V7PTX9|V7PTX9_9APIC	0.9973	1	PY17X_1466200	transcription initiation factor IIA subunit 2, putative	177
tr|V7PU03|V7PU03_9APIC	0.9973	1	PY17X_1330800	DNA-directed RNA polymerase III subunit RPC4,	339
tr|V7PU30|V7PU30_9APIC	0.9973	1	PY17X_1328100	inner membrane complex sub-compartment protein 3, putative	150
tr|V7PNX8|V7PNX8_9APIC	0.9972	2	PY17X_0804500	conserved Plasmodium protein, unknown function	3003
tr|V7PDB9|V7PDB9_9APIC	0.9972	1	PY17X_0902700	membrane associated erythrocyte binding-like protein	1701
tr|V7PI34|V7PI34_9APIC	0.9972	1	PY17X_0414600	vesicle transport v-SNARE protein, putative	197
tr|V7PUK6|V7PUK6_9APIC	0.9972	1	PY17X_0102000	reticulocyte binding protein, putative	611
tr|V7PLN3|V7PLN3_9APIC	0.9971	1	PY17X_1005700	conserved Plasmodium protein, unknown function	855
tr|V7PN97|V7PN97_9APIC	0.9971	1	PY17X_0825400	conserved Plasmodium protein, unknown function	2161
tr|V7PTS5|V7PTS5_9APIC	0.997	2	PY17X_1335900	rab GTPase activator, putative	1581
tr|V7PK32|V7PK32_9APIC	0.997	1	PY17X_0408900	conserved Plasmodium protein, unknown function	280
tr|V7PPE5|V7PPE5_9APIC	0.997	1	PY17X_1423900	GTP-binding translation elongation factor, putative	756
tr|V7PER3|V7PER3_9APIC	0.9969	1	PY17X_1113000	CDK-activating kinase assembly factor MAT1, putative	260
tr|V7PI60|V7PI60_9APIC	0.9969	1	PY17X_0406400	ubiquitin-conjugating enzyme E2, putative	139
tr|V7PPU9|V7PPU9_9APIC	0.9969	1	PY17X_1136000	conserved Plasmodium protein, unknown function	1446
tr|V7PUL6|V7PUL6_9APIC	0.9969	1	PY17X_1232200	nucleolar protein 10, putative	568
tr|V7PGL4|V7PGL4_9APIC	0.9968	1	PY17X_0942000	DNA repair protein RAD51, putative	349
tr|V7PPS8|V7PPS8_9APIC	0.9968	1	PY17X_0815800	conserved Plasmodium protein, unknown function	1219
tr|V7PDK9|V7PDK9_9APIC	0.9966	2	PY17X_1112200	RNA pseudouridylate synthase, putative	9786
tr|V7PS28|V7PS28_9APIC	0.9966	1	PY17X_1224600	protein transport protein USE1, putative	320
tr|V7PMC4|V7PMC4_9APIC	0.9965	2	PY17X_1033400	conserved Plasmodium protein, unknown function	980
tr|V7PT14|V7PT14_9APIC	0.9965	1	PY17X_1356200	exoribonuclease, putative	812
tr|V7PUP0|V7PUP0_9APIC	0.9965	1	PY17X_1233600	ribonuclease, putative	2677
tr|V7PI88|V7PI88_9APIC	0.9964	1	PY17X_0524900	AP-4 complex subunit sigma, putative	146
tr|V7PSK3|V7PSK3_9APIC	0.9963	1	PY17X_1431700	DNA-directed RNA polymerases I, II, and III subunit RPABC3, putative	143
tr|V7PAT9|V7PAT9_9APIC	0.9962	1	PY17X_0711000	Snf2-related CBP activator, putative	1825
tr|V7PGX8|V7PGX8_9APIC	0.9961	1	PY17X_0607900	conserved Plasmodium protein, unknown function	678
tr|V7PPB9|V7PPB9_9APIC	0.996	1	PY17X_1406400	conserved protein, unknown function	512
tr|V7PNF4|V7PNF4_9APIC	0.9959	1	PY17X_1006300	transcription factor, putative	373
tr|V7PR83|V7PR83_9APIC	0.9959	1	PY17X_1457000	polyadenylation factor subunit 2, putative	481
tr|V7PT86|V7PT86_9APIC	0.9959	1	PY17X_1450400	conserved Plasmodium protein, unknown function	1545
tr|V7PK92|V7PK92_9APIC	0.9957	1	PY17X_1006900	AAA family ATPase, putative	625
tr|V7PN06|V7PN06_9APIC	0.9957	1	PY17X_0503400	conserved Plasmodium protein, unknown function	252
tr|V7PGS7|V7PGS7_9APIC	0.9956	1	PY17X_0523200	ribosome-recycling factor, putative	266
tr|V7PS12|V7PS12_9APIC	0.9954	1	PY17X_1222800	cg1 protein, putative	997
tr|V7PSD2|V7PSD2_9APIC	0.9953	1	PY17X_1238900	conserved protein, unknown function	906
tr|V7PHT7|V7PHT7_9APIC	0.995	1	PY17X_0613500	trafficking protein particle complex subunit 5, putative	184
tr|V7PQE1|V7PQE1_9APIC	0.995	1	PY17X_1434400	conserved Plasmodium protein, unknown function	727
tr|V7PWG8|V7PWG8_9APIC	0.995	1	PY17X_0116400	PIR protein	632
tr|V7PF24|V7PF24_9APIC	0.9949	1	PY17X_1209900	protein GPR89, putative	985
tr|V7PHB0|V7PHB0_9APIC	0.9949	1	PY17X_0520000	conserved Plasmodium membrane protein, unknown function	442
tr|V7PMT8|V7PMT8_9APIC	0.9949	1	PY17X_1129700	polyadenylate-binding protein 3, putative	535
tr|V7PD44|V7PD44_9APIC	0.9946	1	PY17X_0604900	major facilitator superfamily domain-containing protein, putative	1040
tr|V7PRY5|V7PRY5_9APIC	0.9941	1	PY17X_1220200	peptidase, putative	873
tr|V7PAC6|V7PAC6_9APIC	0.9939	1	PY17X_1306300	conserved protein, unknown function	298
tr|V7PDF5|V7PDF5_9APIC	0.9939	1	PY17X_0905900	SUMO-activating enzyme subunit 1, putative	369
tr|V7PHN1|V7PHN1_9APIC	0.9939	1	PY17X_0511200	conserved protein, unknown function	1140
tr|V7PJI1|V7PJI1_9APIC	0.9939	1	PY17X_0409600	dual specificity protein phosphatase, putative	471
tr|V7PKU5|V7PKU5_9APIC	0.9939	1	PY17X_0829200	conserved Plasmodium protein, unknown function	362
tr|V7PB62|V7PB62_9APIC	0.9938	1	PY17X_1116200	conserved protein, unknown function	779
tr|V7PF12|V7PF12_9APIC	0.9938	1	PY17X_1104300	protein kinase, putative	684
tr|V7PJV1|V7PJV1_9APIC	0.9938	1	PY17X_1017300	conserved Plasmodium protein, unknown function	1079
tr|V7PTX5|V7PTX5_9APIC	0.9937	1	PY17X_1332300	zinc finger protein, putative	349
tr|V7PF90|V7PF90_9APIC	0.9936	1	PY17X_1215600	GDP-L-fucose synthase, putative	343
tr|V7PJR6|V7PJR6_9APIC	0.9936	1	PY17X_1020400	conserved Plasmodium protein, unknown function	365
tr|V7PIZ6|V7PIZ6_9APIC	0.9926	1	PY17X_1031200	DnaJ protein, putative	381
tr|V7PKQ1|V7PKQ1_9APIC	0.9926	1	PY17X_1029700	conserved Plasmodium protein, unknown function	1194

tr|V7PMY3|V7PMY3_9APIC	0.9926	1	PY17X_1018300	exosome complex component RRP41, putative	246
tr|V7PRM7|V7PRM7_9APIC	0.9926	1	PY17X_1224800	cell division cycle ATPase, putative	1162
tr|V7PDF8|V7PDF8_9APIC	0.9925	1	PY17X_1117000	conserved Plasmodium protein, unknown function	198
tr|V7PV90|V7PV90_9APIC	0.9925	1	PY17X_1248600	conserved Plasmodium protein, unknown function	96
tr|V7PIV8|V7PIV8_9APIC	0.9921	1	PY17X_1215900	SPRY domain-containing protein, putative	2029
tr|V7PLN0|V7PLN0_9APIC	0.9916	1	PY17X_0803600	conserved Plasmodium protein, unknown function	1255
tr|V7PSS8|V7PSS8_9APIC	0.9915	2	PY17X_1220000	conserved Plasmodium protein, unknown function	1751
tr|V7PK17|V7PK17_9APIC	0.9914	2	PY17X_1002800	pre-mRNA-splicing factor CLF1, putative	703
tr|V7PI27|V7PI27_9APIC	0.9914	1	PY17X_0621000	Ham1-like protein, putative	196
tr|V7PFL6|V7PFL6_9APIC	0.9908	1	PY17X_1215500	translation initiation factor eIF-2B subunit delta, putative	1039
tr|V7PFS5|V7PFS5_9APIC	0.9908	1	PY17X_0935800	conserved Plasmodium protein, unknown function	700
tr|V7PFZ3|V7PFZ3_9APIC	0.9904	1	PY17X_0624200	Rab GTPase activator and protein kinase, putative	1634
tr|V7PQQ3|V7PQQ3_9APIC	0.9903	1	PY17X_1456800	vacuolar protein sorting-associated protein 16, putative	965
tr|V7PQT1|V7PQT1_9APIC	0.9902	1	PY17X_1446300	multidrug resistance-associated protein 2, putative	1975
tr|V7PTZ1|V7PTZ1_9APIC	0.99	1	PY17X_1430200	asparagine-rich antigen, putative	993
tr|V7PGT1|V7PGT1_9APIC	0.9897	2	PY17X_0911400	conserved Plasmodium protein, unknown function	1744
tr|V7PIW3|V7PIW3_9APIC	0.9892	1	PY17X_0510300	EF-hand calcium-binding domain-containing protein, putative	908
tr|V7PNS0|V7PNS0_9APIC	0.9891	1	PY17X_0810300	stomatin-like protein, putative	398
tr|V7PVP2|V7PVP2_9APIC	0.9891	1	PY17X_1358700	ABC transporter B family member 5, putative	820
tr|V7PKR9|V7PKR9_9APIC	0.9888	1	PY17X_1028500	conserved Plasmodium protein, unknown function	2793
tr|V7PNZ8|V7PNZ8_9APIC	0.9888	1	PY17X_1411000	RNA-binding protein, putative	154
tr|V7PED3|V7PED3_9APIC	0.9882	1	PY17X_0942800	DEAD/DEAH box helicase, putative	1109
tr|V7PNU2|V7PNU2_9APIC	0.9878	1	PY17X_0807900	mediator of RNA polymerase II transcription subunit 10, putative	257
tr|V7PMM4|V7PMM4_9APIC	0.9876	1	PY17X_0827200	DNA-directed RNA polymerase II subunit RPB3, putative	335
tr|V7PWC1|V7PWC1_9APIC	0.9873	2	PY17X_1240600	inner membrane complex protein, putative	486
tr|V7PI62|V7PI62_9APIC	0.9873	1	PY17X_0416900	inorganic pyrophosphatase, putative	367
tr|V7PUT0|V7PUT0_9APIC	0.9872	1	PY17X_1345400	mitochondrial fission 1 protein, putative	141
tr|V7PKZ0|V7PKZ0_9APIC	0.9869	2	PY17X_0834700	peptidyl-prolyl cis-trans isomerase, putative	590
tr|V7PD57|V7PD57_9APIC	0.9868	1	PY17X_1105200	MOLO1 domain-containing protein, putative	275
tr|V7PU62|V7PU62_9APIC	0.9853	2	PY17X_1324900	conserved Plasmodium protein, unknown function	2979
tr|V7PMY5|V7PMY5_9APIC	0.9847	1	PY17X_0833100	transcription initiation factor TFIID subunit 7, putative	389
tr|V7PRP3|V7PRP3_9APIC	0.9845	1	PY17X_1138500	protein arginine N-methyltransferase 5, putative	729
tr|V7PLY2|V7PLY2_9APIC	0.9832	1	PY17X_1011200	conserved protein, unknown function	374
tr|V7PHJ7|V7PHJ7_9APIC	0.9823	2	PY17X_0607100	conserved protein, unknown function	1196
tr|V7PJQ3|V7PJQ3_9APIC	0.9809	1	PY17X_1012000	conserved protein, unknown function	277
tr|V7PFH9|V7PFH9_9APIC	0.9808	1	PY17X_0910600	conserved Plasmodium protein, unknown function	2069
tr|V7PMS4|V7PMS4_9APIC	0.9806	1	PY17X_1128400	eukaryotic translation initiation factor 2-alpha kinase, putative	2580
tr|V7PXK9|V7PXK9_9APIC	0.9775	1	PY17X_0109300	zinc transporter ZIP1, putative	344
tr|V7PWK6|V7PWK6_9APIC	0.9761	1	PY17X_1248100	phosphoenolpyruvate/phosphate translocator, putative	518
tr|V7PDX1|V7PDX1_9APIC	0.9756	1	PY17X_0927200	calcium-dependent protein kinase 7	1913
tr|V7PRZ4|V7PRZ4_9APIC	0.9745	1	PY17X_1235000	AP2 domain transcription factor AP2-O2	2129
tr|V7PBN5|V7PBN5_9APIC	0.9743	1	PY17X_1102800	conserved protein, unknown function	381
tr|V7PFR0|V7PFR0_9APIC	0.9688	2	PY17X_0609100	conserved Plasmodium protein, unknown function	4285
tr|V7PX28|V7PX28_9APIC	0.967	1	PY17X_1358100	conserved Plasmodium protein, unknown function	271
tr|V7PEF2|V7PEF2_9APIC	0.9652	1	PY17X_0306900	exosome complex component MTR3, putative	271
tr|V7PG51|V7PG51_9APIC	0.9651	1	PY17X_0926000	conserved protein, unknown function	492
tr|V7PHH0|V7PHH0_9APIC	0.9632	2	PY17X_0928100	JmjC domain-containing protein, putative	447
tr|V7PQI2|V7PQI2_9APIC	0.9557	1	PY17X_1403200	methyltransferase, putative	227
tr|V7PTT3|V7PTT3_9APIC	0.9547	1	PY17X_1337600	mediator of RNA polymerase II transcription subunit 6, putative	205
tr|V7PTD9|V7PTD9_9APIC	0.9531	1	PY17X_1415500	conserved protein, unknown function	524
tr|V7PMS3|V7PMS3_9APIC	0.9452	1	PY17X_0823100	gamma-glutamylcysteine synthetase	999
tr|V7PEM6|V7PEM6_9APIC	0.9447	1	PY17X_0312600	conserved Plasmodium protein, unknown function	830
tr|V7PJ48|V7PJ48_9APIC	0.9413	1	PY17X_1035600	DNA damage-inducible protein 1, putative	385
tr|V7PSD9|V7PSD9_9APIC	0.9392	3	PY17X_1240400	conserved Plasmodium protein, unknown function	8949
tr|V7PDX8|V7PDX8_9APIC	0.937	1	PY17X_0313900	autophagy-related protein 11, putative	1423
tr|V7PIS1|V7PIS1_9APIC	0.933	1	PY17X_0513200	methyltransferase, putative	577
tr|V7PJE5|V7PJE5_9APIC	0.9298	1	PY17X_1020200	conserved Plasmodium protein, unknown function	364
tr|V7PZB8|V7PZB8_9APIC	0.921	1	PY17X_1250700	PIR protein	316
tr|V7PE58|V7PE58_9APIC	0.9198	2	PY17X_0935400	GTPase-activating protein, putative	372
tr|V7PAK3|V7PAK3_9APIC	0.9149	1	PY17X_1371500	fam-c protein	94
tr|V7PMS9|V7PMS9_9APIC	0.9094	1	PY17X_1128800	DNA methyltransferase 1-associated protein 1, putative	385
tr|V7PJB0|V7PJB0_9APIC	0.9063	1	PY17X_1031000	zinc finger protein, putative	697

Supplementary Table 3. Primers and oligonucleotides used in this study.

Oligo sequence for candidate genes (except gep1) knockout plasmid construction								
Gene ID	Gene name	Gene size (bp)/ deleted gene size (bp)	Left homologous arm		Right homologous arm		Target site of sgRNA	
			Forward primer	Reverse primer	Forward primer	Reverse primer	Oligo (Forward)	Oligo (Reverse)
PY17X_1243400	7-helix-1 protein, putative	1410 / 756	CGGGGTACCTATATGTGTAACTATTAGGG	CATGCCATGGAGCCACAATGACCTTTTATT	CCGCTCGAGGGAAGTGCACATGGGTATGC	CCCCTTAAGCAGGTCTATCTGGAATGTTA	TATTGCAAATCAATCAATTTATTG	AAACCAATAAATTGATTGATTTGC
PY17X_1431500	integral membrane protein GPR180, putative	2080 / 327	CGGGGTACCTACATTAATGCTTGATATTG	CATGCCATGGCATATTCTATATTGAATCC	CCGCTCGAGCACTAAGCTATGGTATAACA	CCCCTTAAGTAAGCGTATGAAACATGCAC	TATTGTTTATTCACAAAATGGTAT	AAACATACCATTTTGTGAATAAAC
PY17X_0918700	serpentine receptor, putative	1878 / 498	CGGGGTACCTTAATTAGGACCAATGTAA	CATGCCATGGACCTTGACTTGACGTATCC	CCGCTCGAGCTAGTTGGTGATGATAAA	CCCCTTAAGATAAAGACAGACGATAT	TATTGGTAATACTATATCAACATA	AAACTATGTTGATATAGTATTACC
PY17X_1433900	serpentine receptor, putative	1776 / 545	CGGGGTACCTTCATGTATTAACAATGGA	CATGCCATGGATATATATCACGTCTGTG	CCGCTCGAGCAGAACACTCAGATTTGGA	CCCCTTAAGCACACTGATATCCATACTT	TATTGTCATCTTCTTCATAAGAAG	AAACCTTCTTATGAAGAAGATGAC
PY17X_0524600	serpentine receptor, putative	2122 / 434	CGGGGTACCTATATTGTTATGTGTGTACA	CATGCCATGGGATTACACCAATTTGATATG	CCGCTCGAGGATATAGACAATCAATTAGA	CCCCTTAAGGTTTGATGATTCTGTATCTC	TATTGTATCATCAAAAGTAGTATA	AAACTATACTACTTTTGATGATAC
PY17X_1421700	GPCR-like receptor SR25, putative	1347 / 531	CGGGGTACCAGATTACTACGTTGTCGATT	CATGCCATGGAGTTCATCACCACTGTCATC	CCGCTCGAGGCCATCTTATTACAGTATGC	CCCCTTAAGTGACTTTTGATGGTAAAGAC	TATTGAATTTGCTACTATAGTATG	AAACCATACTATAGTAGCAAATTC
PY17X_0605800	sexual stage-specific protein G37, putative	2513 / 459	CGGGGTACCTTAGTAACACCTCAACTTATA	CATGCCATGGGTGGTATATCCTTAAAGACC	CCGCTCGAGGCATGTATCAGTAGGTATAG	CCGGAATTCGTATACCCCATAATGACGAT	TATTGTAAATTTCGCTTCATTGCTA	AAACTAGCAATGAAGCGAAATTTAC
PY17X_0617400	conserved Plasmodium membrane protein, unknown function	2400 / 415	CGGGGTACCCTATAATTCCTTGTAGACGT	CATGCCATGGGATAGCAATTCGTTTAACTA	CCGCTCGAGGTATGTTTACAACTGTTGCA	CCGGAATTCAAAGTTGATACTGGTATCTA	TATTGTTAATTTCGTCTTAGTTAT	AAACATAACTAAGACGAAATTAAC
PY17X_0914700	conserved Plasmodium membrane protein, unknown function	1251 / 343	CGGGGTACCTTACACGTGGCGAATGATAT	CATGCCATGGCGTAGTTCACTAGTAAATGA	CCGCTCGAGGGCTTATTATCAATTATACTC	CCGGAATTCGATGATATAGCTGTACTTATC	TATTGAATATAAAAGAAAGAGTCG	AAACCGACTCTTTCTTTTATATTC
PY17X_1128600	protease, putative	2155 / 385	CGGGGTACCTCCTTCGCTATATGTGCGAT	CATGCCATGGCAAGATATATGAAATTGCCT	CCGCTCGAGCGTTTATCTTTATCTGTTAG	CCGGAATTCGGCAGTTCTGTGTATTCATT	TATTGGTTTTTCTTGTATAGCAAA	AAACTTTGCTATACAAGAAAAACC
PY17X_1313900	conserved Plasmodium protein, unknown function	3636 / 626	CGGGGTACCCGGCATATGTGGATGTTAGC	CATGCCATGGGCCCAAACAACAACAATCTT	CCGCTCGAGAGGGTAGTGAGGAATGTTCAT	CCCCTTAAGCCATTTGTTACTATATATGG	TATTGTTTTGAAAAATATAGAATT	AAACAATTCTATATTTTTCAAAAC
PY17X_0702400	folate transporter 1, putative	1887 / 1102	CCCAAGCTTATCATGTTTCCGTTACTA	CATGCCATGGAGGGTATAATATAATCGA	CCGCTCGAGGTTGTTGAAAAAAGGGAT	CCGGAATTCTGAACTGACCATTACTGC	TATTGATACTTATCAGCTTCATCC	AAACGGATGAAGCTGATAAGTATC
PY17X_0933500	folate transporter 2, putative	1362 / 1404	CCCAAGCTTTGATGTCTTTATGTATTTCG	CATGCCATGGTATTTGTGTTCTTCTTTCTC	CCGCTCGAGATGAGTGGCAAACCCAAAAT	CCGGAATTCTGGGGTTTTCGTCTCTACAA	TATTGGTTTCCGACCTTCTTTTAT	AAACATAAAAGAAGGTCGGAAACC
PY17X_0309400	GDP-fructose; GMP antiporter, putative	1325 / 1325	CCCAAGCTTCCCCACACATACATATCTTT	CATGCCATGGTTGTCTATTTGTTCAGCTTA	CCGCTCGAGATGAACAAGTCAGACAACAC	CCGGAATTCTACCAATTTTGTGAAGAAAC	TATTGTGGTAATTGAAAATAATAC	AAACGTATTATTTTCAATTACCAC
PY17X_0936300	UDP-galactose transporter, putative	1044 / 1044	CCCAAGCTTAATTAACACCTTAACAGC	CATGCCATGGTCCTCACATAGTTATCAA	CCGCTCGAGCCATTTCGTTTCGTACTT	CCGGAATTCAGAAACTGGAGGAGATGT	TATTGAAATGCATCAAACAACATT	AAACAATGTTGTTTGATGCATTTC
PY17X_1436400	phosphate translocator, putative	2650 / 1462	CCCAAGCTTCATACCTAAAGAGGAGAA	CATGCCATGGAAATTAACAGACTGTCTC	CCGCTCGAGTAAGTGCTCTCTGCTCGT	CCGGAATTCGTTATTGTTGTAATCTGA	TATTGATGTTTTTGATACTTAAAA	AAACTTTTAAGTATCAAAAACATC
PY17X_0823700	major facilitator superfamily domain-containing protein, putative	1470 / 1470	CGGGGTACCTTGTTCTCTTTCTCCATCTA	CATGCCATGGATTTTTGTAAGGTACATCAT	CCGCTCGAGTTTCACACTTATTCATTTTG	CCGGAATTCATTGAGTGCGAGAGTAGAAA	TATTGGATATGATATATGCCCAGA	AAACTCTGGGCATATATCATATCC
PY17X_0820300	major facilitator superfamily domain-containing protein, putative	4033 / 1312	CCCAAGCTTCACAAACAGACACATAACAG	CATGCCATGGATCTCTAGAATCAGCTCAAT	CCGCTCGAGGAAGAGAGTAAAACCCCATT	CCGGAATTCATCGAAGATATCATTGACGT	TATTGAAGCTATAAAACAAGCAAA	AAACTTTGCTTGTTTTATAGCTTC
PY17X_0307300	transporter, putative	3986 / 363	CCCAAGCTTAATGAAAGGATAAGAGTGT	CATGCCATGGATTGGGGTAACATGTGCTA	CCGCTCGAGAATCGAACTATACAAGAAG	CCGGAATTCGAATATGTCCATTACCAG	TATTGAGCATATTTTCATTATCTA	AAACTAGATAATGAAAATATGCTC
PY17X_0917400	amino acid transporter	4068 / 444	CCCAAGCTTCTGTCTAATGGTCCCAATAA	CATGCCATGGGAATAACACCTCCCCTCTTT	CCGCTCGAGATTTTGAGTTAGAAGAAG	CCGGAATTCATACATTTCAACAGATGG	TATTGTATCATGTTCATGCTCTTT	AAACAAAGAGCATGAACATGATAC
PY17X_0609400	amino acid transporter, putative	4545 / 370	CCCAAGCTTCGTGCTCATTTTGTGTTC	CATGCCATGGAGCTTCAATTTGTCTGTT	CCGCTCGAGAAACATTCTGGTTGGCTA	CCGGAATTCGACTTCATTTCATTTGCC	TATTGAGACATGTTAAGAGAAAATG	AAACCATTTTCTCTTAACATGTCTC
PY17X_1448600	amino acid transporter, putative	5556 / 388	CCCAAGCTTATTATGAGTAACCTTCGC	CATGCCATGGACTTAAACAAACGCAAAT	CCGCTCGAGGGAAATCTGTTTGTATGC	CCGGAATTCTTTTAATTGGTGTTGGAC	TATTGTTTAATTGATGAAGTAGGA	AAACTCCTACTTCATCAATTAAAC
PY17X_1241000	multidrug resistance protein 1, putative	4266 / 684	CGGGGTACCGAAATCTACCGTTGAGTTGT	CATGCCATGGATTACACTTTCTCCACAAT	CCGCTCGAGTGGGTTCAACTTGCATGG	CCCCTTAAGGTTCAACTATTACACTTCC	TATTGTTGATAGAAATCAAAATAA	AAACTTATTTTGATTTCTATCAAC
PY17X_1446300	multidrug resistance-associated protein 2, putative	5928 / 665	CGGGGTACCCTACATATCCATGATGAATG	CATGCCATGGACACTATGCGTAACTATAT	CCGCTCGAGTCGATATGGAAGTAACTG	CCCCTTAAGGCATACTTGATATGAATTCAC	TATTGATTATTATGAATATAATAG	AAACCTATTATATTCATAATAATC
PY17X_1315500	multidrug resistance protein 2, putative	2877 / 481	CGGGGTACCCACATTAGTTGACATGATTGC	CATGCCATGGGTATATGGCATATCATTACC	CCGCTCGAGGGTTTAGCATCAACTGAAGT	CCCCTTAAGAATTAGATAATGCACCAC	TATTGATTATTATGAATATAATAG	AAACCTATTATATTCATAATAATC
PY17X_0904900	ABC transporter B family member 3, putative	2624 / 755	CGGGGTACCGGAAATCGAAGTTATAGACA	CATGCCATGGCCTTAAAAGACACAACCCT	CCGCTCGAGTAGCACGTCTACACACAACG	CCGGAATTCTCACCTTGGGAAAGTGGATC	TATTGATTATTATGAATATAATAG	AAACCTATTATATTCATAATAATC
PY17X_0403400	ABC transporter B family member 4, putative	3876 / 577	CGGGGTACCGGAAATGCTGAAGATGTAA	CATGCCATGGTTGGCTAAATGTACTAATAT	CCGCTCGAGCACCACATTGTGACATATCC	CCCCTTAAGTGTAACTGTGTGTTGGCTAG	TATTGATTATTATGAATATAATAG	AAACCTATTATATTCATAATAATC
PY17X_1358700	ABC transporter B family member 5, putative	2463 / 679	CGGGGTACCGCTTGGTTTAGGAATTGTTGG	CATGCCATGGCATATAAGGACCTATTCAG	CCGCTCGAGATGTTCATTATCATCTACC	CCCCTTAAGAACACACAATAAATCTGC	TATTGATTATTATGAATATAATAG	AAACCTATTATATTCATAATAATC
PY17X_0928600	protein GCN20, putative	2322 / 991	CGGGGTACCGAAGTATGGGTAATGAGAA	CATGCCATGGCCCCATATATCTATGTGTG	CCGCTCGAGCTTGGTTTTGACTCCAACCTTC	CCCCTTAAGCTCTTAATCTGATAAGCACAC	TATTGATTATTATGAATATAATAG	AAACCTATTATATTCATAATAATC
PY17X_1370600	ABC transporter B family member 6, putative	3087 / 552	CGGGGTACCGGCCTACATGTATAAATGC	CATGCCATGGTACAAGATATGAGAGAGT	CCGCTCGAGCAATGAACATAGTAATGACG	CCCCTTAAGGTAGTAAAGACACTATTCC	TATTGAATCGGCTGCATAATTAAG	AAACCTTAATTATGCAGCCGATTC
PY17X_0610800	ABC transporter B family member 7, putative	2418 / 605	CGGGGTACCGCATATATGGATGTATGGG	CATGCCATGGCTACCTACCTTAACAATCC	CCGCTCGAGATCTATGATATGTCTACTC	CCCCTTAAGGATTCACCATTAAGGAATC	TATTGATTATTATGAATATAATAG	AAACCTATTATATTCATAATAATC
PY17X_1145400	ABC transporter E family member 1, putative	2055 / 690	CGGGGTACCCCGTTTATATCAGTAAACCA	CATGCCATGGCGGTGCTGCTACGATAAATGG	CCGCTCGAGTATGGGGAAAGGCAGGTGCA	CCGGAATTCCGTGTTCGACAACAAAAGCTG	TATTGAATGGCGAGATATATTATC	AAACGATAATATATCTCGCCATTC
PY17X_1019600	ABC transporter G family member 2, putative	1971 / 769	CGGGGTACCCGACATAGACAATGAATGTATAGTG	CATGCCATGGTCTAAGTTTCCATTATCGACTG	CCGCTCGAGGAAGAAGAAGGATATTATATGGA	CCCCTTAAGATTCAGCTAATGCTTGTGACA	TATTGATTATTATGAATATAATAG	AAACCTATTATATTCATAATAATC
PY17X_1425800	ABC transporter F family member 1, putative	3792 / 608	CGGGGTACCTATCATATGGTGTATAAG	CATGCCATGGGCCAACTTTCACACATATC	CCGCTCGAGCAATGGGTGTGGAAAATCG	CCGGAATTCTCACTTCTTTTATCACTTC	TATTGATGATGATAATGATGATTGT	AAACACAATCATCATTATCATCATC
PY17X_1222000	ABC transporter I family member 1, putative	8548 / 520	CGGGGTACCCTTGAAATGAACTCAATGCTC	CATGCCATGGCATACAAGCAAGATCTATG	CCGCTCGAGCGACGCATGCACATATATG	CCCCTTAAGGTCCTATGGAGGTTTGTCGTAG	TATTGCCCAAACGTTTAAACTATT	AAACAATAGTTTAAACGTTTGGGC
PY17X_1031600	FeS assembly ATPase SufC, putative	1083 / 809	CGGGGTACCGCTCACAGATAAGGATTAGTA	CATGCCATGGGATCATCTGTATTAGAATATTCC	CCGCTCGAGGCACAATTTGTTGAGTAGATG	CCCCTTAAGCTCATTGACTATTGGTAGTG	TATTGATTATTATGAATATAATAG	AAACCTATTATATTCATAATAATC
PY17X_0407300	ER membrane protein complex subunit 5, putative	706 / 706	CCCAAGCTTGGGTTGTCACATATTTTAT	CATGCCATGGCCTTTATTTGTATTTCCTC	CCGCTCGAGGTTATCATTGCCCCATTTC	CCGGAATTCGAGTTATTCCTTTAGCATTTTAG	TATTGCAGTTATGATAACCTTGAT	AAACATCAAGGTTATCATAACTGC
PY17X_0929900	CorA-like Mg2+ transporter protein, putative	1466 / 538	CGGGGTACCAATAATACGTGGTTGCTTAC	CATGCCATGGTACGAATATCAACAAACTCA	CCGCTCGAGATAATAACCACAACCCAACA	CCGGAATTCTTTCCAAATCACTACAATCTT	TATTGTTGTTTGGTCTTAAAACATA	AAACTATGTTTTAAGACCAAACAAC
PY17X_1018500	CorA-like Mg2+ transporter protein, putative	1443 / 478	CCCAAGCTTGGAAGATAACTGTGTTCTGA	CATGCCATGGCGAATACAATGGTTTAGTTT	CCGCTCGAGGTTCATAAGATAAGTAACGGAG	CCGGAATTCTATTCGAGTAGCATTTCAGT	TATTGAACGAAAGTGATAGTGATG	AAACCATCACTATCACTTTCGTTC
PY17X_0703300	magnesium transporter, putative	1723 / 999	CCCAAGCTTATTTTTACAACCTTCCAGTC	CATGCCATGGCAACAGTGATGTATAGAGCAG	CCGCTCGAGATGGTAATACTAAAAGGTGC	CCGGAATTCTAGACTACTAAGGAAAACGAT	TATTGCAGTTGTTGCTCCGTTTGT	AAACACAAACGGAGCAACAACTGC
PY17X_1240600	inner membrane complex protein, putative	1461 / 1461	CCCAAGCTTTCCCTATTCAAACCTACAG	CATGCCATGGGTTTTCAATATAATCACCCT	CCGCTCGAGTAGCCATTTTTTCATTGTTC	CCGGAATTCATAGATGTGATGGGTGCTG	TATTGGGATAATTTTGACCGTAAT	AAACATTACGGTCAAAATTATCCC
PY17X_1441100	vacuolar iron transporter, putative	981 / 981	CCCAAGCTTTATGGGGTTTTGTCGTG	CATGCCATGGATTATTGCCAGTCAGGTTA	CCGCTCGAGGCCGAACTAAATGAAAAC	CCGGAATTCTTTACAACATCACCATTATT	TATTGCAATTGTTTCCGGTTGTGT	AAACACACAACCGGAAACAATTGC
PY17X_1367300	E1-E2 ATPase, putative	5705 / 1253	CCCAAGCTTTAACGATTAAAGAGATGTAG	CATGCCATGGGCCAATAGACAATAGAAA	CCGCTCGAGAATAATGGAATAAACTCGG	CCGGAATTCATATGTATCTTCTAATCTTGGA	TATTGTCGTATGGAAATAGCCTTT	AAACAAAGGCTATTTCCATACGAC
PY17X_0109300	zinc transporter ZIP1, putative	2055 / 1462	CCCAAGCTTAAAAATAAAAGGCTGTGAT	CATGCCATGGCGAGTCGTGTAAATAAATAA	CCGCTCGAGTATTTTGCCCCCTTTTTG	CCGGAATTCTGTGAATGCTGATGTGGAG	TATTGTGTGCAATACCTTATATTT	AAACAAATATAAGGTATTGCACAC
PY17X_1424200	cation diffusion facilitator family protein, putative	1557 / 452	CCCAAGCTTAAATTACTACCACAGCGTAC	CATGCCATGGTCGGAGGTTATATTTTTATG	CCGCTCGAGATGTTTGTTACTGCTTTTGT	CCGGAATTCAAGAGGCTATCATTACTCCT	TATTGACAGACCTCTAGTTGGAAA	AAACTTTCCAACTAGAGGTCTGTC
PY17X_1138200	guanylyl cyclase beta	11179 / 864	CGGGGTACCCATTTAATACACACACTTGTATGT	CATGCCATGGACCTCGCTCTTTATTTTATCTG	CCGCTCGAGTGATTCGTTTAAAATCGATGGAT	CCGGAATTCATGCAATAATAATAGTTCAATCA	TATTGTAGCAATTAGATGGGAAAA	AAACTTTTCCCATCTAATTGCTAC
PY17X_0619700	LEM3/CDC50 family protein	1397 / 1397	CGGGGTACCTACGAAATAAATACATGCTAAT	CATGCCATGGACTATGTACATTTTTTTATGACCCA	CATGCCATGGGCTCCAAAAAAGGGGGGAAAAG	CCGGAATTCCGAATTTTTATTTATTTTAAAATATG	TATTGGAATTTTATATTTAATAAT	AAACATTATTAAATATAAAATTCC
PY17X_0916600	LEM3/CDC50 family protein, putative	1122 / 1122	CGGGGTACCAGATCGAACAAGTTGAGCATT	CATGCCATGGATATATTATTAACATTTATCAGAAC	CATGCCATGGGACGAATAAATTAACATAATATA	CCGCTCGAGTCACTATGCAAATTGTACACTC	TATTGGTAATGGGCTTGGAAATGG	AAACCCATTTCCAAGCCCATTACC
PY17X_0809500	P-type ATPase, putative	5295 / 962	CGGGGTACCACACATATCGTTATCCCAATTA	CATGCCATGGTCACATGAAAGCGAAAAAGGA	CCGCTCGAGGGTAGAAAATTTTTGCACACAAT	CCGGAATTCTATGTGTTTCTATACACATGTG	TATTAATTAGAGATTAAATAAATC	AAACGATTTATTTAATCTCTAATT
PY17X_1437200	aminophospholipid-transporting P-ATPase, putative	4838 / 1011	CCGGAATTCATCCAATTATTTAAAAAATCTTGA	CCGCTCGAGCCTTTATGTGTTGCGGCATT	CATGCCATGGATCTGAAGGATCAAGCCATAGA	CGGGGTACCCATAGTAACAATTAAACAAATAGG	TATTGAAACACAAATACGCATCAA	AAACTTGATGCGTATTTGTGTTTC

PY17X_1440800	phospholipid-transporting ATPase, putative	5978 / 1030	CGGGGTACCACATTATTTAGATAATTCTGTAGG	CATGCCATGGCTTCAAATCCGTTAAAATTTACA	CCGCTCGAGTGATGGAGAAACTGATTGGA	CCGGAATTCGTTTCCATTTCCATCTCCTA	TATTGCTTTACGTTAAGCAAAAAA	AAACTTTTTTGCTTAACGTAAAGC
PY17X_0911700	guanylyl cyclase, putative	11553 / 994	CGGGGTACCCTTTCTGCATTCTTAGAATTAAC	CATGCCATGGGTTATTTTTATTGTTTCTTATTTGC	CCGCTCGAGCTGGATATGTGAATAAAGAATT	CCGGAATTCACTTTACAAGTTTATCAAATGTGC	TATTGTCGAAACATCGCTAGTAAA	AAACTTTACTAGCGATGTTTCGAC
PY17X_1105200	MOLO1 domain-containing protein, putative	1594 / 948	CCCAAGCTTGTTGGTATATATCTTTCCCA	CATGCCATGGTGAAGGGCTTTTAAATGGTT	CCGCTCGAGGCTGTAGCTATAGTACCAGA	CCCCTTAAGCGTGTTGGTCAGTTCTGTAA	TATTGCATTCTTATTTTGTTTGCT	AAACGCATTCTTATTTTGTTTGCT
PY17X_1315200	conserved protein, unknown function	765 / 765	CGGGGTACCCGTGAAGTTCAATTTATCCC	CATGCCATGGAGTGCCTTATCCAGAAAGTC	CCGCTCGAGGAAACCAAACAAGAGACGAA	CCGGAATTCCTCAAAGGACATATACTTAC	TATTGATTGTGGAAATTCATCTAC	AAACGTAGATGAATTTCCACAATC
PY17X_1339400	transmembrane protein 43, putative	1869 / 1412	CCCAAGCTTTTTAAATGTCTTATGCTCTG	CATGCCATGGTATCAAACGCTAAACCATAT	CCGCTCGAGCAGAAAGCAAGATTACTAAA	CCGGAATTCCCATTATCTACTTCGTTATT	TATTGTCTATAGTAGATCTAAATG	AAACACCCACTGATACATTTCAAC
PY17X_1342800	conserved protein, unknown function	2358 / 1213	CGGGGTACCCGTTATGCCGAAGAAATTTT	CATGCCATGGGTAATAATGTTCCTTCACAA	CCGCTCGAGGTAATATTGCATGAACACGT	CCGGAATTCCAACGTGTGTTGTAACTAAA	TATTGGTAGAAAGACACCTAAGAG	AAACCTCTTAGGTGTCTTTCTACC
PY17X_1366100	conserved protein, unknown function	2603 / 1347	CCCAAGCTTCTATTCAGTGTTTATATTAAGC	CATGCCATGGGGATAACAAAAAGAGAAGTA	CCGCTCGAGTAAGGACAGCCATATTAAAG	CCGGAATTCCAATTTGGAACTCGGTTACA	TATTGGAGCAAATTGGATTTGCTC	AAACGAGCAAATCCAATTTGCTCC
PY17X_1463300	dipeptidyl aminopeptidase 2, putative	2800 / 1367	CCCAAGCTTGTATTTTTGGTTGTAGAGTG	CATGCCATGGAATATAATGCCACTGTTCAG	CCGCTCGAGCAGAGTGCTATAAAACAGAT	CCGGAATTCTGTAGCTTATCTTTGTCGAT	TATTGATACTTCGGAACATTGTGG	AAACCCACAATGTTCCGAAGTATC
Primers for PCR-genotyping parasite with candidate genes (except gep1) knockout								
Gene name	**Gene ID**	**P1**	**P2**	**P3**	**P4**	**P5**	**P6**	
PY17X_1243400	7-helix-1 protein, putative	ATAACATTTAAACAGATAGGCG	CAGGTCTATCTGGAATGTTA	GAGAATAAAAGGTCATTGTGGC	CTATTAAACCTGCATAACCTTC	GAGAAACATGCAAATCAATCAA	CTATTAAACCTGCATAACCTTC	
PY17X_1431500	integral membrane protein GPR180, putative	TACAAATAACGAAGGTATAGCA	CTATGTATTTATGCTTACGTGG	TACATTAATGCTTGATATTG	CACAATTTCATATTACGCAA	TACAAATAACGAAGGTATAGCA	AACATACAACCATTACGTGCTT	
PY17X_0918700	serpentine receptor, putative	ATATGCCAAATAAACATGCCAA	ATAAAGACAGACGATAT	TATGAACATATAAGAACGCCAA	CTCTCGTTAATAATTACGTAGG	GTGTGTTACCAAATTGATAGCA	CTCTCGTTAATAATTACGTAGG	
PY17X_1433900	serpentine receptor, putative	TCATTATGATTATTCCCCAGCG	TCCTCCAAATCTGAGTGTTCTG	TTCATGTATTAACAATGGA	TGAAATATCTTCAATTGAAT	TCATTATGATTATTCCCCAGCG	CTCCTAACAAAATATATGGCGC	
PY17X_0524600	serpentine receptor, putative	GATGAGGTGTAAAGACTTCGGT	CTTCATACCTTGCTCTTCACAT	TATATTGTTATGTGTGTACA	ATTATTACACTGAAGCGTTC	GATGAGGTGTAAAGACTTCGGT	CACTTGAAAGAATAACGGATCC	
PY17X_1421700	GPCR-like receptor SR25, putative	TGAAGTGAAGTAGTTAGTTTTACT	ATGCATAAACAGAAAAATAGAATATAAC	CGAGTTTGGTAATAATGAAAGAGAT	ATGTGCACATATATATATAGTGC	TGAAGTGAAGTAGTTAGTTTTACT	AGCAAATTCTTGAATTACTAATGC	
PY17X_0605800	sexual stage-specific protein G37, putative	ATCAAGATAGATATGGTGGTCC	CTCTATACCTACTGATACATGC	TTAGTAACACCTCAACTTATA	TTTAACCTGCTACTACCAGTGG	ATCAAGATAGATATGGTGGTCC	TGCTATGGACAATTCGGGACAA	
PY17X_0617400	conserved Plasmodium membrane protein, unknown function	ATGTATGTTCAGTATACATACA	AAAGTTGATACTGGTATCTA	GTTACCATAGGTCAAGCTCTTA	GCCATACAAAATGCAAAACCCA	GCTAGCCAATAACTAAGACGAA	GCCATACAAAATGCAAAACCCA	
PY17X_0914700	conserved Plasmodium membrane protein, unknown function	GTTATTTGGAGTTACATAAATGT	ATCTGTGCCCCAAACTTCTAAAAAG	GTTATGCGCAATTAAAATCAAACT	AGGGCACCAATGAAAAGAGAA	GTTATTTGGAGTTACATAAATGT	ATTGCCATGGACTTATTTGTTTGCATC	
PY17X_1128600	protease, putative	TTGGATTCCTCACATTAAACTA	GAATCTATAATTGAAAACGCAG	TCCTTCGCTATATGTGCGAT	AATATAACCCTGCTGAAGAGCA	TTGGATTCCTCACATTAAACTA	GTAATATCATGAATGCACACCG	
PY17X_1313900	conserved Plasmodium protein, unknown function	TTTATTCGATGGCATTTCAT	CCATTTGTTACTATATATGG	AAGATTGTTGTTGTTTGGGCTT	TTGTTTGCTATGTTTTATGTCC	ATGATACCCAAGAAATTGAGAG	TTGTTTGCTATGTTTTATGTCC	
PY17X_0702400	folate transporter 1, putative	AAAACTGTTAATGCTCTT	ACTAGATGGTGTTGACAT	TTTACATTTCCACCCGTT	TCATGTCCATTTTCTGTG	TTTACATTTCCACCCGTT	GCAAAGAACCTCAACTCC	
PY17X_0933500	folate transporter 2, putative	AAGGAAAAATCAAAGAAT	CGTGCCTTAGTACGTGAT	ATACATGAGTCTGCACCCTA	GATTCTCATCCATTAGGTTC	ATACATGAGTCTGCACCCTA	GTATTTCTGTAATGGCTTCA	
PY17X_0309400	GDP-fructose; GMP antiporter, putative	ATAATGCCGAAAGGTTAA	AAATCCTGATCTCATCAT	GTGCAAACTTAACTAAAATACCCCG	ATCATACTTTTTCACACAAACAAACTG	ATAATGCCGAAAGGTTAA	CATCCTCCCTTTCTCTCT	
PY17X_0936300	UDP-galactose transporter, putative	CATATCCATGTTTAGGTT	TCACCATTGAAACTAGAA	CAGCAAGTTTAGTAGAGCAAGT	ATTGACAATGATGCAAATATCCAAGC	CATATCCATGTTTAGGTT	TTATCTTGTCTTGGTCCT	
PY17X_1436400	phosphate translocator, putative	CAAACCCAAAGGAAGAAC	ATTGATACGAGCAGAGAG	TAGATCTATATACACATCCCTGTGAT	ATCACAGCACCGAGAGATACAAAGCC	CAAACCCAAAGGAAGAAC	GCTTCCTCGTTAGGCTTG	
PY17X_0823700	major facilitator superfamily domain-containing protein, putative	TATTTGTGTGTGCAGTCT	AAAAATGGGCAAATCTACAC	TTTATACAAAATGATGTACCTTAC	ATTGAATAGAAGAAGTTACACTATG	TATTTGTGTGTGCAGTCT	TAAAGGGGTATCCATAGT	
PY17X_0820300	major facilitator superfamily domain-containing protein, putative	GGGTGTATGTATATATGTGTAAGTACTT	ACCGTAAATGTATGCATGGCTCAC	TAAATAGTATGAGGGCAAA	TGGTAAATAAACAACAGGT	AGTGCAAACAGTACGAACT	TGGTAAATAAACAACAGGT	
PY17X_0307300	transporter, putative	TTTCCGTATGTTTAGTATCT	CTTGTTCATAACTTCTTGTA	TTTTGTATTATTGTTAGA	GATATTTGTTCAGGTGTA	TTTCCGTATGTTTAGTATCT	TCTGTTTTCTCAAATCTGTA	
PY17X_0917400	amino acid transporter	AGAAAAAAGTAAGTGGTGTG	GTTTTCTATCTGTTTGCTCA	CCAAATATAAGAAAGAGGGGAGGTGT	ATTCTATCTAATATTGGCTCCC	AGAAAAAAGTAAGTGGTGTG	ATGTTCAGAATTTATCCTTA	
PY17X_0609400	amino acid transporter, putative	CCTCGTGTGTACACATGGCACCT	ATTTGGTATCATTGTCATAGATCG	TTGTGTTCATTTACACCCGT	TCAATATGAGGGTAAGCGGT	TTGTGTTCATTTACACCCGT	CCCTTATGCCTATCACTTTT	
PY17X_1448600	amino acid transporter, putative	TCGTTTTATCGAGCATGT	GCTCAGTTGCTGCTTTTT	TTGCTGCAATTCTATACATA	TCTTAGAACAACTTAACGCT	TTGCTGCAATTCTATACATA	TCAAATAAGCCTACAGACAA	
PY17X_1241000	multidrug resistance protein 1, putative	GTGATAATAATAAGAATAATA	CACTAGTTGTATTTCTCTTA	GAACAAGTAAATGCAGGAATAG	TATCCATATTTGTATCAGTAAC	GTTGATAGAAATCAAAATAA	TATCCATATTTGTATCAGTAAC	
PY17X_1446300	multidrug resistance-associated protein 2, putative	CTATGTATGCAAACAATTTGACAATGTT	ATTGTCGTGATATGGGCTTAA	GTAATTCATGGAATTCATG	CCGAATTAACATCAATATGATC	GGACTGATTTCGGCATTGGCCTAT	CCGAATTAACATCAATATGATC	
PY17X_1315500	multidrug resistance protein 2, putative	CTTATAGCGACATTTTTTGGATGTT	ACATGTGAATATAATACACCCG	GCTGTGTTAATAACATATAACCT	CAATAGTAGAATATAATGTTCC	GATTTAGGTAAAAAATGGGA	CAATAGTAGAATATAATGTTCC	
PY17X_0904900	ABC transporter B family member 3, putative	GTGTGTAAAACACTTAAGGA	CACCACTATGTATAGACATG	GAATTATAAGTTTAGGGTTGTGTCT	AAAGCMAAATAAAGGGCTAG	GTGTGTAAAACACTTAAGGA	CAATTTTGATCAATAATATC	
PY17X_0403400	ABC transporter B family member 4, putative	GAACAACAATATTCACGGATTCAAGAAT	ATTGTCTTCATTAGTGGATATGTCAC	CTGGACATACAGATAACAACAC	CTATCTAAACAGACAATTTTGG	TATACATGGTACTTCTAGTC	CTATCTAAACAGACAATTTTGG	
PY17X_1358700	ABC transporter B family member 5, putative	CGAATAACACATGGACAGCTTGTATCT	ACCCATAGAATGAAAAGGTAGATG	TCAGGAAAATCGACCATATGG	GTCCAGGCTTATCTTGTTCGCC	GATTAGACGATGAACTAAAGG	GTCCAGGCTTATCTTGTTCGCC	
PY17X_0928600	protein GCN20, putative	GATATAGTGACAAAATGGCTGTTGTATCAT	ATTCTCATTCCTCCACTTAGAGAGTTTAC	TGGCCTTTCACATAGCTTA	CTCGAGTCCATATCTACTTC	GTTAAGTTTATTTAAAGAAT	CTCGAGTCCATATCTACTTC	
PY17X_1370600	ABC transporter B family member 6, putative	TATGGCTGCATAAAAATTGG	GTTATTATACAATTGAATAT	TTCGGGGATTGCTTTATTCAAAGT	GTATTTTGTTCTGACTTGTTCAT	AGTATACAATCGACATATCC	GTATTTTGTTCTGACTTGTTCAT	
PY17X_0610800	ABC transporter B family member 7, putative	GGTACTATATATTCCTATGTAGT	AGTGTTTCTTCTTTTCCTCCATAC	GTGATGAAGTACAGTTAGAAG	TCCTACTATAGCAACAGATT	GCAGATTCGAGTTTCGCATG	TCCTACTATAGCAACAGATT	
PY17X_1145400	ABC transporter E family member 1, putative	GTAGTCTTGATTTATGGCA	GGTAAAAGAGTTCAATGTTT	CTGCGATACAGTTATATGATA	CATACCTGCTACTAATGTTTGTG	GAATGGCGAGATATATTATC	CATACCTGCTACTAATGTTTGTG	
PY17X_1019600	ABC transporter G family member 2, putative	GTATATATGCATATATAAAAGG	ATTTCACTATCATGATCATTATGAATTATTG	ATGCATCATACCAATCACCTA	GAATGATCCATATAATGCTA	GCATTTATAAGAGGTATAAG	GAATGATCCATATAATGCTA	
PY17X_1425800	ABC transporter F family member 1, putative	CATATATAAATACAAACATAT	CAACTTTTCAAAATCAGAAA	GGCGCAATAGACGTTAACT	ATTCTTCTTCCTCATCAGAA	GATGAGAATGATGATGAGAATG	ATTCTTCTTCCTCATCAGAA	
PY17X_1222000	ABC transporter I family member 1, putative	GATAATATTGATTTTTGTTCTC	CATTTGCACTGAGATTGTCGA	ACTCACATATATACAGATATG	CTGTAACTATGCTACTATCTG	GCATTATGTCGAATAGCATA	CTGTAACTATGCTACTATCTG	
PY17X_1031600	FeS assembly ATPase SufC, putative	GAGTAAAACGACACAAATGTGAAAT	ATTGTGAACCCTCATATATTGTACATGTTC	GGCTAGCTGTGTCATACTAT	CGCATATTTCTTCGCAATGCTC	GTTAATCATAGATCATTATG	CGCATATTTCTTCGCAATGCTC	
PY17X_0407300	ER membrane protein complex subunit 5, putative	CCTAACAATGTTGCACACAGTAATACT	AGCATTAACAAACTTGTTCCGATTGATG	TAGTATGCTTCTTTTTGCG	ATAGGTCTGTCCTCTTTGC	ATGACTCAACTTTTGCTCTA	ATAGGTCTGTCCTCTTTGC	
PY17X_0929900	CorA-like Mg2+ transporter protein, putative	GTCTGAAGCGCTTCCCCCCCTCAACT	ATCTTTTCGTATTAAAATTGTTGGGTTGTGG	TTTGAGTTTGTTGATATTCG	GGACCATACAGAAACAAAA	GTAGCTGATGATGGAAATG	GGACCATACAGAAACAAAA	
PY17X_1018500	CorA-like Mg2+ transporter protein, putative	GCTAGCTATATATGTAAATATGTTTT	GTAAAAGATAATGAACATTTTCTCCGTTAC	AAACTAAACCATTGTATTCG	GCTAATGTCCAAAAAATGTA	TGTAATGAAAAAGAACCCA	GCTAATGTCCAAAAAATGTA	
PY17X_0703300	magnesium transporter, putative	GCTAAATGCTGTAACATATCGAAT	ATCTCTCCTTTTTATCATCTTCTTTTGTTTCGTC	ACGCTGCTCTATACATCACT	AAATAGAATACTGCGAAGAT	AGTTGTTGCTCCGTTTGT	AAATAGAATACTGCGAAGAT	
PY17X_1240600	inner membrane complex protein, putative	CATTGAAAATTTGTAAAGTTGAAGCATTTG	ATGCACATGCTGCAATAGTAGCATATGTGAAC	AGGGTGATTATATTGAAAAC	TTTTCTTACACTTGAACACA	CTCATATAGGAGATCACCAT	TTTTCTTACACTTGAACACA	
PY17X_1441100	vacuolar iron transporter, putative	GAAGAAGTGGCATTACTAATTAACAAT	AGGTTGGTAACTAAAATGTTAAAAACGCA	TAACCTGACTGGCAATAAT	GTAAGACGATAAAATGTGAA	GTTAGCAGAAAGACAAAGAG	GTAAGACGATAAAATGTGAA	
PY17X_1367300	E1-E2 ATPase, putative	GTATGAATAAAATTGACAAATTTGTATACAT	ACCTGAATTGGTATTACCCGAGTTTATTCC	TTTTTCTATTGTCTATTGG	CATGTTTCTCTATTATTTTC	CTATTTCCATACGACTCTA	CATGTTTCTCTATTATTTTC	

PY17X_0109300	zinc transporter ZIP1, putative	GTTGATGTCGTTCTATATTCATT	ATCTTGAGATTTTGGCTCTGAAAAAGAGTGCAC	GTAATAAATAACTACGGTCA	GATAATAATGTGTCTTCCCT	TTTCTAAAGTCTATCAACGC	GATAATAATGTGTCTTCCCT	
PY17X_1424200	cation diffusion facilitator family protein, putative	CTTATTTTCATTGATAAAACGCTGCCT	ACAAAAGCGATAAATATATTTGCTAGTG	GAGCGTCACAGCTACATGACCAT	ATTGGATCTGTGATTGAATATTTAGGGTTATACC	CAAGTTGAGCAAGTTGATGGAT	ATTGGATCTGTGATTGAATATTTAGGGTTATACC	
PY17X_1138200	guanylyl cyclase beta	GTCTACACCTGACTGGACATA	ATGCAATAATAATAGTTCAATCA	ATGGAGGCTTAATATTGGGT	TAATTCTTAATGTATATAAAAGTATAGACA	GTCTACACCTGACTGGACATA	TGCGTCGAGTGATATCAAC	
PY17X_0619700	LEM3/CDC50 family protein	GGTCATTCTAATGTTATAAGA	GAAATGTTATTGCATATCCACC	CAAGACGATTCCTCTATATGTATGC	TCTACATAATAAAAGCATCGC	CACATTGTGTCTTATTTACAACC	TCTACATAATAAAAGCATCGC	
PY17X_0916600	LEM3/CDC50 family protein, putative	AATTTCCCTTTGGGGTTTCAC	ACATGTTAATATTTATCCGAATGGA	TGTGTGATTATACAATTGCTTATGA	GGAAATATATTACAAAACATAGTG	GGAAATATATTACAAAACATAGTG	TGGATGATACCATCACCATTTAG	
PY17X_0809500	P-type ATPase, putative	GGAAACGTGCATATATCCACA	TGTGTTTACAAGTGATGTACCTCT	ACTTAATGCATACCTTCCTG	ATACATATATATACGCGTATATTGTGT	GGAAACGTGCATATATCCACA	TAGTTGTAACGCCGATATCGA	
PY17X_1437200	aminophospholipid-transporting P-ATPase, putative	TCCTCCACCTTATAAACCATAT	TAGGTGGTAATAATATCACTG	TGAGTATAAAGCATACTCACAAAG	GGTAACTTAACATATTTATCATCAT	CATGAATATGTGTAAAAAGGACGA	TGAGTATAAAGCATACTCACAAAG	
PY17X_1440800	phospholipid-transporting ATPase, putative	TCATCGAAGAAACAAATGAGTA	ACCATATTGATTGTATTTAAACAT	CACTGTCAACAAAATTTATCATAC	GAAGAGATTGTAAATTTTAA	TCATCGAAGAAACAAATGAGTAA	TCTTCATCTTTACTTAAATTTCGT	
PY17X_0911700	guanylyl cyclase, putative	ACACACCCAGCACACATATTTAG	ATGTATTTAAATAAACCATTTGTAGC	ATATTGTTTGATGTTGGTTTTG	CTTGCTTACCTCTATTACTGCA	ACACACCCAGCACACATATTTAG	TCCCATAATGGTTGATTATTTG	
PY17X_1105200	MOLO1 domain-containing protein, putative	GTTATATCTACACATATGCATG	CGTGTTGGTCAGTTCTGTAA	ATGTTGCTTTATCGTCTT	ACAGCCAAACAGTAGTCA	GCATTCTTATTTTGTTTGCT	CGTGTTGGTCAGTTCTGTAA	
PY17X_1315200	conserved protein, unknown function	ACTAACTCGCTATTTAGCCT	CTCAAAGGACATATACTTAC	TATACGCATGTCAATCTT	TTCAGTGCAAATTATGTT	GATTGTGGAAATTCATCTAC	CTCAAAGGACATATACTTAC	
PY17X_1339400	transmembrane protein 43, putative	CATACACTATATGCATATATATAAGC	CATCTTTATTCATGATATTAACTG	AATATTTGTGGGGGTGGTGTTTA	CGTAGAAGATAATTGTACAG	GCAACATCGCTTACTATAATCC	CATCTTTATTCATGATATTAACTG	
PY17X_1342800	conserved protein, unknown function	TGCCATTTTCCCCCACCCTTTTTGTTAGG	TAAACATAATGGGAATAACCATATATGGG	GACGGTTTACAACTTATT	GTAATGATGGCTGTTCTA	GGTAGAAAGACACCTAAGAG	ACTTCGGCCATCAAATTATC	
PY17X_1366100	conserved protein, unknown function	GTGTAACATAAAAGGAAAAT	CTAAATAAACAAATGGACGT	GGTTTAAAATACCTTGAT	CTAACTCGATTTATAGGG	GGAATATTTACAATATTTTA	CTTTAATATGGCTGTCCTTA	
PY17X_1463300	dipeptidyl aminopeptidase 2, putative	TAGTTTGGTACTATTTAGCG	CATAAAATATCCATCCTAATC	ACACCCATTTTGCCTGAA	TCAACTGTTTCGCAAGGA	TACAAAACCAATGTCTAACC	AGAGATAGGCATCTTTGTAA	

Oligo sequence for gep1 (PY17X_1116300) knockout plasmid construction

Gene ID	KO	Gene size (bp)/ deleted gene size (bp)	Left homologous arm		Right homologous arm		Target site of sgRNA	
			Forward primer	Reverse primer	Forward primer	Reverse primer	Oligo (Forward)	Oligo (Reverse)
PY17X_1116300	gep1 N-terminal KO	3333 / 464	CCCAAGCTTTTGGCTAAGCAAATGTAT	CATGCCATGGCCAAAACGAAATTAAATC	CCGCTCGAGAAACAAGATAGAGTAGAA	CCGGAATTCAGATGAACTTAATGTTGT	TATTGTGTTAGTAACAATAAATAAA	AAACTTTATTTATTGTTACTAACAC
PY17X_1116300	gep1 C-terminal KO	3333 / 558	CGGGGTACCCCTTTATGCTTATATCAGCA	CATGCCATGGTGTGCAAAATGTACACATGC	CCGCTCGAGGGGCTATTACTATTATTGCA	CCCCTTAAGGTAGTGTTGTCCAATTTGAA	TATTGTTAAACCAGTCTATATATT	AAACAATATATAGACTGGTTTAAC
PY17X_1116300	gep1 full length KO	3333 / 3333	CGGGGTACCCACAACTCTACAAATAAACA	CATGCCATGGCTTTTTTTCAAACTTACAAA	CCGCTCGAGACAAACATTTTTCATATTTT	CCCCTTAAGGTAGTGTTGTCCAATTTGAA		
PY17X_1116300	gep1 full length replaced with mScarlet							

Primers for PCR-genotyping parasite with gep1 (PY17X_1116300) knockout

Gene ID	KO	P1	P2	P3	P4	P5	P6	P7
PY17X_1116300	gep1 N-terminal KO	ACGCACATTGGCCATAAACATG	CAAAGACACTTGCCATTTCAAT	GCTTGGCTAAGCAAATGTATCA	TCTTGCAATAAAAATGGAGCCG	TATTGACATTAGGATTTCGAAGTGT	TCTTGCAATAAAAATGGAGCCG	/
PY17X_1116300	gep1 C-terminal KO	ATATACTGCACATACCTGATTG	GGCACATACACATACACATATA	ATATTCCGTCTTTCAATGGA	CTTAAGAGTACGCGATATATAGACAAGA	ATATACTGCACATACCTGATTG	GAATTCGAGTTGGATATGCTTT	
PY17X_1116300	gep1 full length KO	ACGCACATTGGCCATAAACATG	CCCCTTAAGGTAGTGTTGTCCAATTTGAA	CGGGGTACCCACAACTCTACAAATAAACA	CTTAAGAGTACGCGATATATAGACAAGA	ACGCACATTGGCCATAAACATG	TCTTGCAATAAAAATGGAGCCG	
PY17X_1116300	gep1 full length replaced with mScarlet							ACGCACATTGGCCATAAACATGCCGCTCGAGCTACTTGTACAGCTCGTCCA

Oligo sequence for gene knockout plasmid construction

Gene ID	Gene name	Gene size (bp)/ deleted gene size (bp)	Left homologous arm		Right homologous arm		Target site of sgRNA	
			Forward primer	Reverse primer	Forward primer	Reverse primer	Oligo (Forward)	Oligo (Reverse)
PY17X_0619400	nek4	1709/1709	CCCAAGCTTGTAAGCAAAGGTTAATACAC	CATGCCATGGTTGTGAGGACGTGTATAATA	CCGCTCGAGGAGTATAATATTACAGTCCA	CCGGAATTCGAAATGGTACACCCTGTTCT	TATTGAACAAGTATGAAAAAATAA	AAACTTATTTTTTCATACTTGTTC
PY17X_0935700	map2	1587/1587	CCCAAGCTTAGTCTCCCAATTTTTCTGTG	CATGCCATGGAAGGAGAATGTGCGTATCTA	CCGCTCGAGTATGTTTCGTCGAGAAAGGT	CCGGAATTCTTGGGAATATGAGCATTCGT	TATTGAAAAATTTATTCACGAATC	AAACGATTCGTGAATAAATTTTTC
PY17X_0617900	cdpk4	1792/465	CGGGGTACCGAAGTAGATGCAGCTAGAATA	CATGCCATGGGTTCTAATGCATCTCTTGCTG	CCGCTCGAGCTGCAAATGAATTAGCTCAAT	CCCCTTAAGTGTGTATATTCCACGATATTT	TATTGACAGAAATGAATTAATAAT	AAACATTATTAATTCATTTCTGTC

Primers for PCR-genotyping parasite with gene knockout

Gene ID	Gene name	P1	P2	P3	P4	P5	P6	
PY17X_0619400	nek4	CTTTTGAAAACCGATAAAAAGTG	CCGGAATTCGAAATGGTACACCCTGTTCT	CCCAAGCTTGTAAGCAAAGGTTAATACAC	TCACACCGTATCATATTGTGTC	GAGTAAGATTGTGTGATTTTGG	TCACACCGTATCATATTGTGTC	
PY17X_0935700	map2	GGGAAATACTGATAATAGCGACAA	CCGGAATTCTTGGGAATATGAGCATTCGT	CCCAAGCTTAGTCTCCCAATTTTTCTGTG	AGACACACTCACATTACGATTG	GATATATGGTCTACTGGTTGTA	AGACACACTCACATTACGATTG	
PY17X_0617900	cdpk4	GCTCTTCCTTTGGACATAGTTA	GGGCTGAAAACCAAATAAGTAT	GAAGTAGATGCAGCTAGAATA	AGACGGATAAAATGTCGGAT	AGTACACAAAAGTTAGCACAAG	CCTTTTCTAATCTCTCAGTTGA	

Oligo sequence for gene knockout in P.berghei ANKA plasmid construction

Gene ID	Gene name	Gene size (bp)/ deleted gene size (bp)	Left homologous arm		Right homologous arm		Target site of sgRNA	
			Forward primer	Reverse primer	Forward primer	Reverse primer	Oligo (Forward)	Oligo (Reverse)
PBANKA_1115100	gep1	3166/785	CCCAAGCTTGCACATTGATCATAAACTTG	CATGCCATGGCTTGTCTGTACATGGACAAA	CCGCTCGAGCGAATTTCATAATTATGATG	CCGGAATTCCATACATCCCTATTGATATA	TATTGTTATAATATAAAATATGAG	AAACCTCATATTTTATATTATAAC
PBANKA_0933700	map2	1572/807	CCCAAGCTTGTCTCCCAATTTTATGTGT	CATGCCATGGTGATCGTATGGGAAAACGCT	CCGCTCGAGTCACGAATCAGGTATTATCC	CCGGAATTCCATCTGAAATAGATGGGTAT	TATTGCAATGAAGAAGATAAAAGT	AAACACTTTTATCTTCTTCATTGC

Primers for PCR-genotyping parasite with gene knockout in ANKA

Gene ID	Gene name	P1	P2	P3	P4	P5	P6	
PBANKA_1115100	gep1	GCACACACAAACTCTTATGCGCATAC	ACAAATCTCCCTCCATTTATTTCTTG	CGAGATTTGTCCATGTACAG	CTCAATAAGGGAGAAATCACGT	GGAAACGACAAATAAAGAAA	CATTATATGATATACCAATAG	
PBANKA_0933700	map2	GCTATTATGAAAAAAGGAGCTAACAT	TTATGTGGCCCTGGTTCTTCATTTTC	CGATTTTGTCAATCCATATATTT	GCCTGGTCAATTGTGATTCGTT	GATGATAGCACATATATAGAT	GTCCGAATCGGCTATTTCTA	

Oligo sequences for gene tagging plasmid construction

Gene name	Tag	Gene ID	Left homologous arm		Right homologous arm		Target site of sgRNA	
			Forward primer	Reverse primer	Forward primer	Reverse primer	Oligo (Forward)	Oligo (Reverse)
sep1	C-terminal 4Myc	PY17X_0526200	CCCAAGCTTTTGCCTTTTTATTGGCCATA	CATGCCATGGGTGTGATGCTGGTGGATAA	CCCCTCGAGTTCTAATTTCTGATGGTTAT	CCCCTTAAGCACGGTACTACTTACAATAA	TATTGTATTAGTTTCTGGTGCGGG	AAACCCCGCACCAGAAACTAATAC
gep1	N-terminal 6HA	PY17X_1116300	CATGCCATGGCACAACTCTACAAATAAACA	CCGGATATCCTTTTTTTCAAACTTACAAA	CCGCTCGAGGAAACATCAAATAAAGAAAT	CCCCTTAAGTATACCAATAGATACAAGAT	TATTGAGCTATTTTATGAGAATAA	AAACTTATTCTCATAAAATAGCTC
gep1	N-terminal 4Myc	PY17X_1116300						
gcα	C-terminal 6HA	PY17X_0911700	CGGGGTACCGTGTATACCAAATTTAAATATGAGA	CATGCCATGGGCAAAATTGAACTTGTGTCTTTGGA	CCGCTCGAGTACTTTTAGAACTTTCTAATTTATG	CCGGAATTCCCATGTACTGTGAACATATCA	TATTAATCGTCATATAAAATATTT	AAACAAATATTTTATATGACGATT
gcα	C-terminal 4Myc	PY17X_0911700						
gcα	N-terminal 6HA	PY17X_0911700	CCCAAGCTTCTTTCTGCATTCTTAGAATTAACATGTATTATTGGAT	CATGCCATGGCTTTTATATCTTTATCTGTTATTTTTTATTGTTTC	CCGCTCGAGATGCAGACGAAAAAAGGAAATGAAAAAGT	CCGGAATTCGAAGTTGATCCATCTATGATGTGACATAATC	TATTCAATAGTAATATGAAAAATC	AAACGATTTTTCATATTACTATTG

Primers for PCR-genotyping with gene tagging

Gene name	Gene name	Gene ID	P9	P10	P11	P12		
sep1	C-terminal 4Myc	PY17X_0526200	CATGTGCAAAAATGAAATTAGCAAAAGC	CCCCTTAAGCACGGTACTACTTACAATAA	GCTAGCGCCGGTTCTGCTGCTAGA	GTAATGGTGATTCAGGGT		
gep1	N-terminal 6HA	PY17X_1116300	GCTTGGCTAAGCAAATGTATCA	CCCCTTAAGTATACCAATAGATACAAGAT	CATGCCATGGCACAACTCTACAAATAAACA	CAAAGACACTTGCCATTTCAAT		
gep1	N-terminal 4Myc	PY17X_1116300						
gcα	C-terminal 6HA	PY17X_0911700	TTAGAAATGGCATATTCAATG	CCATGTACTGTGAACATATCA	GTGTATACCAAATTTAAATATGAGA	ATGAAATTAATTTCCAAAATGGA		
gcα	C-terminal 4Myc	PY17X_0911700						
gcα	N-terminal 6HA	PY17X_0911700	CACACACCCAGCACACATATTTAGAT	ATCCAAGCAGCTTCTGCTGTTGC	CCTTGCTTACCTCTATTACTGCACCATTGAT	ATCTGCAGGTACTTGCTCATTTTCTACTAAGCG		

Oligo sequences for gcα promoter swap plasmid construction

Gene name	Tag	Gene ID	Left homologous arm		Right homologous arm		Target site of sgRNA	
			Forward primer	Rerverse primer	Forward primer	Reverse primer	Oligo (Forward)	Oligo (Reverse)
gcα	N-terminal 6HA & promoter swap	PY17X_0911700	CCCAAGCTTCTCAATATGGTTGCATATAT	CATGCCATGGAAGAAGATAATGTGCATACAC	CCGCTCGAGCAGACGAAAAAAGGAAATGA	CCGGAATTCGAAGTTGATCCATCTATGAT	TATTCAATAGTAATATGAAAAATC	AAACGATTTTTCATATTACTATTG
Primers for PCR-genotyping with gcα promoter swap								
Gene name	**Gene name**	**Gene ID**	**P9**	**P10**	**P11**	**P12**	**P13**	**P14**
gcα	N-terminal 6HA & promoter swap	PY17X_0911700	TCATCCAGGTGTAGACTAAAAT	CCGGAATTCGAAGTTGATCCATCTATGAT	CCCAAGCTTCTCAATATGGTTGCATATAT	AGCGTATAATACTACCTACAGT	AAACACAGACATAACTCCTTTAGA	AGCGTATAATACTACCTACAGT
Primers for RT-PCR								
Gene name	**Gene ID**	**Forward Primer**	**Reverse Primer**					
18s Rrna	PY17X_0522400	GGTTTTATAATTGGAATGATGGGAAT	ACGCTATTGGAGCTGGAATTACC					
gcα	PY17X_0911700	GTTGTAATCATAGTGATGGTTC	TCACATGTTATTCTTCCTCTAA					
Peimers for gene in situ complementation								
Gene name	**Tag**	**Gene ID**	**TS**		**Left homologous arm**		**Right homologous arm**	
			Oligo (Forward)	**Oligo (Reverse)**	**Forward primer**	**Reverse primer**	**Forward primer**	**Reverse primer**
Pygep1	C-terminal 6HA	PY17X_1116300	TATTGCGGACGCTAATCGTAGCTA	AAACTAGCTACGATTAGCGTCCGC	CGGGGTACCCCTTTATGCTTATATCAGCA	CATGCCATGGACCCCTTATTGAAAATTCAC	CCGCTCGAGACAAACATTTTTCATATTTT	CCCCTTAAGGTAGTGTTGTCCAATTTGAA